ENERGY OPTIMIZATION OF THE YANKEE-HOOD DRYER

A THESIS SUBMITTED TO
THE GRADUATE SCHOOL OF NATURAL AND APPLIED SCIENCES
OF
THE MIDDLE EAST TECHNICAL UNIVERSITY

BY

SELİS ÖNEL

IN PARTIAL FULFILLMENT OF THE REQUIREMENTS FOR
THE DEGREE OF MASTER OF SCIENCE
IN
THE DEPARTMENT OF CHEMICAL ENGINEERING

AUGUST 2000

Approval of the Graduate School of Natural and Applied Sciences.

Prof. Dr. Tayfur Öztürk
Director

I certify that this thesis satisfies all the requirements as a thesis for the degree of Master of Science.

Prof. Dr. Timur Doğu
Head of Department

This is to certify that we have read this thesis and that in our opinion it is fully adequate, in scope and quality, as a thesis for the degree of Master of Science.

Prof. Dr. Güniz Gürüz
Supervisor

Examining Committee Members

Prof. Dr. Canan Özgen (Chair)

Recep Parlak (İpekkağıt)

Prof. Dr. Güniz Gürüz

Prof. Dr. Suzan Kıncal

Assoc. Prof. Dr. Deniz Üner

ABSTRACT

ENERGY OPTIMIZATION OF THE YANKEE-HOOD DRYER

Önel, Selis
M.S., Department of Chemical Engineering
Supervisor: Prof. Dr. Güniz Gürüz

August 2000, 130 pages

The Yankee-Hood dryer in 'İpek Kağıt' tissue paper mill is evaluated since it is the gargantuan energy consumer. Mass and energy balances are set and optimization studies are made in order to achieve the desired production rate whilst keeping the drying parameters within limits at the minimum energy costs.

The approach to solve the problem is to develop a steady state analytical model. The complicated drying system is simplified as the overall and sub systems. Material and energy balances are set up for each system. Data of machine parameters at several paper grades are collected at the mill during production. Material and energy balance equations are solved with the available data for the unknown parameters and for the determination of the drying parameters most effective on energy consumption. The critical drying parameters are the air supply velocity, wet- and dry-hood temperatures, and steam pressure in cylinder. Efficiency, defined as the ratio of energy required to evaporate the water to energy input through the system boundaries, is calculated as 28-30% for the overall system for different grades of tissue paper production. The overall

system involves the cylinder, burners and the hood. Efficiency at the heat transfer area that is between the cylinder and upper surface of the paper web is found as 80-85% for different paper grades.

Steady state rate of heat transfer to the wet sheet is analyzed considering the two-way mechanism, from steam through the cast iron shell and from heated air. The transfer of heat is eased in both mechanisms by the lightweight tissue paper that has a comparatively lower internal thermal resistance with respect to other types of paper products. Steam side is modeled considering different thermal resistances in series: Condensate layer, shell, shell-sheet contact, and paper sheet. These resistances are to the same order of magnitude, cast iron shell being the largest and paper sheet the smallest in value. Sheet-shell contact heat transfer coefficient is strongly dependent on sheet moisture content that is assumed to vary almost linearly due to the angular position on the Yankee dryer. Air side heat transfer is mostly affected by the temperature, humidity and velocity of the air that is blown on to the sheet. Calculations resulted out that rate of heat transfer from air side is 55-65% while that from steam side is 35-45% of their total for different paper grades indicating the dominance of air side on drying. Electricity is not used to directly dry the paper but is used to blow the air on to paper surface.

In general for the Yankee-Hood system, energy from gas, steam and electricity is about 45-55%, 35-45% and 10-15%, respectively. Electricity consumption should be minimized since it is found to be greatly effective on the total cost of drying due to the relatively high cost.

Keywords: Yankee-Hood Dryer, Paper Drying, Conduction, Energy Consumption in Paper Drying

ÖZ

YANKEE-HOOD KURUTUCUSUNDA ENERJİ OPTİMİZASYONU

Önel, Selis
Yüksek Lisans, Kimya Mühendisliği Bölümü
Tez Yöneticisi: Prof. Dr. Güniz Gürüz

Ağustos 2000, 130 sayfa

Yankee-Hood kurutucusu harcanan enerji miktarı açısından kağıt makinasının en önemli bölümüdür. Sürekli artan enerji fiatları sonucunda, hem ipek kağıdı makinasının en verimli halde çalışmasını hem de kağıt kalitesini sağlamak bakımından, uygun çalışma koşullarının belirlenmesi büyük önem kazanmıştır. Bu çalışmanın amacı 'İpek Kağıt' kağıt fabrikasındaki Yankee-Hood kurutucusunu incelemek ve kurutma değişkenlerini en az enerji tüketimini sağlayacak sınırlar içinde tutarak hedeflenen üretim hızını sağlamak için optimizasyon çalışmaları yapmaktır. Diğer değişkenlerin de kurutma ve kağıt kalitesi üzerindeki olası etkilerini açıklayabilmek için sürecin ayrıntılı olarak anlaşılması gerekmektedir.

Bu çalışmada sistemin yatışkın durum analitik modeli geliştirilmektedir. Karmaşık kurutma sistemi, tanımlanarak basitleştirilmiş ve ana ve yan sistemler olarak sınıflandırılmıştır. Her sistem için madde ve enerji denklikleri kurulmuştur. Kurutma makinası değişken verileri, fabrikada üretim sırasında, değişik gramajlarda ürünler için kaydedilmiştir. Kütle ve enerji denklikleri, bu veriler kullanılarak bilinmeyen değişkenlerin hesaplanması ve enerji tüketiminde en etkili kurutma degişkenlerinin belirlenmesi için çözülmüştür.

Sistem üzerinde uygulanan toplam kütle ve su denklikleri tutarlı bulunmuştur. Analiz sonucunda kritik kurutma değişkenleri, hava besleme hızı, yaş- ve kuru-haube sıcaklıkları, Yankee silindir hızı ve silindir içindeki buhar basıncı olarak tespit edilmiştir. Suyu buharlaştırmak için gereken enerji miktarının sistem sınırlarından giren enerjiye oranı olarak tanımlanan toplam verimlilik değeri, farklı gramajlarda ipek kağıdı üretimi için %45-55 olarak hesaplanmıştır.

Yatışkın durumda kağıt yüzeyine aktarılan ısı, silindir içindeki buhardan ve yüksek sıcaklıktaki havadan olmak üzere iki yönlü bir mekanizma öngörülerek incelenmiştir. Buhar tarafı, yoğuşmuş buhar tabakası, silindir kalınlığı, silindir-kağıt yüzeyi ve kağıt olmak üzere seri halde farklı dirençler öngörülerek modellenmiştir. Bu dirençlerin büyüklüğü, kağıdınki en küçük olmak üzere, 10^{-4} $W/m^2 \cdot K$ seviyelerinde bulunmuştur. Kağıt nem miktarının, Yankee üzerindeki açısal konuma göre, doğrusal bir şekilde değiştiği varsayılmıştır. Silindir-kağıt yüzeyi ısı aktarım katsayısı, kağıt nem miktarının bir fonksiyonu kullanılarak hesaplanmıştır. Hava tarafı ısı aktarımını en fazla etkileyen değişkenlerin yüzey üzerine üflenen havanın sıcaklığı, nem oranı ve hızı olduğu belirlenmiştir. Hesaplar sonucunda, hava tarafından ısı aktarım hızının her iki tarafın toplamının %55-65'i iken buhar tarafınınkinin bu toplamın %35-45'i olduğunun bulunması kurutmada hava tarafının önemini göstermektedir. Bu sistemde elektrik enerjisi kağıdı doğrudan kurutmak için değil; sıcak havayı kağıt yüzeyine üflemek üzere kullanılmaktadır.

Genel olarak Yankee-Hood sisteminde toplam enerji kullanımı %45-55 gaz, %35-45 buhar ve %10-15 elektrik tarafından gerçekleşmektedir. Elektrik enerjisi tüketimi çok daha pahalı olması ve toplam kurutma masrafı üzerindeki farkedilir etkisi açısından en aza indirilmelidir.

Anahtar Kelimeler: Yankee-Hood Kurutucusu, Kağıt Kurutma, Isı Aktarımı, Kağıt Kurutmada Enerji Sarfiyatı

ACKNOWLEDGMENTS

My deepest gratitude is to my supervisor Prof. Dr. Güniz Gürüz for all her guidance, motivation and tolerance she provided during the course of my masters study. She has always reassured me especially during the last year in my masters study, which has been the busiest and most apprehensive and ambiguous time period in my life-time due to some vital decisions I took upon both my academic and personal future. I have always respected her with my deepest sincerity.

I, also, would like to show my appreciation to all the professors in Chemical Engineering Department whom I deeply esteem and thank for their great appetite in shaping the Chemical Engineer candidates with very good instructions and strong knowledge. Thus, making the Chemical Engineering Department of Middle East Technical University a very good and special place of science.

I present my thanks to the 'Selüloz ve Kağıt Sanayii Vakfi', the pulp and paper foundation of Turkey and its members under the name of its current president Erdal Sukan, for their support with this thesis. They have put forward a great step in industry-university relationships by bringing together the industry and the university and providing the necessary occasions so that both may benefit from each other.

On the occurrence and continuation of the industry-university relationship, it is also my thanks with my regards that I would like to present to Prof. Dr. Canan Özgen, the previous head, and Prof. Dr. Timur Doğu, the current head of the Chemical Engineering Department.

It was great pleasure to spend some several days and then several weeks at 'İpek Kağıt Sanayi ve Ticaret A.Ş.' tissue paper mill in Yalova. I did not only meet the requirements to my thesis study, but also breathed the sincere ambience of the

mill. It would not only be my thanks but my appreciation, too, to the General Director Dr. Baki Gökçümen and the Director Sertaç Nişli of this model mill. I am grateful to the Paper Machine II Process Manager Recep Parlak and the Process Engineer Oktay Orhan. I first had to get to learn and know the mill and the drying system. Then I had to collect data in order to use in the calculations. In the meantime, I was provided with the necessary information and privilege that I could reach the answers to my questions. I thank the directors and employees for all their help and kindness.

I thank the ICHMT (International Centre for Heat and Mass Transfer) Secretariat for their understanding. I have worked as an assistant at ICHMT since 1998.

My family is worth of lots of gratitude for their great encouragement, moral support and patience during my uneasy times.

Finally, thank you my husband, Berker Evren, to whom I got married on the 22nd of July, exactly one month before the approval of my thesis. Thank you for being a supporter in my every step and keeping continuous interest in my thesis subject.

From the heart, to the most precious of mine...

TABLE OF CONTENTS

LIST OF TABLES

TABLE

LIST OF FIGURES

FIGURES

LIST OF SYMBOLS

CF : Creping factor (%)

CPa : Specific heat of air (kJ/kg·K)

CPng : Specific heat of natural gas (kJ/kg·K)

CPp : Specific heat of pulp (kJ/kg·K)

dng : Density of natural gas at the present T8 and P8 (kg/m^3)

E13 : Exhaust air on hood exit stream 13 (tons dry air/h)

h# : Humidity of stream # (g water/kg dry air)

H# : Enthalpy of stream # per hour (kJ/h)

HgT51 : Enthalpy of water vapor at cylinder exit at saturation temperature T51 (kJ/h)

HlT51 : Enthalpy of liquid water at cylinder exit at saturation temperature T51 (kJ/h)

HP50 : Enthalpy of steam at the inlet of cylinder at pressure P50 (kJ/h)

HT21 : Enthalpy of water vaporization at T21 (kJ/h)

m21 : Grammage of product paper on Yankee exit stream 21 (g/m^2)

Mbt : Amount of blowthrough steam (kg/h)

Mcy : Amount of steam condensated in the Yankee cylinder per hour (kg/h)

Mi : Rate of net mass transfer through system boundaries (kg/h)

Midh : Rate of mass infiltration by the dry side hood (kg/h)

Miwh : Rate of mass infiltration by the wet side hood (kg/h)

Mms : Amount of motive steam (kg/h)

Mp# : Amount of solid pulp fiber in stream # (kg/h)

Msy : Amount of steam leaving the Yankee cylinder as steam per hour (kg/h)

MWng : Molecular weight of natural gas (kg/kgmole)

NG# : Volumetric flow rate of natural gas in stream # (m^3/h)

P50 : Pressure at stream 50 (bars)

RDng : Relative density of natural gas at 288 K (15°C) and 1.03125 bar

T# : Temperature of stream # (K)

Tref : Reference temperature (K)

Trxn : Temperature at the exit of combustion rooms at which reaction takes place (K)

VR : Reel velocity (m/min)

VY : Yankee velocity (m/min)

w : Width of paper on Yankee (m)

W# : Mass flow rate of water in stream # per hour (kg/h)

Wa : Mass flow rate of water entering the system within fresh air (kg/h)

Wc : Rate of water produced by combustion of natural gas (kg/h)

Wr : Rate of overall water removal (kg/h)

Wrdh : Amount of water removed by the dry side hood (kg/h)

Wrwh : Amount of water removed by the wet side hood (kg/h)

x# : Water percentage on mass basis in stream #

α : Fraction of net mass transferred through system boundaries in wet side

β : Mass fraction of net water transferred through system boundaries in wet side

λd : Mass fraction of stream 18 circulated back to the dry side in stream 19.

λw : Mass fraction of stream 12 exhausted in stream 13.

CHAPTER 1

INTRODUCTION

The Yankee-Hood dryer is an extremely energy intensive section of the paper machine, which makes it the focus of crucial interest and studies. Massive dehydration process takes place in the dryer. As a consequence of continuously increasing energy costs, determination of the proper operating conditions is essential to operate the tissue machine in the most efficient and economic means while ensuring paper quality.

The pulp and paper industry, even with modern technology, ranks forth behind chemicals, steel, and petroleum in energy consumption, and is the leading industry in terms of energy expended during drying operations [1]. The dryer section of a typical tissue paper machine removes via evaporation the final 60% of the water originally present in the fiber/water suspension. This drying process accounts for approximately 80% of the total energy consumption of the paper machine. It corresponds to nearly one-third of the energy consumption in an integrated paper mill [2].

Yankee-Hood dryer is the heart of the tissue machine as mentioned by many scientists. It plays part in pressing, drying and creping of the paper web. It consists of a steam-heated cylinder and a high-velocity air impingement hood. The cylinder conveys the sheet from the press roll to a creping doctor, transferring heat continuously to the sheet. The cylinder shell must be thick enough not to crack, able to conduct heat well and sufficiently hard to resist the pressure inside. Part of the cylinder is wrapped by a hood, blowing drying air at high velocity against the sheet. The main part of the drying air is recirculated. The evaporated water is swept away

by the exhaust air. In order to calculate the evaporation efficiency, it is necessary to be familiar with the heat transfer coefficient from the inside of the cylinder to the paper and the heat transfer from the drying air to the paper. In general, the drying air has become more effective on drying such that about 50-60% of the drying energy is from the hoods and 40-50% is from the steam-heated cylinder.

Operating parameters such as the blowing air temperature and velocity as well as the steam pressure in the Yankee cylinder reveal diverse influences on the consumption of gas, steam and electric power. Nevertheless, the inflated energy costs have increased the necessity that the air system is aerodynamically well engineered and both the air and steam systems are thermodynamically optimized. Steam heated cylinder and high velocity hood should always be kept in balance. This is a difficult task to perform while aiming high product quality since changes in the drying conditions of one lead to changes in that of the other. Gigantic amount of air, approximately 15 tons/h, enters the system. Air balance of the system must not be disturbed while maintaining balanced flow across boundary in terms of controlled infiltration into the system and spill out of the hood.

The dryer is sometimes the production limit of a paper machine and can impact the profitability [3]. However, it is not an attractive proposition to decrease the energy required per unit mass of dry product by adding new drying equipment and increasing the capacity due to the high investment cost. There are a large number of factors or parameters that affect the dryer performance by means of energy consumption and product quality. Factors starting with the raw material, type and life of the felt, which determine the web moisture content and the vacuum level before the Yankee cylinder, Yankee cylinder crown, shell thickness and its distance from the hood, product type and basis weight, all designate the quality and drying energy per unit mass of product. Consequently, tissue paper drying is a complex and complicated process. Drying parameters all interact with each other. It is difficult if not impossible to discover the dependencies of these parameters without a mathematical model. Therefore, quantitative understanding of the effect of these variables and their interaction is required in order to optimize the drying process in a scientific way.

A very live example of the seemingly simple production, but indeed the very intricate unit operations of tissue paper is at "İpek Kağıt Sanayi ve Ticaret A:Ş.", a leader tissue paper producing company of Turkey placed in Yalova. There are three operating paper machines in the mill, the third of which has very recently started. The thermal drying section in each paper machine is composed of the Yankee cylinder and the hood dryer. The first machine is thirty-one years old, rather simple and equipped with older machinery, which are controlled manually with the addition of some automatic control improvements recently. Each part of it and its operation is very well identified and understood by the mill. It has probably reached its maximum production through years. However, the second paper machine, which is the case of the present study, is a modern, mostly automatically controlled, complex machine. It is investigated in terms of the net rate of overall heat and mass transfer within the system boundaries, the effects of the most important of the many operating parameters on each other and the corresponding results on energy consumption.

In the present work, the Yankee cylinder and the hood with the burners are the only parts of the drying section in the second paper machine to be considered. Actually, the drying section of the paper machine consists of mechanical and thermal drying sections. After the headbox, the wire and felt systems with the press roll make the mechanical drying by vacuum or suction. Following, the Yankee cylinder, hood and the burners are responsible for the thermal drying, finally the product being winded at the reel. Each of the parameters within these processes plays great part in production. Nevertheless, being the most energy consuming section of the paper machine, the thermal drying section is worth studying.

Accordingly, the objectives of this study have been to

- Collect data for different paper grades at İpek Kağıt mill site
- Use these data to perform overall mass and energy balances on the overall system and the subsystems of the Yankee Hood dryer
- Solve the set of equations for the unknown parameters

- Investigate the two way mechanism of heat transfer from steam and from air on to the paper web and determine the thermal resistances to heat transfer

- Study the interaction and effects of drying parameters on system efficiency

- Optimize the energy utilization of the dryer with respect to the most vital drying parameters.

CHAPTER 2

PAPER AND DRYING

2.1 Early History of Pulp and Paper

It is a fact that paper and paper products have occupied a great place in modern life. Even though there were not so many types of paper during the times of early civilizations, literally thousands of different paper types and grades, and paperboard are made today. Since its invention, paper has played a great role on the development of civilization through its influence on communication. The earliest surfaces upon which people communicated such as stone and clay tablets, wooden slates, metal plates, sticks, and strings has much influenced the use of paper. They have been inferior to paper in terms of transportability, surface quality and efficiency. Some other common early writing surfaces are bricks, lead sheets, brass sheets, bronze sheets, pieces of wood, large tree leaves, inner bark of trees, vellum, parchement, and papyrus [4]. In addition to the writing surfaces, cloth material has also influenced the use of paper but in a more household used way. Cloth material has especially been inferior to paper used for sanitary purposes such as toilet and facial paper, napkins, sanitary napkins, towels and wipers due to its properties such as liquid absorptivity and softness.

Paper has derived its name from the reedy plant, papyrus. Egyptians invented papyrus around 3000 BC. They kept papyrus-manufacturing technology as a trade secret, a know-how, and prevented the dissemination of the knowledge. The exact date of the invention of paper and papermaking is not known. However, a Chinese Minister of Agriculture, Tsai Lun, is given credit for the invention of papermaking. Tsai Lun, in year AD 105, beat silk and mulberry bark together to prepare pulp and

screened the fibers from water with a bamboo mold. The basic technique was kept secret in China until the year AD 807 as had done the Egyptians for papyrus-manufacturing technology. Samarkand is known as the first place outside China to make paper in year AD 751. The art of papermaking then spread through Central Asia, Asia Minor and Egypt and in to Europe. In Europe, it was quite well established by 1400. It is interesting to note that, travellers had reported use of toilet paper in China in year AD 875 [4].

2.2 Pulp and Paper Processing

Pulp is the previous form of paper just before being dried and taking the product form. Considering the primitive methods, paper is traditionally defined as the felted sheet of fibers formed on a fine screen from a water suspension. However, the papermaking process is not that simple today, namely production of paper is dependent on the production of pulp. Pulp is a material prepared by chemical or mechanical methods, primarily from wood but also from rags and other fibrous materials, into a structure appropriate for making paper and other cellulose based products [5]. The most important sources of fiber are the forests of the world. More than 90% of the total world production of fiber comes from wood [4]. In short, paper is always made from a fibrous material.

Papermaking, actually, is a long, costly process and shows many distinctions within the intermediate steps depending on the type of the product. However, the basic and most common steps to papermaking can be stated as follows:

- The logs and wood product residuals are reduced into smaller pieces of relatively uniform chip size.
- The fiber source is pulped and bleached for white papers.
- The pulp is washed and screened.
- The pulp is refined to insure the fibers are separated from each other and roughen the surface for better fiber bonding.
- A paper web is formed from a dilute pulp slurry letting most of the water drain by gravity.

- Additional water is pressed from the web.
- The remaining free water is removed by evaporation to give the product [5].

Pulping operation involves the selection of raw materials and the liberation of fibers. Then in stock preparation, fiber modification and furnishing takes place. Papermaking starts with the performing considerations such as cleaning and refining processes, continues with forming and consolidation of the web and the product is formed after drying. In web modification operation, the surface of the web may be modified either chemically or physically depending on the type of the product. Finally, during the converting operation, the product takes its final form with the correct design, size and package ready to enter the market.

2.3 Structure of Paper

Paper is a complex matrix of wood fibers. It has an extremely anisotropic porous structure. The fibers are oriented with their axes roughly parallel to the web surface and they are randomly located in that plane [6]. Fibers are first suspended in water with relatively small quantities of non-fibrous additives such as fillers, sizing agents, retention aids, wet strengthening agents, colors and etc [7]. The concentration of the fibrous suspension, named as "consistency", as it passes on to the web formation section, is between 0.5-1.5% for paper and board and between 0.1-0.3% for tissue paper.

Vegetable fibers make the 98% of the fibrous raw materials used in pulping and papermaking operations. Vegetable fibers consist of fruit, stem and leaf fibers. Corn and cotton are plants that have fruit fibers. Wood fibers and grasses such as cereal straws, bamboo, esparto and reeds are stem fibers whereas leaf fibers can be obtained from pineapple and sisal.

Non-vegetable fibers are used as the remaining 2% of the total fibrous materials. There are man-made or artificial fibers, mineral fibers and animal fibers. Man-made fibers involve regenerated cellulose (viscose rayon), polyamide (nylon),

polyacrylic (orlon), and others. Mineral fibers involve asbestos and glass, and animal fibers involve wool.

2.3.1 General Structure of Wood Fibers

Wood is classified as softwood or hardwood. The softwoods are the sources of all long-fiber wood pulp. They have needle-like or scale-like leaves, appear to be evergreen and are the largest trees in the world today. Hardwoods are the source of short-fiber wood pulp. They are broad-leaved and largely deciduous, even though some may retain their leaves for one or more years especially in subtropical or tropical zones. Altogether, 30,000 hardwood and 520 softwood tree species are known.

Fibers are cells of vegetable matter that geometrically have a tubular structure. Fiber walls are made up of various amounts of cellulose. Fibers from different sources have different physical properties and chemical composition. The most apparent differences in physical properties are length, width, wall thickness, and lumen or cavity diameter. Chemically, fibers are made up of three main polymeric constituents found in wood, namely cellulose, hemicellulose and lignin. Generally, the wood fibers that have a length between 0.5 mm and 5.0 mm are considered to be more important. Fiber length of native softwoods vary from 3 to 5 mm while that of hardwoods vary from 1 to 2 mm.

2.3.2 Porous Structure of Paper

As stated by Polat et al. [6], the size of the pore spaces range from gaps between fibers to interstices of molecular dimensions. Paper porosity can be the most important single structural feature of the end product, for example high porosity is required for sanitary and filter paper. Some other products require low porosity. Low porosity can be achieved by coating, impregnation, or lamination.

The raw material and the paper making process all influence the porous structure of paper. The raw material involves the type of wood, either soft wood,

hard wood or a mixture, and the type of pulping process. There are many types of pulping processes such as mechanical, stone-ground-wood, refiner-mechanical, semi-mechanical, kraft, sulfite, and chemi-thermo-mechanical pulping processes. Papermaking processes also play a great part on the porous structure of the web while this structure is being developed starting from the refining of the pulp to the formation, drainage and drying. Polat et al.[6] states that the drainage of a freshly formed web is a function of its water permeability. Dewatering by suction and pressing depends on both water and air permeability of the web. The very complex heat and mass transfer processes that take place within the web during drying depend strongly on many structural properties of paper. These structural properties of paper include air permeability, water transport characteristics, porosity, specific surface area, and pore size distribution of the paper. For example, in through drying, flow rate of air across the paper, which is a function of the paper permeability, is the primary variable that affects the drying rate. Rates of heat and mass transfer between the blowing air and the fibers are, as a result, strongly affected by the fiber matrix.

2.4 Tissue Paper Production

It is a fact that the tissue grades are seemingly quite simple and few, but the manufacturing methods are diverse [8]. Toilet and facial tissues are similar, but not truly identical in either their manufacture or their processing and packaging. Napkins can also be made and processed in a variety of ways. Toweling includes both the kitchen towels sold in rolls and the white or brown towels folded to fit dispensers. Generally, the very basic manufacturing processes are at least similar to all grades and only some very special considerations for a special grade may differ from the norm.

2.4.1 Pulping Operations

Softwood sulfite pulp has been the preferred raw material for most tissue and towels because of its softness. The sulfite process produces a softer, more flexible fiber, which gives paper the same characteristics. For towels that require greater

strength, kraft or high-yield pulps may be preferred. With the pollution problems faced by the sulfite process, there has been a shift to craft and recycled fibers for tissue and towel grades.In general, the brown-colored towels can be assumed to be either kraft or high-yielded pulps, and the white towels and tissue bleached kraft, sulfite or recycled fibers. It is difficult to detect the use of recycled fibers in these grades, since fairly white, clean waste grades are used and impurities are removed in the mill. Hardwood fibers have the ability to contribute bulk and softness to paper, but they are not entirely satisfactory for use in these grades. For lightweight tissue, the small hardwood fibers would not be retained well on the wire and would be lost during the formation of the web.

2.4.2 Stock Preparation

Fibers require refining to develop the bonding ability needed to make strong paper. Bonding, however, creates a more dense, brittle and generally less soft sheet. Accordingly, the tissue and toweling manufacturer must balance strength requirements against softness requirements. Lightly refined softwood fibers can satisfy both requirements. Wet-strength agents, which can help the tissue or towel retain strength when wet, are an obvious need for towels and facial tissue. Urea and melamine formaldehyde have traditionally been used for these applications. However, their use can affect softness and contribute to environmental concerns, so they must be used sparingly.

2.4.3 Papermaking Operations

2.4.3.1 Formers

Within the several types of formers, especially Fourdrinier and twin-wire machines are used for lightweight paper grades. The forming section for lightweight grades tends to be shorter than normal for printing or writing grades, since the stock tends to drain faster. There is a large breast roll and the stock is delivered to the wire above the breast roll to drain the web quickly or the web is formed around a solid

forming roll squeezed by the wire. The high-speed forming can benefit the web by freezing the turbulent flow coming from the headbox, or it can hurt the web by removing too many fibers and fines from the web. The exact location of the point at which the stock is delivered to the wire varies from mill to mill. Drainage on the wire is assisted by either large table rolls or foils. The web is lifted from the wire by a pickup felt since the web is too light and fragile to be able to sustain a free draw at this point. The same pickup felt delivers the web to the Yankee dryer. Actualy, the way the web is delivered to the felt differs from machine to machine. Additional equipment to remove water from the web is generally not needed for tissue but could be used for towelling. The older large headboxes are not being used anymore with the fast formers. It is stated by Kline [8] that the reduction in the length of the forming section and contomitant fast drainage goes well with the turbulent-flow nozzle headboxes. These headboxes can be designed with two compartments so that two different stock furnishes can be laid on the wire at the same time. The strength of the web is improved by the use of long softwood fibers, but softness is improved by the use of shorter secondary or hardwood fibers. By forming a two-layer web, the two types of fiber can be combined. By putting them in the layer next to the wire, the longer fibers help retain the short fibers on the wire in the forming section of the machine.

2.4.3.2 Presses

In tissue, the need for pressing to develop strength through bonding must be balanced against the increased density that can be created. Towels and napkins can tolerate more pressing perhaps, but the balance between strength and bulk cannot be forgotten. The press sections tend to be rather simple and are generally double felted. By pressing the web between two felts, the density is not increased too much and the web will continue to adhere to the felt. If the web is to be dried with a Yankee dryer, as most tissue and related grades are, the web is carried through the press section on the pickup felt and applied to the dryer by that same felt.

The need for water removal in the press section without actually pressing the web has led to the development of the through dryer as shown in Figure 2.1. In this

device, the web and felt or carrying wire are passed around a porous-surfaced roll, which permits hot air to be forced through the web. This helps evaporate water without increasing the density of the web. The device may be limited in its ability to remove water and may not be able to dry the web completely. Through dryers are in use either before or after Yankee dryers in today's tissue mills.

2.4.3.3 Dryers

In major, Yankee drying cylinders are used for the drying of lightweight paper. The primary advantages of the Yankee are: (1) the web is not made more dense, (2) the web need not be strong enough to make it through the open draws of the normal dryer, and (3) the web can be creped. The Yankee is represented by the drawing in Figure 2.2. At the lower left, the web is pressed against the surface of the dryer can, to which it adheres due to the moisture it contains. The web cannot be too dry, or it will not adhere properly. At the same time, the web must not be too wet or it will not be able to be dried in one pass around the dryer. Dryer can be assisted by the use of hot-air caps, which blow hot air on the outside surface of the web. These caps need to be installed in such a way that they can be slid back away from the Yankee for maintenance.

If the web is allowed to dry completely, it will pop free of the can and the product is machine-glazed paper. If the web is scraped from the cylinder while it is still stuck to the cylinder, the web is distorted into long wrinkles in the cross-machine direction, an operation called creping. An essential part of the operation is the removal from the creping doctor.The web is pulled away from the doctor at a speed designed to remove some of the crepe, but not all of it. The web still is not too strong and cannot sustain a very strong pull without breaking. This particular part of the machine is the problem point where web-breaks often occur. The creping operation does not necessarily make the web weaker; in fact, the increase in extensibility is a plus factor in its strength. Creping improves the water absorbency and softness of the web by increasing bulk.

Noncreped papers may be dried by Yankee dryers if they are strong enough, or may be dried by Yankee dryers without using the creping doctor. The Yankee dryer

will lead to a higher bulk in the web even though the creping doctor is not used. Many of the noncreped grades are embossed to improve absorbency and softness.

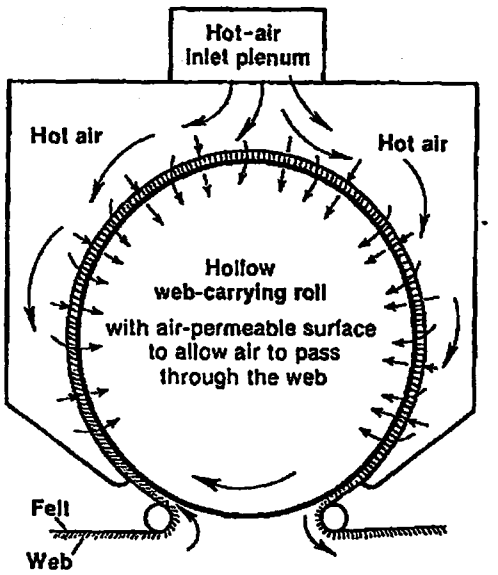

Figure 2.1: Through Dryer for Drying Tissue [8]

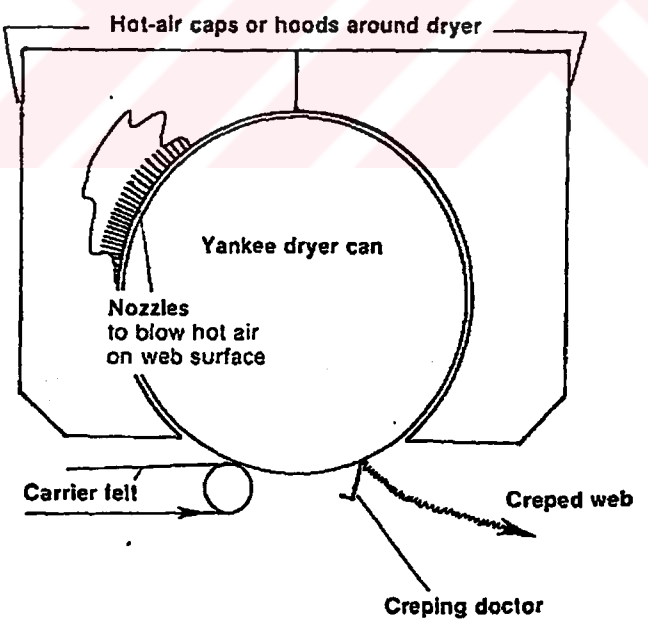

Figure 2.2: Yankee Dryer for Tissue [8]

2.4.4 Converting Operations

Most tissue and related grades are converted into consumer products at the plant at which they are manufactured. The reason for this is simply that the soft paper rolls made on the paper machines are too bulky and difficult to handle to be transported any great distance.

2.5 Yankee-Hood Dryer

2.5.1 General

In the manufacture of creped paper grades, such as toilet and facial tissues, many varieties of paper napkins, towel, wadding for sanitary padding and other special products, high speed Yankee drying cylinders are used. Yankee cylinder is most commonly made of cast-iron. A Yankee consists of a shell, two heads, one centerstay, two journals and the apparatus for condensate extraction, which is fixed to the centrestay as shown in Figure 2.3. Upper section of the cylinder is wrapped by a hood that blows hot air at high velocity on to sheet surface, sucks back and exhausts it. Yankee cylinder is characterized as the heart of the paper machine in the tissue industry because of the high contact-drying rate. The principle function of the cylinder with its high velocity impingement hood is the evaporation of water in the sheet of paper and the evacuation of water vapor formed in the drying process.

Generally, one or more pressure rolls are placed just before the Yankee cylinder to decrease the amount of water in the sheet while transferring it on to the Yankee cylinder. The sheet remains stuck on to the Yankee surface while being dried and conveyed to the creeping doctor blade which removes it. The cylinder surface is heated from inside by steam and from outside by air heated with natural gas and blown by electric power. The advantage of the system is that it enables high evaporation rates, but with the disadvantage of a relatively high-energy consumption

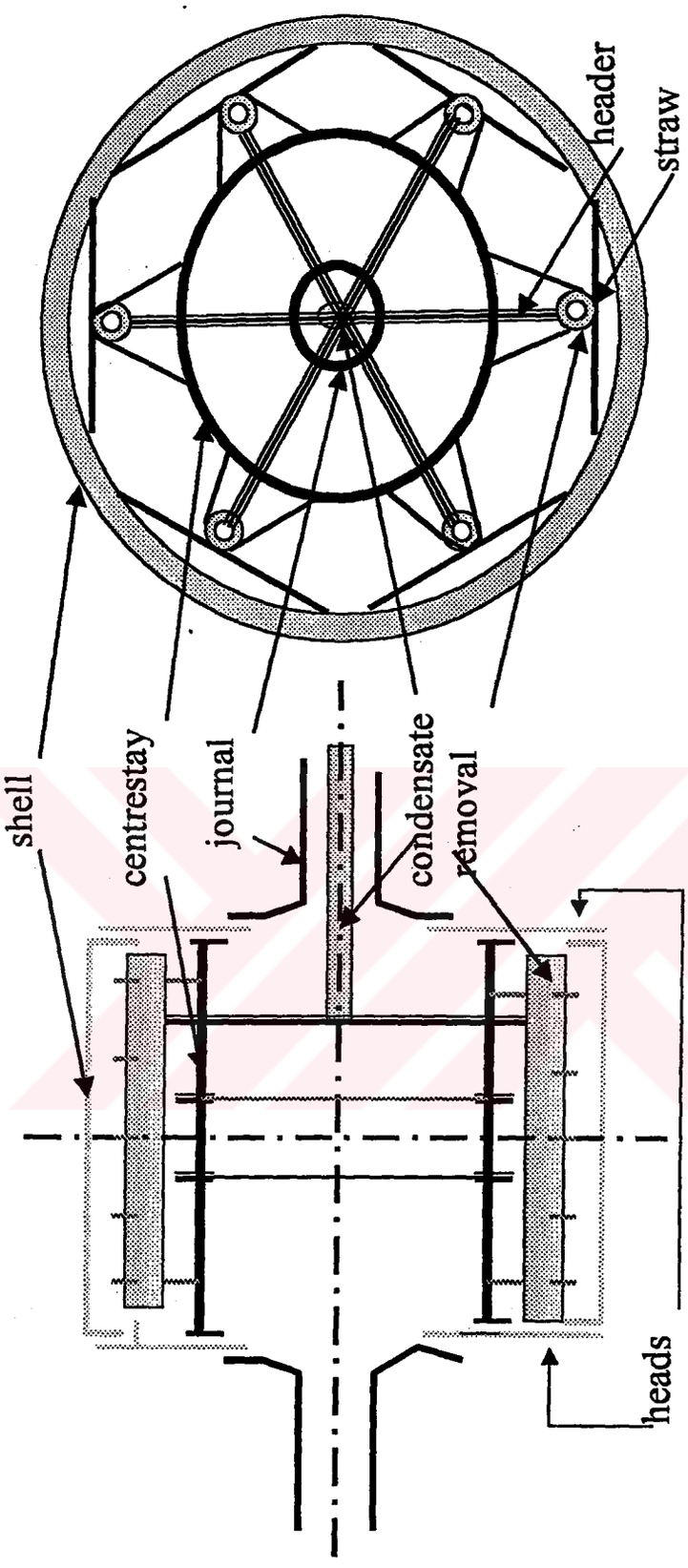

Figure 2.3: Construction of a Yankee Cylinder

rate resulting in high costs. Intuitively, it is not expected to achieve as high a drying rate with for example the machine glazed kraft paper as with lightweight tissue [9]. This is a result of the difference in the extent to which moisture is bound with in the web. Using the air impingement system, moisture in tissue and toweling is more readily available for rapid evaporation and removal. Therefore, the air impingement drying method has made it most important contribution with tissue paper.

2.5.2 The Hood

A high velocity, high temperature dryer hood is located around the outside circumference of the Yankee cylinder to further increase the drying rate. Jets of hot air are impinged on the sheet surface at temperatures about 500°C and velocities around 120 m/sec [10]. After impingement on the sheet surface, the spent air and the evaporated moisture are collected with the air and a large portion of the flow is recirculated in the air system. A cutaway view of a hood, namely air impingement dryer is presented in Figure 2.4.

There are number of devices which can be utilized in tissue drying for cross machine moisture correction. Many of the dryer hoods involve cross machine dampers, which can be used to modulate the airflow. These are normally spaced on about 0.5-meter intervals. This method reduces average drying capacity and efficiency of the hood, because only the parts with dampers fully open are working at full capacity [11]. Other devices include profiling steam boxes located just upstream of the pressure roll and infrared type units are also in use.

The most important parameters of the hood design on drying are the nozzle configuration, the nozzle itself, and the drying distance. The nozzle configuration and the nozzle generate the drying force, i.e. the air to sheet heat transfer. Toivonen [12] studied the importance of the nozzle geometry by first equipping a Yankee hood with slot nozzles and then replacing them by round nozzles. As a result of the study, the round nozzles were found to be much more beneficial such that the air volume and the fan power were reduced by 30% for the same evaporation efficiency and problems like dust buildup were eliminated.

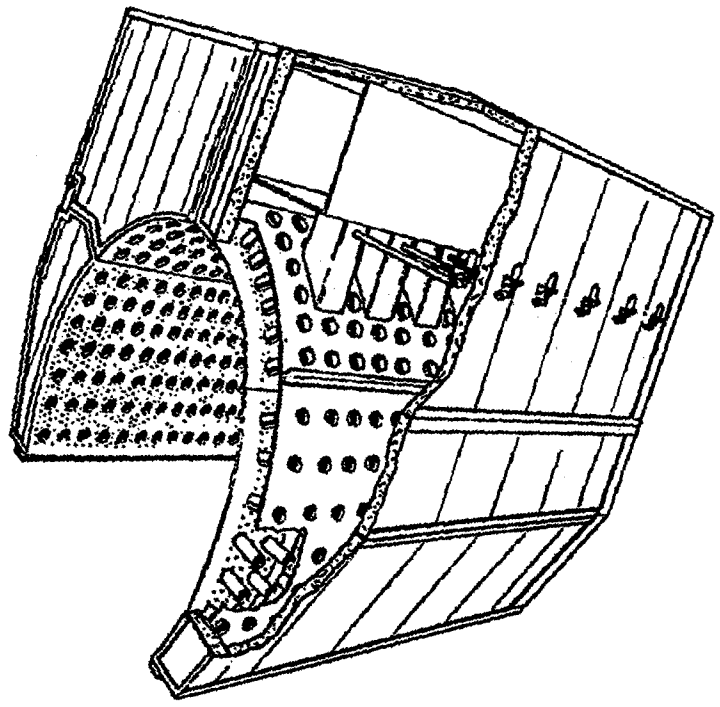

Figure 2.4. Air Impingement Dryer (Hood) [10]

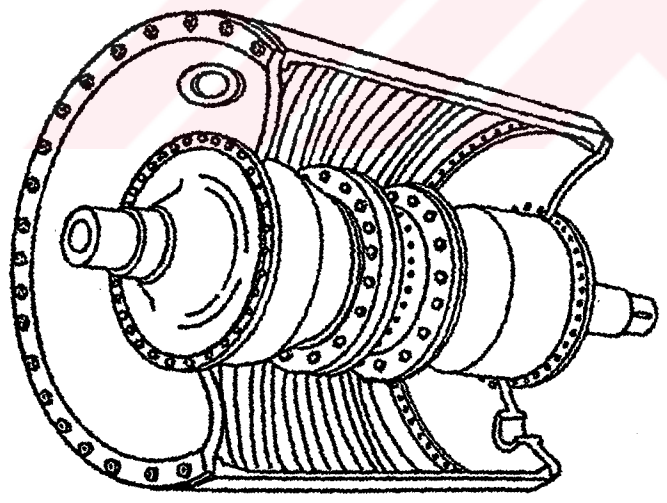

Figure 2.5. Ribbed Yankee Dryer [10]

The nozzle to sheet distance gains much importance as a consequence of a structural problem of the high temperature Yankee hood. The problem is that when the hood reaches the operating temperature, the toe moves away from the dryer. The size of this movement is very much dependent on how the hood design takes care of the existing thermal expansions of the hood. Unfortunately, movements of up to 50 mm can still be seen in the machines of today [11].

2.5.3 Steam Supply and Condensate Removal

Steam provides the dryer with heat by giving up its latent heat of evaporation and at the same time forming condensate. At high machine speeds, over 500 m/min, the condensate forms an almost even water layer on the dryer surface; this regime is called rimming. The transfer of heat takes place from steam to the condensate film and through the film to the metal. The heat transfer of the condensate layer depends on the machine speed and the thickness of the condensate layer according to Appel and Hong [13].

Practically, steam is used as the heating medium condensing on the inner surface of all paper-drying cylinders. Other heat transfer media such as special heat transfer oils have also been tried. These media have the advantage that high pressures are not required to accomplish high temperatures. However, steam is preferred since the best results are achieved with temperatures that are easily attainable with steam at reasonable pressures.

Most of the Yankee dryers being produced today are of the ribbed design as shown in Figure 2.5 [10]. Grooves are machined into the inside wall of the dryer shell. As heat is transferred to the tissue, the condensate collects in the grooves. Individual siphon tubes, placed in each groove, are used to take away the condensate. These dryers are very efficient from a drying viewpoint because heat no longer has to be conducted through the stagnant condensate layer. Heat is actually conducted around the condensate layer through the cast iron fins machined into the dryer wall.

2.5.4 Dryer Doctors

A drying doctor comprises a blade holder, a blade, and brackets to support the ends of the blade holder. The blades are placed around the cylinder such that there remains a certain distance and angle in between as shown in Figure 2.6. The angle between the blade and the dryer surface is obtuse on the side on which the dryer surface is approaching the blade, and acute on the side on which the dryer surface is leaving the blade.

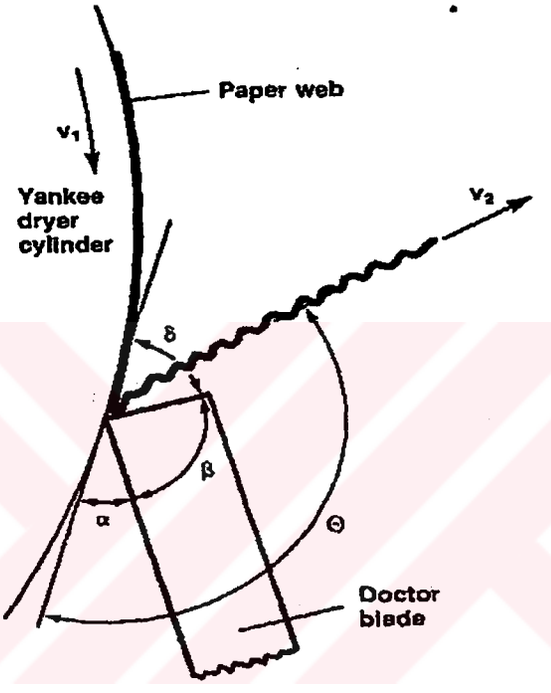

Figure 2.6: Creping Doctor Blade Geometry [14]

The material of the doctor blade must be chosen such that it will function with a minimum of wear of the dryer surface. Steel, bronze or plastic blades may be used. On one hand, a large dryer cylinder is very expensive due to its manufacturing, transportation and installation, so the wear problem should be handled with care. On the other hand, paper quality is greatly influenced by the condition of the dryer surface, so doctor blades should be used. A layer of dirt will impair paper quality especially for the lightweight paper products. It will also reduce the heat transfer rate and as a result, the drying capacity. The doctor blades will remove fuzz or dirt from

the dryer surface and prevent the sheet from wrapping the dryer cylinder, which is an advantage especially during breaks. However, the dryer surface wear caused by the oscillation of the blades would be outweighed if blades were not absolutely necessary.

CHAPTER 3

STUDIES ON HEAT AND MASS TRANSFER IN PAPER DRYERS

3.1 General

The operation of a Yankee dryer is a complex procedure. It is typically the largest energy user in the paper machine complex. The control of temperature, speed, and consistency of the pulp throughout the paper machine is very complex and has always been viewed as an art until computer control became available. Computer control has brought the advantages of fewer web breaks and faster as well as easier changing of one grade of paper to another. However, sudden great temperature changes of 150°C are not uncommon during start-up breaks, where a lot of energy is lost and the Yankee hoods face significant thermal stresses associated with the high temperature and prevailing static pressure. In order to prevent heat losses from the hood and to maintain safety, the hood is generally insulated with panels having mineral wool insulation and covered with pressure resistant steel.

Yankee hoods are designed for high speeds, temperatures, corrosion resistance, and high burner loads. It is mentioned by Schukov [15] that total burner loads are about 53 million Btu/h (56 million kJ/hr) and air circulation fans are driven by motors of up to 500 hp (377 kW, $1.34 \cdot 10^6$ kJ/h). World's largest Yankee Hood of the time (1989) at Flakt Ross in Montreal was designed to dry tissue paper at a speed of more than 1830 m/min. It is stated that efficient heat transfer at the dryer face is essential.

In the study of Schukov [15], typically the properties of the impinging air were in the order of 482°C temperature at the nozzle and a velocity of 142.25 m/h. Hood efficiency was 3955 kcal/kg of water evaporated, which he specified as the most efficient system available then.

It is stated by Schukov and Haberl [16] that two types of energy are consumed by the Yankee hoods: Electrical and thermal.

1. The electrical energy consists of the horsepower consumed in operating the fan motors. Consumption of electricity is relatively constant during operation and is approximately 15% of the total energy on a Yankee hood system.

2. Thermal energy supplied by the burners is consumed by:

- Raising the sheet temperature (Energy consumption is a function of production variables)
- Evaporating water from the sheet (Energy consumption is a function of production variables)
- Radiation and other losses from the hood and ductwork (Energy consumption is a function of temperature)
- Heating the make-up air from room temperature to supply temperature. Air system offers energy saving opportunity (Energy consumption is a function of flow of make up air)

Many attempts have been made to analyze the paper drying process both theoretically and experimentally. Most theoretical models contain critical assumptions that considerably simplify the heat and mass transport phenomena within the sheet during drying. Most of the existing simulation models assume variables such as temperature, moisture content, or thermal conductivity remain uniform through the sheet thickness, and that water fluxes are negligible. It is a general idea that better understanding of the transport phenomena in the paper sheet is needed to model the heat and mass flow through the paper accurately. All agree that a flexible model for the entire drying system could aid in the design and

maintenance of dryer systems, overall system efficiency, and improved product quality.

Seyed-Yagoobi et al. [17] worked on multi-cylinder drying considering each felt-covered cylinder in four phases. The first and third phases involved the paper and the cylinder, the second phase involved the paper between the cylinder and felt, and finally the forth phase was the paper web only. Internal dynamics of the drying process was studied and variations in sheet properties throughout the dryer section were characterized especially for temperature and moisture content profiles. Mass balance was used to calculate the moisture content distribution in the paper sheet. Energy equation included both the liquid and vapor migration and variations in sheet properties. The contact coefficient was calculated assuming the heat was transferred across a stagnant air gap, where it was a function of the interface temperature. The convection coefficient was calculated assuming flow over a cylinder. Temperature and moisture content profiles along the thickness of the paper sheet were studied for each cylinder.

As a result of the studies by Seyed-Yagoobi et al. [17], it was found out that except for the initial cylinder, temperature was higher inside the sheet than on the interfaces (top and bottom surfaces). At the end of the three phases in each cylinder, the temperature of the paper at the cylinder-paper interface increased due to the heat conduction from the dryer. The temperature at the air side was the lowest due to the heat being removed by evaporation and convection. By the end of the forth phase the temperature became higher within the sheet than on the edges with an exception of the initial cylinder. Inlet moisture distribution was assumed to be constant. As the web got in touch with the shell, moisture began to move from the heated side of the paper sheet to the middle of the sheet. Following the warm-up period, moisture content at the paper-air interface dropped due to evaporation. As the drying continued, moisture content at the cylinder-paper interface decreased sharply. Towards the end of the drying section, moisture content profile within the sheet was almost uniform.

Asensio and Seyed-Yagoobi [18], in their study of a theoretical model for the simulation of conventional steam-heated cylinder dryers, aimed to describe a model

of the drying process that can be used for process optimization. The model considered heat and mass transfer in a porous sheet during drying. The movement of water, water vapor migration within the sheet, moisture content and temperature profiles and effect of contact conductance on average evaporation rates were observed, sheet thickness and sheet porosity during drying were studied and the internal dynamics of the drying process were explained. Drying was specified in three distinct stages, that were, an initial warm-up period followed by a relatively constant rate period and a falling rate period.

It was noted by Asensio and Seyed-Yagoobi [18] that the change in sheet moisture content initially was negligible as the sheet entered the drying section indicating a warm-up period. High pocket humidity caused moisture from the ambient to initially condense on the sheet. After the warm-up period, that is, reaching a maximum, the average evaporation rate was observed to decrease gradually while the sheet was being dried. Moisture content started to drop continuously but not constantly. The reason is with constant dryer surface temperature, heat input into the sheet decreases as the sheet gets drier due to decreasing contact conductance at the paper/dryer interface. Towards the end of the drying process, the change in the moisture content decreased significantly and reached a constant. Sheet thickness was hypothesized to be of three layers: A layer of fibers, a layer of air, and a layer of water. Sheet at the end of the drying section contains very little water most of which is chemically bonded to the paper fibers. Therefore, the final sheet thickness was assumed to be equal to the bone-dry sheet thickness.

As a part of their study, Asensio and Seyed-Yagoobi [18], observed the average sheet temperature to initially rise abruptly and then continue to increase gradually until the last cylinder. The net water flux, initially, was slightly greater than the net vapor flux due to the high moisture content of the sheet. As the sheet warmed up, the magnitude of the water flux towards the heated surface increased. During drying, the net water flux decreased since there was less water present in the sheet and much of the water vaporized. In the middle of the dryer section, although the water flux towards the outer sheet surface decreased, the liquid appeared to be flowing equally to both surfaces. Water flew to the outer control volume and directly evaporated, that is, the net vapor flux quickly exceeded the flux for liquid water and

became the dominant drying mechanism. The sum of the water and vapor fluxes entering the surface control volumes was greater than the evaporation rate from these control volumes, indicating that some moisture accumulated in these outer surface control volumes located slightly inside the sheet. As the sheet dried, this moisture was removed since the net water and vapor flux rate was less than the average evaporation rate at lower moisture contents. However, the magnitudes of both water and vapor fluxes calculated by Asensio and Seyed-Yagoobi [18] were stated to be inexact due to the empirical correlations used for capillary pressure and apparent vapor diffusivity, respectively.

Effective web transport affects the speed of the paper machine as concluded by Wahren [19]. The known transport mechanisms that take place in the web during drying are capillary flow of liquid, diffusion, vaporization-condensation, and heat conduction. Ramaswamy [20] stated that during paper drying conduction, convection and radiation could take place but conduction and convection were the more probable mechanisms as radiation in a fiber mat could be expected to be negligible. He added that vaporization-condensation cycles, apart from contributing to mass transfer, might also contribute significantly to heat transfer.

Consequently, it was stated by Lehtinen [21] that when there was air inside the web in conventional (multi-cylinder) hot-surface drying, the net heat transfer locally due to the evaporation-diffusion-condensation process was of the same order of magnitude as the heat transfer by thermal conduction through the wet fiber matrix. He assumed that there are active heat pipes inside a drying paper web and these conduits are slightly open to the ambient at their cold end. He analyzed the performance of a simplified heat pipe conduit. His primary purpose was to study the difference between the operation of an intraweb heat pipe conduit when originally air fills the conduit with everything at 60°C, and when originally vapor fills the same conduit with the vapor at 100°C in equilibrium with the wet walls.

Lehtinen [21] explained the main conduit in the heat pipe had many smaller branches. Vapor from the main conduit moved easily to these branches and condensed there. Naturally, a pressure drop occurred between the main conduit and the condensation locality. It was assumed there was a hole at the far end of the pipe

opening into a large reservoir at a lower pressure such as the ambient. When there was air originally in the conduit, it hampered the functioning of the heat pipe. And if the temperature of the wet walls was lower, for example 60°C compared to 100°C, then vapor condensed more readily on the walls, keeping the pressure near the hot surface lower and thus causing more vapor generation there, near the hot end. In real application, important factors that interrupted the operation of heat pipe were collapse of the heated web layers just above the hot surface, and accompanying increase in density. The period was a few milliseconds at the most for the wall thickness (thermal mass) of a heat pipe conduit of length 0.1-0.2 mm had an effect on the total heat absorbing capacity of the heat pipe. After the few milliseconds, all heat pipes acted mainly as vapor conduits of high internal flow resistance.

It is stated, in conclusion, by Lehtinen [21] that the heat pipe mechanism and the thermal conduction mechanism transfer the total energy at about the same rate, as time approaches 1 millisecond. The heat-pipe mechanism, unlike the thermal conduction mechanism, transfers the energy to regions far from the hot surface into the web interior, whereas thermal conduction heats up only the immediate vicinity of the hot surface. However, at smaller time values (time starting at hot surface-web contact), the total energy transferred by the heat pipe is roughly ten times as great as that transferred by the conduction mechanism.

Polat et al.[6] and Bond et al.[22] showed that the state of bonding of water in the web did not affect dryness that is, the concept of critical dryness was not a characteristic at the molecular level but depended on the drying conditions. This according to Wahren [19] meant that there was no end to improvement of drying sections and there was potential for increased capacity.

3.2 Thermal Contact Conductance

Drying efficiency is very dependent on the contact conductance between the dryer drum and the paper web [18]. Estimates made by several investigators show that 35-75% of the total resistance to heat transfer in paper drying is encountered at the contact surface [23]. The adhesion of the fiber matrix onto the cylinder dryer is

very important in order to achieve the maximum possible rate of heat transfer at the cylinder paper interface while maintaining the quality of the paper. However, there is the risk of web burning at very high drying temperatures such as 700°C. If the web is loose on the steel plate, those parts easily get dark color or burn out totally. If the paper adheres properly to the surface of the steel plate, thermal contact is very good and heating up of the web to high temperatures is prevented [11].

Many studies have been done in order to clarify the dependencies and the magnitude of the contact coefficient in various types of paper machines for different types and grades of paper. However, Wilhemsson et al. [23] concluded that it is very difficult to determine an accurate temperature of paper surface during contact, so it is difficult to find a correct value of the contact coefficient.

Seyed-Yagoobi et al. [24] constructed an apparatus to determine the thermal contact conductance of bone-dry paper handsheet/metal interface and the effective thermal conductivity of handsheet samples. The effect of pressure on thermal contact conductance was studied and the effective thermal conductivity at various sheet basis weights was measured in their study. The overall joint conductance was defined as the sum of conductances of the handsheet, that is, the reciprocal of the heat transfer coefficient of the bulk material, and the thermal contact conductances of the upper and lower handsheet/metal interfaces in $W/m^2 \cdot K$. Bulk conductance was expressed as a function of the effective thermal conductivity and the paper thickness. The type of the handsheets used and the results are presented in Table 3.1 and it was concluded that:

- Handsheet thickness is logarithmically dependent on the applied pressure. Sheet thickness affects the overall joint conductance by changing the thermal resistance of the sheet.

- The overall joint conductance increases with increased pressure or decreased basis weight. A logarithmic relation exists between the overall joint conductance and the applied pressure while the conductance changes almost linearly with respect to the basis weight of the handsheet. In conclusion, an expression for the

overall joint conductance is a function of the applied pressure, handsheet thickness and the basis weight.

- At low basis weight, handsheet preparation results with smoother surface, making better contact with the metal. Sheets of lower basis weight make better contact with the surface improving the contact conductance.

- The contact conductance increases with increasing pressure or decreasing basis weight. As the applied pressure increases, the handsheet/metal contact area increases, resulting in better heat transfer across the interface.

It was stated that the values for contact coefficient were found to be lower when compared to the previous studies done by other scientists. The results of the thermal conductance and the contact conductance found by other scientists were summarized and tabulated by Seyed-Yagoobi et al. [24] as presented in Table 3.2. The reasons put forward were that the samples used were bone-dry and a completely dry contact zone would cause greater resistance to heat transfer than one that included a partial water interface. Besides, surface roughness of the handsheets might be greater than that of paper webs considered in other studies, due to limited pressing. Finally, contact coefficient increases rapidly at low basis weights and the basis weights considered in the study were greater than the basis weight of newsprint.

Conversely, the results of Seyed-Yagoobi et al. [24] for paper effective thermal conductivity were found to be higher when compared to the previous studies done by others. This may be due to the fact that determination of effective thermal conductivity is very sensitive to the predicted value of contact coefficient and handsheet thickness. Any decrease in the predicted value of the contact coefficient results in higher estimates of the effective thermal conductivity. Since the contact coefficient is found to be lower when compared to the results obtained in previous studies, it is logical to find the effective thermal conductivity relatively higher. In addition, effective thermal conductivity was found to increase with increasing density because of the reduction of air within and between the fibers of the sheet.

Table 3.1: Effective Thermal Conductivity and Thermal Contact Conductance for Different Types of Paper

Author	Paper Type	Dryer Type	Mach. Speed (m/min)	Drum Diam. (m)	Moisture Cont. (initial,final) (wet/dry basis) db* (%)	Basis Weight (db) (g/m^2)	Contact Pres. (kPA)	Interface Temp. (lower,upper) (°C)	Ave. Paper Temp. (°C)	Sheet Density (kg/m^3)	Effective Ther.Conductivity. (W/m·K)	Ther. Contact Conductance. ($W/m^2 \cdot K$)
Seyed-Yagoobi et al. (1992)	Bd bleached sth.mixed Kraft hands	Exp. App.		--	0	348.7-68.0	2.3 300	--	85	90 - 500	0.14 -0.7	97 – 200 146 – 452
Asensio et al. (1993)	Unbleached sth.pine handsheets .8sw+.2hw	Exp. App.		--	5, 50, 100, 150	90, 150, 300*	0.69-328	130, 40	85	137-1108*	0.06-0.54*	
Seyed-Yagoobi et al. (1992)	Paper & Fiberboard	Multi-Cyl			5-150 db 5-60 wb.	300	2.3	130, 40	85			240 - 380
				1.52	150 db, 6	300		100, 49.9	~90*	600		
Wilhemsson et al. (1996)	Fine paper Fluting Paperboard Newsprint Fine paper	Multi-Cyl.	708 600 454 1200 189	 1.83	121, 1.2 200, ~10 170, ~8-10 --, 8 db	77 133 213 48.8 132		80-120* 80-110* 80-100*	~90 ~95 85-105			500 300 400 500 1400
			>300		0						0.08	200-500

Table 3.2: Summary of Thermal Conductivity and Contact Conductance from Seyed-Yagoobi et al. [24]

Author	Paper Grade	Moisture Content (wet basis)	Pressure (kPa)	Heated Surface Temperature (°C)	Thermal Conductivity (W/mK)	Thermal Contact Conductance (W/m^2K)
Han &Ulmanen (1958)	Sulphite Pulp Handsheet	0%-67%	-	---	0.07-0.79[1]	794-1362[2]
Redfern (1963)	Bleached Sulfate	0%-70%	0.57-2.9	70-100	---	78-1078
Sunberg & Osterberg (1966)	Unbleached Sulfate	5%-23%	---	---	---	400-4500
Lau & Pratte (1969)	Newsprint	0%-70%	---	24-30[3]	0.027-0.195	---
Han (1970)	Tissue	wet	---	---	0.216[4]	2271
		dry	---	---	0.144[4]	1987
	Paper	wet	---	---	0.288[4]	1420
		dry	---	---	0.115[4]	1136
	Board	wet	---	---	0.577[4]	1136
		dry	---	---	0.072[4]	568
Kirk &Tatlicibasi (1972)	Bleached Sulphite[6]	6.7%-7.9%	0	---	0.084-0.117	---
Kerekes (1980)	Newsprint					
	uncalendared	7.4%	---	72.5-78	0.127	875
	calendared	7.4%	---	68-73.5	0.169	1610
Lee & Hinds (1981)	Bleached Douglas Fir Kraft	0%-55.6%	2.8	105	0-0.57	226-475
Byrd (1982)	Linerboard	40%	13.8	121-288	---	191-1565[5]
		65%	13.8	121-288	---	205-1806[5]
Burnside &Crotogino (1984)	Newsprint	5.7%-7%	---	53-83	0.102-0.126	540-1760
Seyed-Yagoobi, Ng & Fletcher (1991)	Bleached	0%	0-300	85	0.12-0.68	90-450

[1]Apparent Thermal Conductivity
[2]Estimated
[3]Sheet Ave. Temperature
[4]Calculated
[5]Apparent Heat Transfer Coefficient
[6]Front Surfaces Coated with Graphite

In a study carried by Asensio et al. [25], which is a continuation of a previous study by Seyed-Yagoobi et al. [24], a linear model was developed to analyze the data in order to find the experimental overall joint conductance as a function of contact pressure, sample basis weight and thickness. It was also aimed to derive the (interface thermal) contact conductance between the iron shell surface and the paper surface and the effective thermal conductivity of each sheet. Sample basis weight, dry basis moisture content and the operating conditions such as contact pressure and sheet thickness are given in Table 3.1. The lower and upper interface temperatures were 130°C and 40°C respectively and the average paper temperature was taken as 85°C. Critiques of the results of their study are as follows:

- It is known that joint conductance is related to sample surface smoothness and density, which to some extent are dependent on fiber type and composition. However, results indicated that handsheet composition has less effect on the joint conductance than what would be expected.

- The top and bottom interface contact conductances were assumed to be the same in the calculation of the effective thermal conductivity, even though the top interface temperature was greater than that of the bottom interface and the contact conductance was indicated to increase with increasing temperature. However, it was indicated that the heat transfer across the bottom interface increased due to the thin layer of condensate because the conductivity of water (0.673 W/m·K at 85°C) is greater than the conductivity of air (0.0306 W/m·K at 85°C). Therefore, contact conductances at the interfaces can be considered similar, since under experimental operating conditions the temperature and moisture differences at the top and bottom interfaces may offset each other.

- Analysis of the heat and mass transfer occurring within the sheet indicated that a slight, non-uniform moisture content profile through the sheet thickness existed continuously during the steady-state period of each experiment.

- It was found that contact conductance increases with increasing contact pressure, decreasing basis weight, and increasing moisture content As the applied pressure

increases, the handsheet/metal contact area increases, yielding increased heat transfer across the interface. At lower basis weight, the interfacial contact area increases due to smoother or more uniform sheet surfaces (observed visually) for the handsheet samples considered. Contact conductance is also enhanced by softer handsheet fibers at higher moisture content since softer fibers provide a better effective contact area between the handsheet and metal surfaces.

- Overall joint conductance must lie between the fiber conductivity of 0.12 W/m·K and water conductivity of 0.68 W/m·K.

- Effective thermal conductivity increases with increasing handsheet density due to the decrease in air within and between the fibers of the handsheet. Effective thermal conductivity of a moist handsheet, at constant basis weight, increases slightly with increasing moisture content due to greater conductivity of water. But contribution of moisture content to thermal conductivity is very small due to the fact that moisture condenses out of the sheet during the experiments. Also, liquid and vapor migrates through the sheet coupled with evaporation near the hotter interface and condensation near the cooler interface and this could in some cases, create a heat pipe effect yielding relatively high values of paper thermal conductivity.

In connection, Lehtinen [21] stressed the importance of the intraweb diffusion processes in addition to conduction through the wet fiber matrix for the case of air inside the web in conventional, hot-surface drying. He included the evaporation-diffusion-condensation process for the intraweb heat transfer for local web temperatures below 100°C. Consequently, the equation of the effective thermal conductivity he used for the web included the thermal conductivity of the wet fiber matrix and the term representing the heat transfer capability due to Stefan diffusion in the pores. He stated that in a typical web-drying situation, with the intraweb temperature at 90°C, the magnitudes of the dry web thermal conductivity and the heat transfer capability due to Stefan diffusion in the pores are 0.13 W/m·°C and 0.39 W/m·°C, respectively.

If there is no air inside the web, the name of the drying regime changes to high-intensity paper drying where the temperature is comparatively higher.

Heat transfer by radiation was included in the paper drying studies carried by Wilhemsson et al.[23]. It was stated that the mechanism of heat transfer between the cylinder and the sheet is in theory a combination of conduction, radiation and natural convection. It was shown that if the cavities at the web surface on average were assumed to be one fiber diameter deep (on the order of 30μm), natural convection was negligible compared with conduction. Besides, it was found for a typical case where the cylinder surface temperature was 140°C and the paper surface temperature was 100°C, the apparent radiation heat transfer coefficient did not exceed 5 $W/m^2 \cdot °C$, which indicates that conduction is the main mechanism of heat transfer in the web.

Wilhemsson et al.[23] stated that in steam heated dryers, heat transfer from the heat source, i.e., steam, to the heat sink, i.e., water within the web, is subjected to several kinds of resistances. The study was done on multi-cylinder dryers. Seven different layers exerting thermal resistance were considered for each dryer cylinder, which are: 1-Steam and noncondensable gases, 2- Condensate, 3- Scale and rust, 4- Cylinder shell, 5- Dirt and air, 6- Paper web, and finally 7- Fabric. The most significant of these layers was indicated as the fifth one, the interface between the cylinder and the web, which is quantified by the contact heat transfer coefficient. Contact coefficient was defined as the heat flux across the interface divided by the temperature difference across this interface. Since, the contact coefficient is not constant, their study aimed to find the knowledge of how it was affected by factors such as moisture content, fabric tension, and temperature. The results of the literature review and the experimental studies were as follows:

- It was found out in both the literature and experimental studies that contact coefficient is strongly dependent on moisture ratio of the paper, that is, contact coefficient decreases as the moisture ratio of paper decreases. A qualitative reason for this is that the voids at the paper surface are progressively depleted of liquid water, so a dried surface layer with low thermal conductivity is formed.

- Contact coefficient is temperature dependent. It was found out that an increase in surface temperature increases the contact coefficient, even though the opposite is claimed in some of the literature they reviewed [26]. The reasoning for the increase was that it is possible that fibers at the cylinder surface become more ductile at higher temperatures, which leads to an increase in the contact area of the web. Since conduction is shown to be the principal mode of heat transfer in multi-cylinder drying, the result will be larger contact coefficient at higher temperature.

- The concept of large number of contact points of the fabric, that is, large contact area being beneficial to heat transfer was not detected. It was shown that neither fabric tension nor fabric type influenced the heat transfer to any significant extent.

- According to experimental results, contact coefficient was not likely to be basis weight dependent.

Finally, it was claimed that the values of the contact coefficients obtained from the studies done on this subject were not readily applicable to an arbitrary dryer section. In short, it is almost impossible to simulate in the laboratory the unique combinations formed by certain dryers that produce certain paper grades.

Wilhemsson et al. [27] worked on a simulation model based on both empirical results and fundamental theory of heat and mass transfer for the drying of paper in a multi-cylinder drying section. Their model did not involve internal mass transfer phenomena in the web and evaporation took place only at the surface of the web. It was based on the unsteady state, one-dimensional heat conduction equation, which was applied to both the cylinder shell and the paper web in perpendicular direction. The simulation program based on a mathematical model was applicable to newsprint, fine paper, fluting, and paperboard. The aim of the study was to find the proper heat and mass transfer coefficients written as the integral parts of the boundary conditions in the equations. Different machine speeds and basis weight were used in determining the condensate coefficient and contact coefficient ranges. Nine cases were studied and for each machine, the simulation program was applied by using the

experimental data obtained for that machine. Fitting parameters of the model were the contact coefficient at zero moisture content and the condensate coefficient. These two heat transfer coefficients were determined by the best fit between the predicted and measured paper moisture contents, and the cylinder surface temperatures.

There were several cases of boundary conditions in the study by Wilhemsson et al. [27]. They found out that if there was fabric above the paper, that is, at the paper-fabric-air interface, mass transfer coefficient reduced by 30-50%, whereas heat transfer coefficient remained unaffected. If there was no fabric above the paper, at the paper-air interface, heat used for evaporation of water was either conducted to the surface or convected from the ambient air. A corrected convective heat transfer coefficient was used since drying involves simultaneous heat and mass transfer. At the cylinder-paper interface, the contact heat transfer coefficient was found to be a linear function of the web moisture content. The intercept when there is no moisture was found to be in the interval 200-500 $W/m^2 \cdot °C$ as presented in Table 3.1. At the cylinder-air interface, only convective heat transfer was considered and radiation effects were neglected. The cylinder-air heat transfer coefficient was calculated using the Nusselt correlation for parallel flow past a flat plate. In the case of a fabric placed between the cylinder and the paper web, only convective heat transfer was considered. The heat transfer coefficient from the cylinder to the paper through the fabric was calculated as 300 $W/m^2 \cdot °C$.

The effective thermal conductance was represented by a lumped parameter in the work of Wilhemsson et al. [27]. It took into account all the heat transfer processes in the paper web, that is, conduction, evaporation and condensation phenomena within the process. It was assigned a value of 0.08 $W/m \cdot °C$ for dry paper at no moisture, which was used in all the simulations. Shrinkage of paper was taken into consideration in a direction perpendicular to the cylinder and an expression for the paper thickness was written as a function of the moisture content.

3.3 Condensate and Condensate Coefficient

The supply of steam to the dryer and the removal of condensate is a critical part of the dryer section operation. The manner in which this is handled affects:

- Drying efficiency
- Energy efficiency
- Paper quality
- Overall paper machine efficiency

At very high speeds, condensate layer approaches to a laminar film inside the cylinder and a small change in the condensate layer depth causes major variations in heat transfer.

Appel and Hong [13] considered the behaviour of condensate at fully rimming state that is, at sufficiently high speeds. According to their studies, maximum depth was found to occur at the top of the dryer and the minimum depth at the bottom, and conversely the minimum absolute velocity of condensate occurred at the top of the dryer and the maximum at the bottom. It was suggested that, since all areas of the dryer perimeter became exposed to the full cycle of variation in condensate depth and pattern of variation was fixed in space, the change in depth did not contribute to non-uniformity of heat transfer in dryers. As the dryer rotated faster, the variation in depth around the perimeter decreased.

In most Yankee dryers the variation in depth due to flow towards siphons can be neglected. In real dryers, average condensate velocity is the same as the dryer speed when a fully rimming condition is obtained. Appel and Hong [13] found out that resistance to flow of heat decreased as both the sloshing velocity and the sloshing amplitude increased. So, the resistance to heat flow increases for increasing dryer speeds both because the amplitude of sloshing and the Reynolds number of sloshing is decreased by increasing speed.

For plain-shell dryers, as the speed increases in dryers, whether they be small paper dryers or large Yankee dryers, it is important to maintain a thin condensate film if maximum drying for a given steam pressure is to be attained [13]. Sometimes the blowthrough steam may not be sufficient to produce critical depths at higher condensate flows. So, careful attention should be given to the condensate removal system, the siphons and to the limiting depth, that is, the critical depth at the siphons, which can be realized for a given condensate flow.

Heat transfer coefficient for the ribbed dryer is not dependent to a significant extent on the dryer speed due to condensation occurring primarily on the sides of the ribs where the condensate has little effect on heat transfer. It was reported by Appel and Hong [13] that values of the inside heat transfer coefficient for the ribbed dryer were actually equal to those for the condensate layer in a plain shell at the lowest speed range and distinctly greater than the plain shell at the higher speeds. So, as the machine speed increases, ribbed dryers should be used to attain high heat transfer rates. But still in this type of dryer, too, the depth of condensate in the grooves should be minimized as stated by Appel and Hong [13]. For this reason, critical depth may then be reached beneath the siphons and the siphon head perimeter may be increased to get further reduction in depth.

Wilhemsson et al. [27] worked on a mathematical model of a multi-cylinder dryer section in order to find the condensate and paper contact heat transfer coefficients. As a result of their studies, they suggested that the condensate coefficient ranged between 800-5000 $W/m^2 \cdot °C$, as presented in Table 3.3. The range is wide such that as the machine speed increases, the condensate heat transfer coefficient decreases.

It was suggested by Wilhemsson [27] that the heat transfer was promoted by the presence of spoiler bars and relatively high values for both slow and fast machines were obtained. For example, a high value of 1900 $W/m^2 \cdot °C$ at 1200 m/min was obtained for a modern newsprint machine with cylinders of 1.83 m diameter and a state-of-the-art condensate removal system. It was mentioned that the condensate removal system and large cylinder diameter promoted heat transfer. According to the

Table 3.3: Summary of Steam Condensing Coefficients with Operating Conditions Found in the Literature

Author	Paper Grade	Dryer Type	Drum diameter and width (m)	Machine speed (m/min)	Steam Pressure (kPA)	Basis Weight (g/m^2)	Ave. Paper Temp. (°C)	Moisture content (%) Inlet and Reel	Steam Condensing Coefficient ($W/m^2°C$)	Thermal Contact Conductance (W/m^2C)
Pearson (1986)	Corrugating Medium	Multi Cylinder	1.52 and 4.06	387-457	1240 413	125	66	60 and 7	850 – 2840	
Wilhemsson et al. (1996)	Newsprint Fine Paper	Multi-Cylinder	1.83	1200 189		48.8 132		--and 8 db	1900 3300	500 1400

study, at high cylinder velocities, during rimming, condensate coefficient was low, but at slow cylinder velocities, during ponding, condensate coefficient was high such that 3300W/m^2.°C was a realistic value. Generally, slow machine rates when the condensate rests in a puddle at the bottom of the cylinder and the steam condenses directly on the inner cylinder wall are characterized by very high heat transfer rates.

3.4 The Felt

Felt is the transmission belt to turn the cylinders. It may be made of wool, polyamide or polyesters. A good felt should be permeable to water otherwise hydraulic pressure, which damages the paper web, occurs. Felt tension and felt tension variation both around the felt loop and across the machine width is often overlooked. However good control of felt goes hand in hand with good machine efficiency.

The purpose of the use of the felt in tissue making and in making higher grades of paper differ such that multi-cylinder dryers are used for higher grades of paper in which the paper web is carried on a felt. Respectively, Seyed-Yagoobi et al. [17] who have worked on multi-cylinder dryers, define the felt as a highly porous material whose main purpose is to hold the paper sheet in close contact with the dryer shell. The aim is to increase the heat transfer between the paper and dryer, as well as to help prevent shrinkage and deformation of the paper sheet.

3.5 Yankee Drying

Ahrens [28] claimed that the average heat flux from the Yankee to the moist paper is commonly several times that in a conventional paper/board machine multi-cylinder dryer section. The primary reasons for this are as follows:

- Light weight sheet has lower internal thermal resistance compared to a heavier paper or board sheet

- Lightweight sheet is applied to the Yankee surface through a high-pressure press roll instead of being held against a dryer cylinder by a fabric at a comparatively low pressure via tension, as is the case in a multi-cylinder conventional dryer section.

Factors that affect the heat flux at the surface of the Yankee with respect to circumferential position are:

- Low initial sheet temperature
- Strong dependence of paper-Yankee contact heat transfer coefficient on sheet moisture content
- Less than 360° wrap angle for the sheet on the Yankee
- Hygroscopic nature of paper that reduces the drying rate in the final stage of drying (local moisture ratio < 0.2 g H_2O/g fiber)

As a consequence of the high average value and the variation in heat flux observed in Yankee dryer systems and the typical cast iron Yankee shell, Ahrens was lead to the expectation that circumferential change of the surface temperature might be significant in common Yankee dryer applications. He stated that experimental results by Brauns and Jansson [29], Sundberg [30], and Zabel [31] showed that circumferential surface temperature changes of at least 5°C were typical, but the quantitative effect of this level of temperature variation on the drying behaviour, sheet temperature, and drying rate was not assessed. Accordingly, the aim of a study done by Ahrens [28] was to compare the local and overall drying behaviour predicted by a Yankee dryer model with a corresponding uniform surface temperature model.

In Ahrens' models [28], since applications to lightweight paper were of interest, the sheets were assumed to be thin enough that temperature and moisture variations in the thickness direction were unimportant. This assumption was proved by Karlsson and Heikkila [32] to be a good approximation for the tissue paper. The models also included a moisture-dependent contact coefficient and a dynamic sheet model, which predicted the variation in sheet temperature and moisture ratio with circumferential position.

The Yankee-hood model was not treated in a very detailed manner by Ahrens [28] in order to develop the more essential features more easily and quickly. For example, the heat transfer coefficients between the sheet and hood air, and between steam and inner cylinder wall, hood air temperature, water vapor mass fraction in hood air were all specified directly, rather than being calculated from mass and energy balances involving many parameters. As a result, he found out that the full shell thermal dynamics model and the uniform surface temperature model gave almost the same results in terms of final sheet moisture content and Yankee velocity especially for low basis weight paper. Thus, the uniform surface temperature assumption is beneficial if the product has low basis weight such as tissue paper, but the full shell thermal dynamics model becomes more necessary for accurate drying predictions when the sheet is heavier.

3.6 Efficiency and Optimization of System

In the large, competitive industry, the common goal of paper manufacturers is increased productivity and quality through increased machine throughput, lower production costs, and more uniform drying of the web [18]. Since the drying process is the major energy-consuming process in papermaking, the use of an economical dryer or even a very small improvement in paper-drying efficiency will result in a significant amount of energy savings. It was recorded by Chiogioji [2] that the Yankee dryer was more economical than the conventional dryer sections, consuming 6400-8100 kJ/kg of sheet compared to 7500-14500 kJ/kg sheet for the conventional dryer.

Schukov [15], who worked on Yankee cylinders, suggested that optimum thermal efficiency was kept by maintaining high system humidity (recirculation) and extensive makeup air recovery. Flow of make-up air can be adjusted if a control system based on feedback from a humidity sensor, which is a system similar to the one in İpek Kağıt factory, is used. However, minimization of the energy consumption must not disturb the net air balance of the system. If a balanced flow across the

boundary is maintained, it prevents over-drying at the edge of the web caused by thermal infiltration or machine room discomfort caused by thermal spill.

Similarly, Schukov and Haberl [16] added that significant energy savings, i.e. optimum energy performance, in a Yankee hood could be obtained by controlling and adjusting the air system dampers in response to a measured humidity. As a result of their study, humidity was found to be dependent on machine speed, paper grade, and entering moisture. At higher humidity electric consumption was more but there was considerable reduction in thermal energy consumption due to increased use of recirculated air and the consequent reduction in the amount of cool makeup air fed to the system. A control system with a humidity sensor responded to a humidity set point by reducing the flow of makeup air. But if the humidity was set too high, the driving force for evaporation (gradient between the sheet and the impinged air) decreased.

Toivonen [12] made a performance analysis of a Yankee dryer system by using a simple mathematical model based on mass and energy balances. The analysis showed that in addition to the evaporation rate, also the overall specific energy consumption characterized the efficiency of the dryer section. Drying air temperature and the impingement velocity on the hood side and the steam pressure on the cylinder side affected the evaporation rate, while the exhaust air humidity affected the overall specific energy consumption. A definite conclusion driven by the analysis was that high exhaust air humidity as well as effective heat recovery systems are the primary factors in reducing energy costs of a Yankee dryer. It was also stated that improving the hood sealing enables higher exhaust humidity. An important conclusion was that optimization of the drying conditions results only in minor savings when the production rate is near maximum, that is, greater than 90%. However, the more the production rate decreases the more important the optimization becomes.

Pearson [33] worked on the mathematical modeling of paper machine drying to analyze its drying capability and optimize dryer efficiency. The product in his case was corrugating medium and the paper machine involved a conventional multi-cylinder dryer. Data inputs were machine operating data, steam pressure, and number

of dryers. Fixed variables were press moisture, dryer area, sheet temperature, and heat transfer coefficients except for the sheet contact coefficient, which was dependent on the moisture content of the sheet. He calculated the heat transfer rate, evaporation rate, and resulting moisture percentage of the sheet leaving the dryer section. He assumed the sheet temperature profile in the machine direction to be constant in all cases, but also mentioned the assumption to be invalid in case of large variations in speed. Another limitation to his model was that he did not consider the effect of the variations in pocket ventilation on sheet contact coefficient. As a result he used his model to predict the pressure in any section of the dryer for a base case and for an alternative case. He was able to identify the energy cost savings and make summer time economical modifications such as replacing the 12.4 bar steam by 4.13 bar steam in some section of the dryer in order to use the rest of the steam for additional electrical generation.

Asensio and Seyed-Yagoobi [25] also worked on multi-cylinder drying and stressed the importance of conduction and steam in this drying method. They concluded that any enhancements of the drying rate can easily be related to energy savings associated with reductions in the dryer section steam requirements. Energy costs associated with the dryer section can be minimized by finding the optimal steam pressures for each cylinder, which yields the same average drying rate or paper production, but with the least steam consumption.

Reese [34] calculated the drying rates for heavier paper grades than tissue paper. The parameters considered in the calculation were the number of dryers, dryer diameter, machine speed, basis weight, ream size, and entering and leaving web consistencies. The importance of the factors such as sheet furnish, siphon design, use of dryer bars, pocket ventilation, dryer fabric application, and use of single top and bottom dryer-fabric runs, which affect drying rates, was stressed. However, these factors were not considered in the calculation of the drying rates. It was observed that except for the paperboard, higher drying rates were achieved on grades made from full chemical pulps. This was due to the fact that there is less bound water in chemical sheets and water is more easily evaporated from the web. As would be expected, the drying rates were found to increase with steam temperature, but interestingly, the drying-rate lines for all the grades were found to be nearly parallel.

CHAPTER 4

İPEK KAĞIT SYSTEM

4.1 Introducing the Plant

"İpek Kağıt Sanayi ve Ticaret A.Ş." is a leader tissue paper producing company of Turkey placed in Yalova. It involves three operating paper machines enrolled with producing several grades of tissue paper for both the local market and the global market. The main grades of paper produced are toilet paper, handkerchiefs of several plies, facial tissues, serviettes, and towels

The first paper machine, PM1, has first started in 1969 with a capacity of 6,000 tons product per year and has reached a capacity of 10,000 tons per year after revisions of the paper machine. Finally, the capacity of PM1 has become 14,000 tons per year as a result of the small-scale efficiency improvement efforts applied on the machine. The second paper machine, PM2, has been running since 1991 with a starting capacity of approximately 24,000 tons per year. There has not been much variation in this capacity since then. The new third paper machine, PM3, has very recently started operating at the beginning of May, 2000 with a larger capacity of 50,000 tons of tissue paper production per year. The company aims to fulfil the whole capacity and implement a forth paper machine in the future while observing and decreasing the energy costs of each paper machine.

PM1, on one hand, is an old, more simple but efficient machine. It is mostly directed by manual control. It has exhibited improvement in production and saving in energy consumption since its start. PM2, on the other hand, is a very complex modern machine. It is mostly controlled automatically by a DCS (Distributed Control

System). Therefore, the net rate of overall heat and mass transfer within the system boundaries, the effects of the most important of the many operating parameters on each other and the corresponding results on energy consumption need to be studied.

4.2 Flowsheet of the İpek Kağıt Paper Machine

The papermaking process for the second paper machine, PM2, starts at the pulper since the plant does not involve a pulping unit. A large proportion of the pulp used in the mill is imported virgin pulp. Secondary fiber, i.e. recycled paper is also used in the first paper machine, PM1, in the production of certain grades of tissue paper. Imported pulp is dispersed in water and refined. Then it passes to the papermaking machine. A simple flow sheet of the processes taking place in PM2 is presented in Figure 4.1.

Cellulose and water are mixed in the pulper together with certain amounts of some additives such as indigo dye, optical brightners, forming agents, etc. The fibers are separated from each other and the resulting pulp with 45% solids is sent to the high-density cleaners and next with 4.5% consistency to the refiners. In the refiners, the pulp is diluted with water up to 3.5% consistency and an even dispersion of the fibers is attained. After some more dilution, the very dilute fiber suspension with 0.1-0.2% consistency is fed to the headbox. Dehydration processes by mechanical drying and thermal drying in the paper machine starts just after the headbox. Mechanical drying section of the İpek Kağıt second paper machine is presented in Figure 4-2.

The headbox is a multilayer headbox that is capable of forming two layers of sheet, so that the tissue to be produced is based on two furnishes. The blend of short fibers coming from the dust collectors and the broke paper stocks is layed on the dewatering side and the blend of long fibers coming from the line shown in the flowsheet in Figure 4.1 is layed above the short fibres.

The headbox spreads the fiber suspension evenly over a moving continuous felt around the forming roll. While on the perforation roll, the furnish is squeezed in between the moving continuous wire-mesh band and the continuous felt.

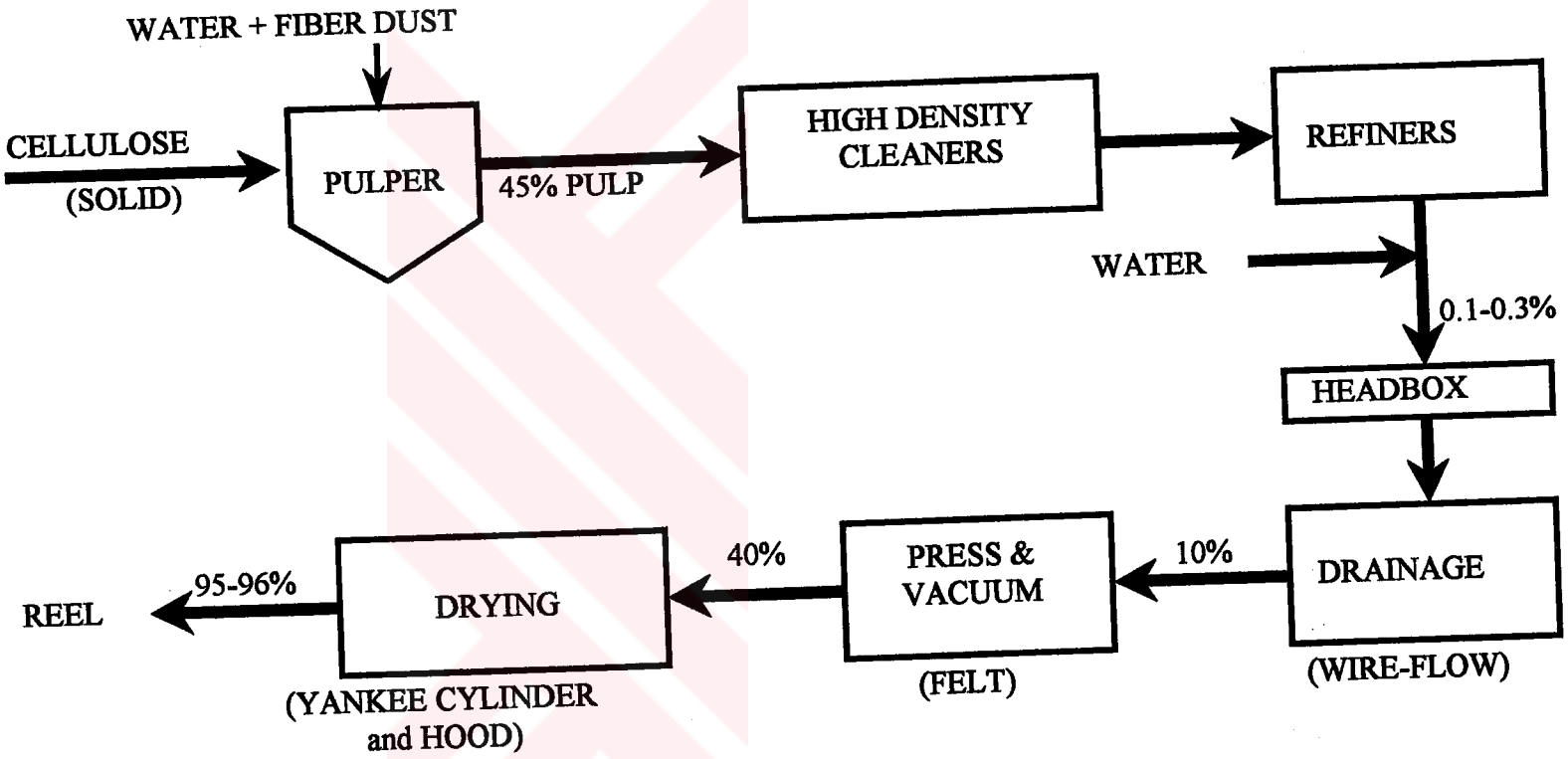

Figure 4.1: Flow Sheet of İpek Kağıt Tissue Paper Mill

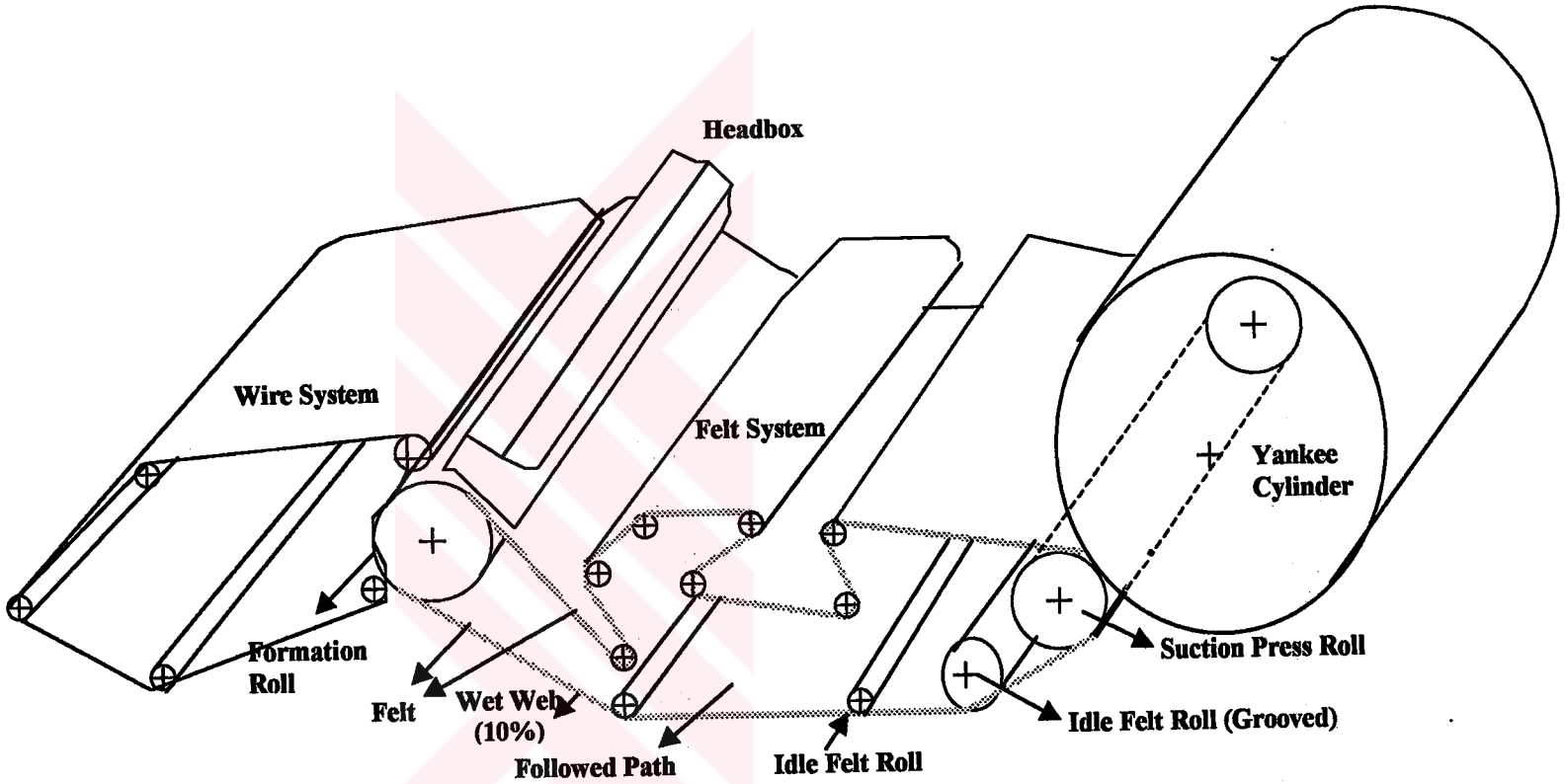

Figure 4.2: Mechanical Drying Section of İpek Kağıt Second Paper Machine Consisting of the Formation Roll, Wire System, Felt System and Suction Press Roll.

The wet paper web with a consistency of 10% solids is then taken off the wire to under the felt. The water removed by the wire drains out by gravity. Some more water is removed out of the wet paper web while it is carried under the felt to the suction press roll. At the press roll, the water in the web is removed by vacuuming and pressing the wet paper web onto the Yankee cylinder. The consistency of the wet paper just before the Yankee cylinder, thus, reaches 40% solids by mass. As the sheet gets stuck on the Yankee cylinder, it is dried thermally by conduction and convection and the remaining water is removed until a consistency of 94-95% solids is reached. Finally, the product with 5-6% moisture is creped and removed out of the cylinder by the help of the creping doctors and sent to the reel.

The product tissue paper is expected to have improved softness due to the laying of the short fibers on the dewatering side, just next to the wire, at the headbox. Accordingly, when the wet web is passed onto the Yankee cylinder, the short fibers are located next to the cylinder surface. Paper softness increases while on the cylinder due to the softening influence of the Yankee surface, and paper strength increases due to bonding of the longer fibers. Besides, both the strength and softness of the product is conserved and increased with the breakage of the short fibers and not the long fibers during the removal of the sheet from the cylinder by the creping doctors.

4.3 Drying Strategies

The Yankee cylinder and the hoods with the burners are shown in a diagram in Figure 4.3. The air streams in the hood area, the steam and condensate in the cylinder, and entering wet paper and leaving dry paper sheet are presented clearly. The paper sheet is dried by two mechanisms: Conduction through the Yankee shell and convection from the hood.

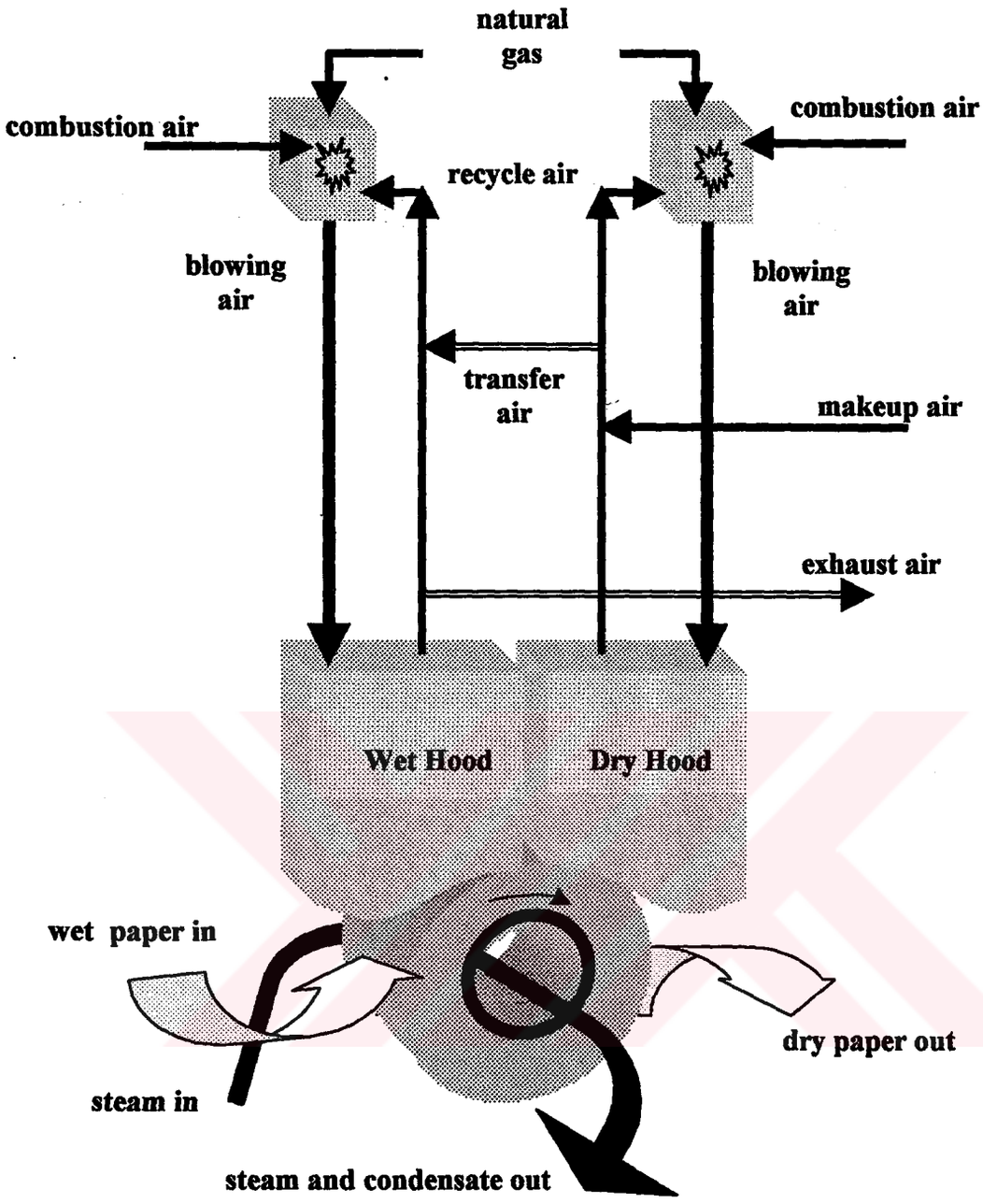

Figure 4.3: The Yankee-Hood Dryer in İpek Kağıt Mill

The cylinder is heated from above by hot air blown on to the paper at high velocity through the hoods and from inside by steam as represented in Figure 4.4. The Yankee cylinder is manufactured by Beloit-Warmsley. The hood is supplied by Beloit but it is a Flakt hood. The heat recovery unit, air circulation system and dust collecting system of the paper machine are supplied by Flakt. The specifications of the Yankee cylinder updated by the Mill in 1998 are presented in Table 4.1.

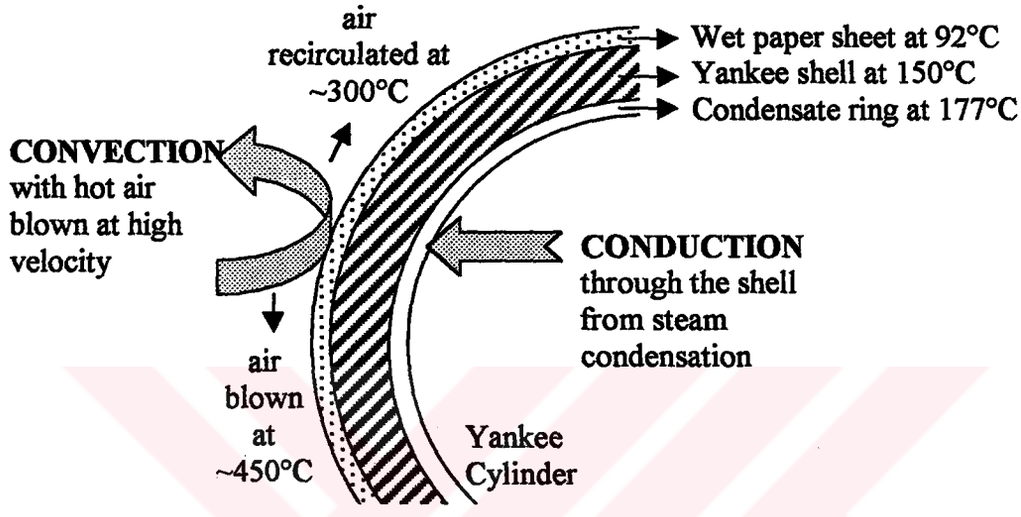

Figure 4.4: The Two Mechanisms of Drying Tissue Paper in İpek Kağıt Yankee Cylinder and Hood System.

Yankee-Hood dryer is composed of two sections as shown in Figure 4.3: Wet side and dry side. After the single press roll in 'İpek Kağıt' where the concentration reaches 40%, the sheet is conveyed by the cylinder on to the wet side and through the dry side to the blades. There are three doctor blades placed at the end of the dryer section in İpek Kağıt, one of which is for removing the paper sheet in case of paper break, one for creping, and one for cleaning.

More than half of the water, about 60-70%, is removed in the wet side making the process more difficult for the dry side. Therefore, the temperature of the air fed to the dry side is greater than that of the wet side.

Table 4.1: Yankee Dryer Status Updated by İpek Kağıt on 11/25/1998

Specification	
Yankee Manufacturer	Beloit-Warmsley
Type (plain or ribbed)	Ribbed
Rib Depth (if ribbed)	28.575 mm
Original Startup	July-1991
Bearing Center Width	4381.5 mm
Face Width	3289.3 mm
Over Heads Width	3454.4 mm
Original Dimensions	
Original Shell Diameter	4576.5 mm
Original Root shell Thickness	47.09 mm
Original Maximum Rated Steam Pressure	10.20 bar
Original Maximum Pressure Roll Pressure	88 kN/m
Present Situation	
Current Location (P.M., Storage, Scrap)	On Machine
Current Shell Diameter	4569.08 mm
Current Root Shell Thickness	43.86 mm
Current Maximum Rated Steam Pressure	10.00 bar
Current Maximum Pressure Roll Pressure	88 kN/m
Headbox Deckle	2785 mm
History of Refurbishments	**Change in Diameter**
Regrind	1.6 mm
Sealing of Yankee Leakage	--
Regrind	1.4 mm
Regrind	0.95 mm
Regrind	2.3 mm

Fresh air is heated previously at the energy recovery unit up to 140-160°C. It is then sent to the wet and dry combustion rooms, where combustion with natural gas takes place reaching reaction temperatures of up to 300-460°C. Hot air blown on to the wet paper, which is stuck on the Yankee cylinder also heated by the cylinder, heats up, evaporates and sweeps the water vapor away. Some of this vapor is exhausted out of the system and the rest is fed back to the system through the recycle fans.

The important thing about the hood is that in addition to fresh air, makeup air is fed to the system. The makeup air is first used in the dry hood where it collects moisture, then in the wet hood collecting more moisture. It is then exhausted. It is a logical procedure using the driest air during the final drying stage. According to the manufacturer of the hood, this procedure gives a reduction in natural gas consumption of about 2 to 5% and a reduction in exhaust airflow of 10 to 20% with the same drying conditions compared to having separate makeup processes. Besides, it is a simple process since there is only one air exhaust ducting with one set of heat recovery units and one exhaust fan.

In the current system, steam is introduced through the rotary steam joint and through the center of the front-end journal as presented in Figure 4.5. Steam pressure inside the cylinder varies between 7 to 10 bars. Using a thermocompressor creates the required differential pressure. Some of the steam condenses on the inside walls of the cylinder while the heat is taken away through the shell and lost through the heads. The siphons remove the condensate to the other end of the cylinder and out through the center of the drive-end journal. Actually, a mixture of condensates and steam is extracted from the Yankee. In the cylinder, about half of the steam used, which is over pure drying requirements, passes out through the straws as steam and is named blowthrough steam. Thus, the density of the condensates and the difference in the required pressure is reduced. The vapor and condensates mixture is sent to a separator from where blowthrough steam is sent to the thermocompresssor. Blowthrough steam is mixed with high-pressure motive steam from the boiler and the new steam is sent back into the cylinder.

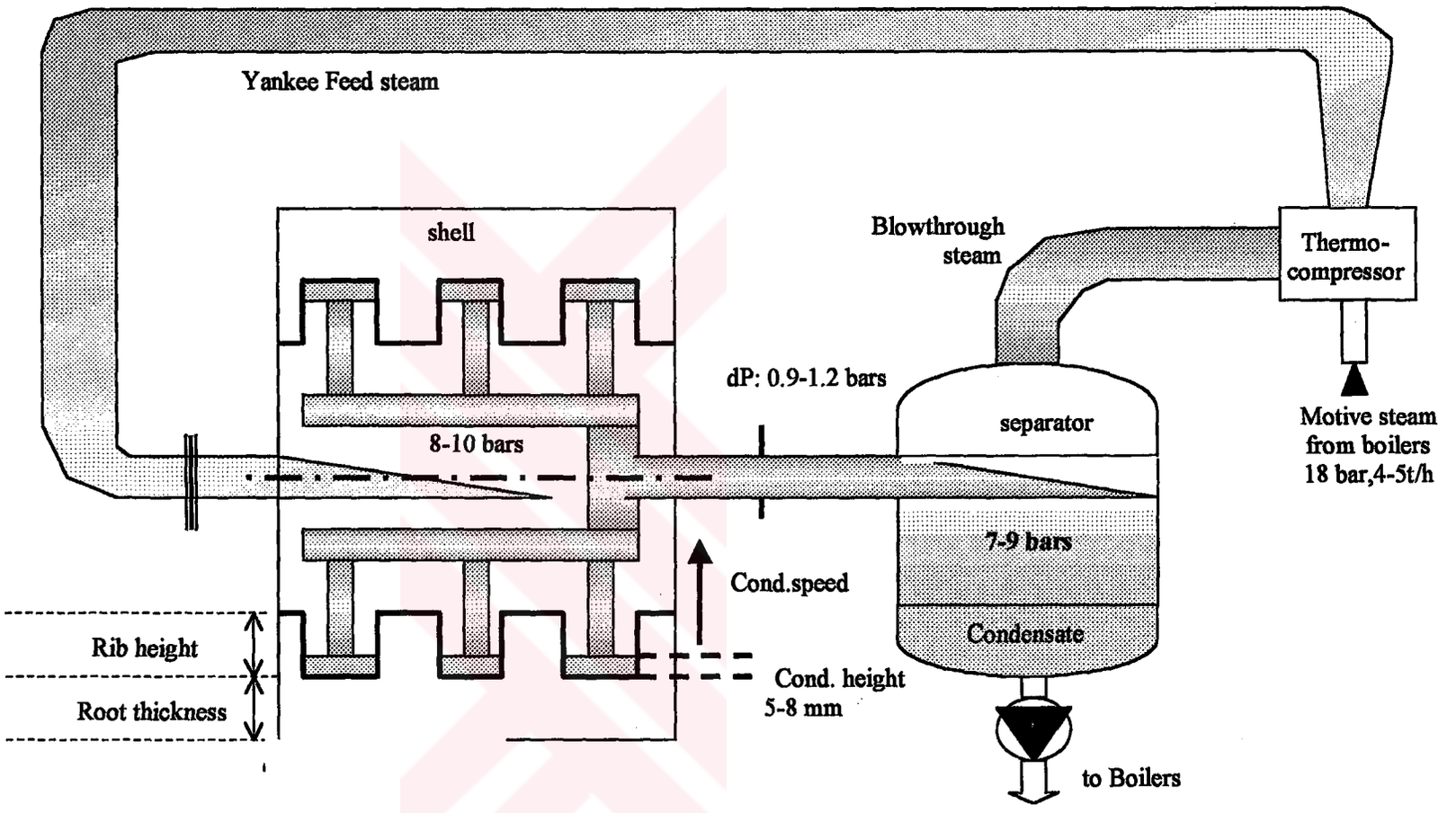

Figure 4.5: Steam and Condensate and Steam Reuse at İpek Kağıt

The drying can be assumed to be uniform. Condensation takes place at constant temperature, where the temperature depends on the pressure of the steam. The pressure is constant throughout since the dryer is large compared to the rate of steam flow and if there are no noncondensable gases.

CHAPTER 5

ANALYSIS OF THE YANKEE-HOOD DRYER IN TERMS OF MASS AND ENERGY BALANCES

The physical system considered is the thermal drying section of the second paper machine, PM2, located at the mill site of "İpek Kağıt Sanayi ve Ticaret A.Ş." in Yalova. An illustration of this system with the flow streams is presented in Figure 5.1. The Yankee cylinder and the hoods are responsible for thermal drying by conduction from the steam inside the cylinder to the cylinder surface and by convection from the blowing air to the paper sheet, respectively. The main sources of energy are steam and hot air heated by natural gas and electricity is used to turn the fans in order to blow the hot air onto the wet paper sheet on the Yankee cylinder.

It is an elaborate task to analyze the complicated Yankee cylinder and the hood system. Therefore, to go forward to analyze the physical system it is simplified as the overall and sub systems. The approach to solve the problem is to develop a steady state analytical model. Given the operating parameters by the Distributed Control System, the necessary material and energy balances set up for each system can be solved for the unknowns and for the rate of net mass and heat transfer through system boundaries, and system efficiencies can be calculated. Optimization studies are made in order to achieve the desired production rate whilst keeping the drying parameters within limits at the minimum energy costs. Eight different products are taken into consideration in the study. The explanation of the systems and the basic assumptions for the calculations are stated in this section. The data obtained from the mill with the results of the calculations especially for a specific product, Product-1, are tabulated.

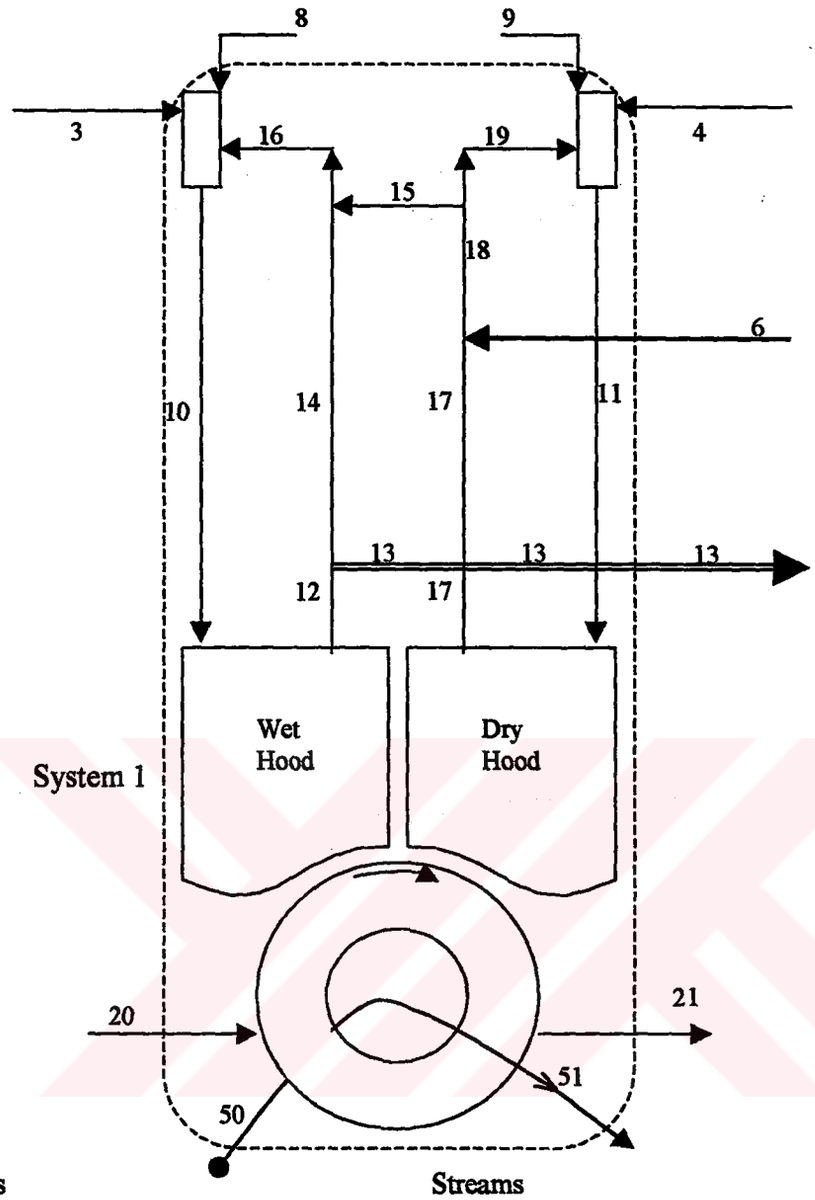

Streams		Streams	
3and 4	Combustion air	13	Exhaust air
6	Makeup air	15	Transfer air
8 and 9	Natural gas	20 and 21	Fiber and water
10 and 11	Blowing air	50	Steam
12,14,16,17,18,19	Recycle air	51	Steam and condensate

Figure 5.1: Overall System With the Yankee Cylinder, Hoods and the Burners (System 1) Showing All the Flow Streams

The calculations, operating data and the corresponding results for the other products, Product-1 through 8 are tabulated and presented in the Appendices.

5.1 Mass Balance

5.1.1 Overall System

The overall system involves the Yankee cylinder and the hoods with the burners. The overall system with the mass flow streams is presented as "System 1" in Figure 5.1.

5.1.1.1 Total Mass Balance On The Overall System

Continuity equation is used to set the mass balance on the overall system in order to calculate the rate of net mass transfer in to or out of the system. Mass flow rate of each stream entering or leaving System 1 is either already known or can be calculated. Streams 3, 4, 6, 8, 9, 20 and 50 enter System 1 while streams 13, 21 and 51 leave. Streams 50 and 51 have no effect on the total mass balance since they are equal. The system is open and at steady state.

Ranges of all the possible data collected at the mill site, involving eight different products, to be used in the total mass balance are presented in Table 5.1. The data involve the parameters required to determine the mass flow rate of each stream entering and leaving System 1. In the total mass balance, mass flow rate of each stream is calculated on kilogram per hour basis.

The transfer of mass in the system mainly consists of the three materials: dry air, water in both liquid phase and vapor phase, and the solid fiber that constitutes the main mass for paper. Solid fiber enters the drying system in stream 20 and leaves as paper in stream 21. Assuming negligible fiber loss due to dust collectors and other vacuum equipment, the fiber balance is consistent and does not affect the rate of net mass lost or infiltrated by the overall system.

Table 5.1: Total Mass Balance Data for the Overall System (System 1)

Stream #	Stream	Data range	Given in units	Flow rate kg/h
3	air in	1.9-2.2	tons/h	1900-2000
4	air in	3-3.2	tons/h	3000-3200
6	air in	5-10	tons/h	5000-10000
8	natural gas in	130-160	Nm^3/min	125-154
9	natural gas in	170-200	Nm^3/min	163-192
13	air out	10-15	tons dry air/h	14480-21720
		h13=400-500	g water/kg dry air	
20	pulp in	VY=1250-1650, VR=1050-1300	m/min	6000-8000
		m21=15-20	g/m^2	
		w=2.7	m	
		x20=0.60 x21=0.05-0.07		
21	paper out	VY, VR, m21, w		2500-3500
50, 51	steam in, steam and water out	Mms=4000-5000	kg/h	6000-8000
		Mbt=2000-3000	kg/h	

Table 5.2: Total Mass Balance Data on the Overall System for a Specific Product

	Product Type-1	
Stream #	**Flow rate data in given units**	**Flow rate, kg/h**
3	2.2 tons/h	2200
4	3.2 tons/h	3200
6	8.2 tons/h	8200
8	148 Nm^3/h	142
9	194 Nm^3/h	186
13	E13=12.2 tons dry air/h	17670
	h13=448 g water/kg dry air	
20	VY=1500 m/min	8231
	VR=1291 m/min	
	M21=16.8 g/m^2	
	w=2.7 m	
	x20=0.60	
	x21=0.063	
21	VY, VR, m21, w	3514
50	Mms=4542 kg/h	6992
	Mbt=2450 kg/h	
51	Mms, Mbt	6992
Σ streams in	Min	29151
Σ streams out	Mout	28176
Σ out - Σ in	Mi	-979

The amount of mass lost by the overall system per hour can be observed for a specific product, Product-1, in Table 5.2. Table 5.2 involves the machine parameters for the specific product and the flow rate of the streams entering and leaving the overall system, System 1. Appendix A can be referred for the details of calculations presented in Table 5.2. As a result of the total mass balance for Product-1, it is found out that 975 kg of mass is lost by the system per hour.

The rate of net mass transfer out of the overall system is in the range 394-1322 tons/h observing the total mass balance results for different products presented in Appendix B.

5.1.1.2 Water Balance

Large amount of water enters System 1 in the feed pulp at 60% moisture content. Most of this water is vaporized and removed by the system to reach the desired moisture content of the product, usually around 6%. Generally, the wet hood removes 55% of the total amount of water removed out of paper while the dry hood removes the remaining 45%. The amount of water removed out of wet paper per hour is found by the difference between the flow rates of pulp feed stream and paper product stream, since the amount of solid fiber in both streams is the same assuming negligible fiber loss. Table 5.3 presents the rate of water removal in kilograms per hour basis for a specific product. The details of calculations can be found in Appendix A.

Table 5.3: Water Removed out of Wet Paper per Hour during Yankee-Drying

Rate of Water Removal During Drying for Product-1		
Product type	Product-1	Symbol
Pulp fed, kg/h	8231	M20
Paper produced, kg/h	3514	M21
Water removed, kg/h	4717	Wr

Water balance is performed on the overall system, System1, shown in Figure 5.1. The system is open and at steady state. The conservation of mass rule is applied for water in order to determine the net rate of water transfer in or out of System 1 boundaries. Amount of water in each stream as well as the water generated as a result of the combustion reaction is calculated on an hourly base.

As can be observed in Table 5.4, the amount of moisture in the feed air entering the system in streams 3, 4 and 6 is very small compared to the other streams. Fresh air has almost negligible contribution in the overall water balance, but it is included in the overall water balance in this study.

Natural gas is assumed to be dry, however, it has contribution to the overall water balance through a combustion reaction at the burners. It is assumed that natural gas is composed of pure methane and 100% combustion takes place due to the single reaction of methane with oxygen. The combustion reaction considered is:

$$CH_4 + 2\,O_2 \rightarrow CO_2 + 2\,H_2O \qquad (5.1)$$

Two moles of water are produced per mole of methane. The amount of water produced at the wet burner and the dry burner is referred as the water generated.

In general, temperature of the dry side must be slightly higher than the wet side due to the drying requirements. It is more difficult to remove the water out of the wet paper as it gets dried and the water remained is the molecules that have attached to the cellulose fibers [21]. Therefore, the amount of fuel fed to the dry side is more than that fed to the wet side thereby causing the generation of more water in the dry hood.

The main portion of water enters the system in the pulp fed, around 5 tons/h, depending on the grams of product per meter square. The amount of water removed per hour is close to this value as presented in Table 5.3. The water balance for the overall system is found out to be consistent applying the rule of conservation of mass for water. The details of the material conservation equation set up for water are presented in Appendix A. Substituting the evaluated values in the equation,

Table 5.4: Water Content of Streams on the Overall System and the Water Balance

Water Balance		**Product-1**
Stream #	Stream	kg / h
3	in	3
4	in	4
6	in	10
8	in	0
9	in	0
13	out	5466
20	in	4938
21	out	221
50	in	6992
51	out	6992
Wet side burner	generation	313
Dry side burner	generation	410
Win		11947
Wgen		723
Wout		12679
(Win+Wgen) -Wout		-9

5.1.1.3 Summary of the Overall System Mass Balances

A summary of the total mass and water balances is presented in Table 5.5. The percent contribution of each constituent can clearly be seen. Most of the mass both entering and leaving the overall system is air and moist air. 7% of the mass entering the system, excluding the pulp and steam, is lost. Since the solids (fiber) and steam balance are assumed to be and the water balance is found to be consistent, what spills out of the system boundaries is air.

Table 5.5: Summary of the Mass Balances on the Overall System

(kg/h)	Input	Generation	Output	Net
Total Mass bal.	29151	0	28176	979
	47% air 28% paper 24% steam 1% natural gas	--	63% exhaust air 13% paper 16% motive steam 9% blowthrough steam	spill out 3.4% (input) ≈ 7% (air + ng)
Water bal.	4955 (air + pulp) 6992 (steam)	723	5687 (moist air + paper) 6992 (steam)	-9

In order to be able to compare the amount of mass transferred by the inlet air (streams 3, 4, and 6) and exhaust air (stream 13) streams, a mass flow balance is applied between these streams. It is simply the arithmetic between the mass flow rates of the air streams entering and leaving the overall system:

$$\underset{\text{(stream 13)}}{\text{Exhaust air flow}} = \underset{\text{(streams 3 and 4)}}{\text{Combustion air flow}} + \underset{\text{(stream 6)}}{\text{Makeup air flow}} + \text{Infiltration flow} \quad (5.2)$$

Substituting the total mass flow rates of the streams mentioned in Equation 5.5, it was found out that air has gained 4066 kg/h of mass. This mass is water, however the amount of water vapor removed out of paper is 4717 kg/h considering the inlet and exit moisture contents of paper. Since, 723 kg/h of water is generated at the

burners during the combustion reaction of methane with oxygen, the expected amount of water in the exhaust stream is about 5440 kg/h. This value matches with the value calculated, 5466 kg/h, according to the reading recorded (0.448 g water/kg dry air in 12.2 kg/h of dry air) by the Yokogawa analyzer on the exhaust stream.

Using the mass flow rates for dry air on Equation 5.5, it was found out that 1400 kg/h of dry air has been lost. 723 kg/h of the dry air is used to generate water due to the combustion reaction of natural gas with air, so 677 kg/h of the air seems to be lost. Therefore, 677 kg/h and more air due to the overall mass balance (979 kg/h) escape at the hood before the cylinder.

5.1.2 System 2 and 3: Wet and Dry Sides

The system has already been classified by the manufacturer as the wet and the dry sections. This classification has been done due to the existence of the two hoods and the decreasing moisture content of the paper web as it travels under the hoods. Wet section involves the wet-side burner and the wet hood, and it is represented as System 2 in Figure 5.2 and dry section involves the dry-side burner and the dry hood, and it is represented as System 3 in Figure 5.3. The flow of each stream is labeled in Figures 2 and 3. The mass balance is performed on kilograms per hour basis.

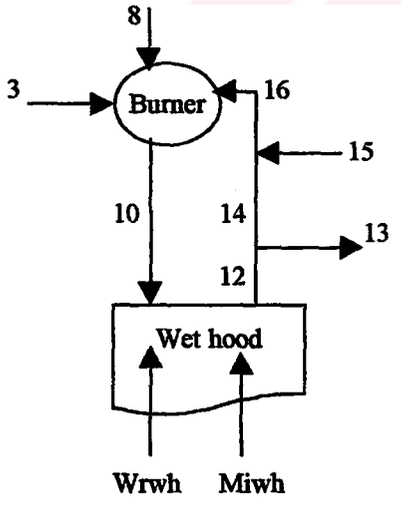

Figure 5.2: System 2, Wet side streams

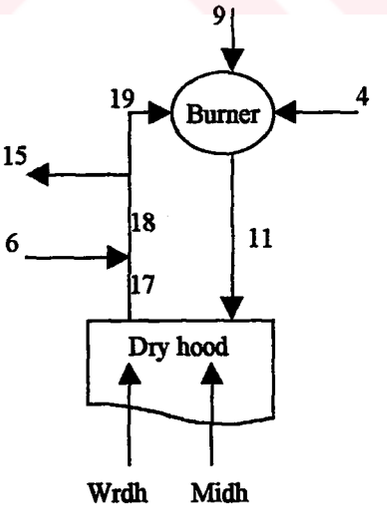

Figure 5.3: System 3, Dry side streams

The pipelines entering and leaving the systems are given numbers for easy identification of the streams during calculations. The streams representing the net transfer of air and water are given letters and shown by two separate streams. Wrwh and Wrdh represent the removal of water by the wet- and dry-side hoods out of the wet paper-sheet while Miwh and Midh represent the net transfer of air through the system boundaries.

The known data required for the mass balances accomplished on both sides is given in Table 5.2 and Table 5.3. The explanation of each stream involved in System 2, i.e. wet-side streams, and in System 3, i.e. dry-side streams, is presented in Table 5.6. For the specific product, Product-1, the value of streams 3, 4, 6, 8 and 9 is converted to kilograms per hour basis in Table 5.2. As a result of the total mass balance in Table 5.2, the net rate of mass transfer through System 1 boundaries is calculated and presented as Mi. Rate of water removal presented as Wr is given in Table 5.3 for Product-1. Both Mi and Wr are multiplied by certain percentages in order to be encountered in the wet and dry side mass balances.

Table 5.6: Explanation of the Streams Involved in Wet Side and Dry Side Systems, Systems 2 and 3

Stream Explanation	**Wet side**	**Dry side**
Hot Fresh air	3	4 & 6
Natural Gas	8	9
Heated air blown from burner to the hoods (Blowing air)	10	11
Humid air returning from the hoods	12, 14	17
Exhaust humid air	13	--
Air transfer from dry hood to wet hood recycle stream	15	15
Recycle humid air feed to the burner	16	19
Net rate of mass transfer through system boundaries	Miwh	Midh
Net rate of water transfer from paper to the hoods	Wrwh	Wrdh

Mass balance sheets for both the wet section over System 2 and the dry section over System 3 are prepared. Both the wet and the dry section systems are divided into subsystems around the burner, the hood and the other mixing points. A mass balance equation is written for each subsystem. The set of linear equations written for both sides are to be solved together to obtain the unknown parameters as shown in Tables 5.7 and 5.9. As a result of the degrees of freedom analysis on each side, both the wet and dry-side systems are found to be undefined, number of unknown parameters are more than the number of independent equations.

There are five unknowns to be solved for in the wet section, which are mass flow rates of stream 10, 12, 14, 15 and 16 presented in Table 5.7. Practically, five independent equations are required in order to be able to solve the system. Five equations are written including the overall wet side balance since only four of the subsystem equations are found to be independent. These equations are represented as "Set of Equations 1" in Table 5.7. The system is solved, however the result is too large to be considered for the wet side. The rank of the five-to-five coefficient matrix and the rank of the five-to-six augmented matrix are checked where the rank of both matrices comes out to be four. This indicates that this set of equations does not give a unique solution.

In order to be able to solve the system, an extra independent equation with a new parameter, λw, is added to the system to replace the overall mass equation for the wet side. The second set of equations is found to give unique solution. λw is the mass fraction of stream 13 (exhaust stream) in stream 12 (recycle stream). The value of λw varies from 0.1 to 1.0. The solution to the system where λw is zero is undefined since it practically means no mass leaves the wet hood and there is no circulation, which is realistically impossible. The value for λw is determined by solving the wet-side equations with the design values of the wet-side. The data is taken from the flow sheet of "İpek Kağıt Air Cap and Heat Recovery System". λw is found to be 0.48. Table 5.8 shows the values of the unknown mass flow rates of the wet side streams calculated when λw is 0.48.

Table 5.7: Wet Side Mass Balance Flow Rate Parameters and Equations (System 2)

Known	**Unknown**	**Set of Equations 1**	**Set of Equations 2: Solution with λw**
M3	M10	M10=f(M12,Miwh,Wrwh)	M10=f(M12,Miwh,Wrwh)
M8	M12	M12=f(M13,M14)	M12=f(M13, λw)
M13	M14	M14=f(M15,M16)	M14=f(M12,M13)
Mi	M15	M15=f(M3,M8,M13,Miwh,Wrwh)	M15=f(M14,M16)
	M16	M16=f(M3.M8,M10)	M16=f(M3,M8,M10)
	Miwh	Miwh=f(Mi,α)	Miwh=f(Mi,α)
	Wrwh	Wrwh=f(Wr,β)	Wrwh=f(Wr,β)

Table 5.8: Mass Flow Rates of the Wet Side (System 2)

Mass Flow Rates of the Wet Side Streams Calculated for λw=0.48			
Calculated from given data		Calculated using set of equations 2	
Symbol	kg/h	Symbol	kg/h
M3	2200	M10	34700
M8	142	M12	36800
M13	17670	M14	19140
Mi	-979	M15	13220
		M16	32360
		Miwh	-490
		Wrwh	2594

In the dry section, the number of unknowns to be solved for is five including the rate of mass flow through the air transfer stream, M15. The other unknowns are the mass flow rates of stream 11, 17, 18 and 19 as can be seen in Table 5.9. As in the wet section, five independent equations are required to obtain a solution in the dry section. However, only four of the several equations that can be written for the overall dry system and the subsystems are found to be independent.

Two sets of equations are written for the dry system as shown in Table 5.9. The first set does not give a unique solution. The rank of the five-to-five coefficient matrix comes out to be four. The rank of the five-to-six augmented matrix also comes out to be four, which indicates that the system has a solution that is not unique. The first set of equations that gives awkward results cannot be used to solve system. The second set of equations, where equation for M18 is replaced with a new equation, has unique solution.

In order to be able to solve the dry side equations, an equation with a new variable, λd is added to the system. λd is the mass flow ratio of stream 18, which is the part of the dry-side recycle stream that has been fed with hot fresh air, to stream 19, which is the final part of the recycle stream that is fed to the burner. The rank of both the five-to-five coefficient matrix and the five-to-six augmented matrix is five. This indicates that the second set of equations has unique solution.

Two set of equations are solved since two different equations can be written for M15, which both end up with the same results. λd varies from 0 to 0.9. This means that the system has a unique solution for each λd between 0 and 0.9. The solution to the system where λd is unity is undefined since it means rate of mass in stream 18 is equal to that in stream 19 and no mass is transferred through stream 15 to the wet side.

λd is determined by solving the dry-side equations with the design values of the dry-side. The data is taken from the flow sheet of "İpek Kağıt Air Cap and Heat Recovery System". λd is found to be 0.75. Table 5.9, shows the unknown mass flow rates of the dry side streams calculated for λd is equal to 0.75.

Table 5.9: Dry Side Mass Balance Flow Rate Parameters and Equations (System 3)

Known	Unknown	Set of Equations 1	Set of Equations 2: Solution with of λd
M4	M11	M11=f(M17,Midh,Wrdh)	M11=f(M17,Midh,Wrdh)
M6	M15	M15=f(M4,M6,M9,Midh,Wrdh)	M15=f(M18,M19) or M15=f(M4,M6,M9,Midh,Wrdh)
M9	M17	M17=f(M6,M18)	M17=f(M6,M18)
Mi	M18	M18=f(M15,M19)	M18=f(M19, λd)
	M19	M19=f(M4,M9,M11)	M19=f(M4.M9,M11)
	Midh	Midh=f(Mi,α)	Midh=f(Mi,α)
	Wrdh	Wrdh=f(Wr,β)	Wrdh=f(Wr,β)

Table 5.10: Mass Flow Rates of the Dry Side Streams (System 3)

Mass Flow Rates of the Dry Side Streams Calculated for λd=0.75			
Calculated from given data		Calculated using set of equations	
Symbol	kg/h	Symbol	kg/h
M4	3200	M11	34700
M6	8200	M15	13220
M19	186	M17	44680
Mi	-979	M18	52880
		M19	39660
		Midh	-490
		Wrdh	2123

The hoods not only remove the water in wet paper, but infiltrate air during the suction operation. The rate of the water removed out of paper, Wr, and the net mass transfer into the overall system, Mi, is included in the equations written for the subsystem around each hood. The ratios of these variables in the wet and dry sections are not known. In order to determine these ratios, two new variables, α and β are introduced to the system. α is defined as the fraction of Mi, rate of net mass transferred into or out of the system, in the wet side. β is defined as the fraction of Wr, rate of water removal, in the wet side. $(1-\beta)$ indicates the fraction of water removed by the dry side. The values of α and β are to be found by trial and error and by using the design data of the cylinder and hood system represented in the flow sheet of "İpek Kağıt Air Cap and Heat Recovery System". The solutions of the dry and wet sides are compared for the rate of mass flow through the air transfer stream, M15, between the two sides and for the validity of the mass flow rate of each stream in the wet and dry sides. Mass flow rate of the air transfer stream, M15, must come out to be the same as a result of the mass balance calculations done for both the wet and the dry sections. As a result of the analysis, α and β values are determined as 0.50 and 0.55.

According to calculations made depending on the design values of the hood streams, approximately 53% of the mass is infiltrated by the wet hood and the remaining 47% is infiltrated by the dry hood. The percent removal of water, infiltration of air and their total is presented in Table 5.11.

Table 5.11: Hood operation depending on design values

Hood Operation Depending on Design Values	Wet-Side (mass %)	Dry-Side (mass %)	Total (kg/h)
Water removed by each hood	55	45	4885
Dry air infiltration by each hood	50	50	4000
Infiltration by the hood	53	47	8885

The mathematical operations are done using the Mathcad mathematical software program. The matrix solution is also applied on the set of linear equations for the wet side and dry side in order to check the liability of the solutions obtained by using other Mathcad tools.

5.2 Energy Balance

5.2.1 Overall System, System 1

The general energy balance is applied on the overall system under steady state conditions in order to calculate the rate of net heat transfer through System 1 boundaries, which is represented by Q. The energy required to evaporate and remove the water out of the wet paper to reach the desired product conditions with the appropriate moisture content is aimed to be found for certain products. The efficiency of the system under the given conditions needs to be determined. In order for the stated calculations to be done, the contribution of each stream or component to the system on heat transfer rate basis must be calculated.

The overall system involves the Yankee cylinder, the wet- and dry-side hoods and the burners. The intensive variables as well as the extensive parameters are required since the energy balance is considered. The overall system used in the total energy balance, showing the feed and exit streams with the symbols of the corresponding stream temperature or pressure is presented as "System 1" in Figure 5.4.

The system is open and at steady state. Streams 3, 4, 6, 8, 9, 20 and 50 enter the system while streams 13, 21 and 51 leave. Chemical reaction takes place within the system boundaries, at the burners. The ranges of the available intensive parameter data collected at the factory site during the production of several different tissue paper types are presented for each stream in Table 5.12.

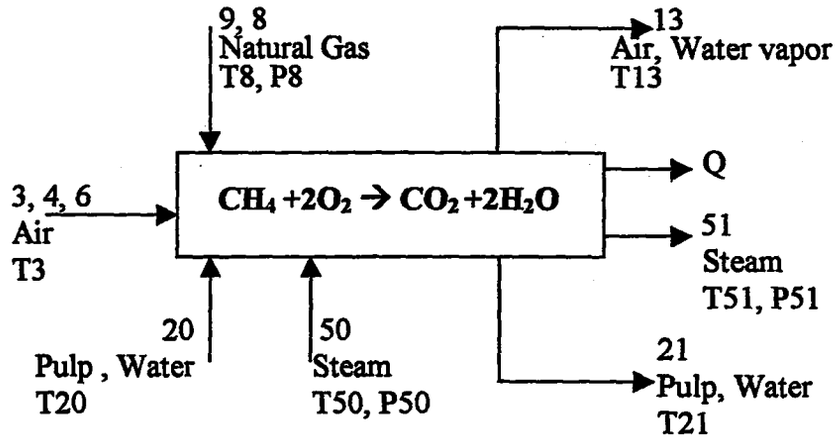

Figure 5.4: System 1, Overall System Used in Total Energy Balance Including the Cylinder, Hoods and Burners

Table 5.12: Total Energy Balance Data for the Overall System (System 1)

Data Collected on System 1			
Stream	Stream #	Stream Property	Data Range
Air in	3,4,6	T3=T4=T6	130-160 C
Natural gas in	8,9	T8=T9, P8=P9	10-35 °C, ~1.4 bar
Air out	13	T13	270-290 °C
Pulp in	20	T20	~30 °C
Paper out	21	T21	85-98 °C
Steam in	50	P50	8-9.8 bar
Steam-water out	51	T51	170-180 °C
Combustion of natural gas	Burners	Trxn	350-460 °C

Energy input and output through system boundaries for each stream can be calculated depending on the data collected at the mill site. Concerning this system, mass flow rates of the feed and exit streams have already been determined on kilogram per hour basis within the total mass balance calculations. The ranges of parameter data required for the total mass balance and the ranges of mass flow rates are presented in Table 5.1 titled as "Total Mass Balance Data for the Overall System".

Main components to be considered in the overall energy balance are air, natural gas, steam, water, and cellulose fiber. Calculations for the rate of heat transfer are made on kilo-joules per hour basis. Enthalpy input and output through the system boundaries for each component and enthalpy generation within the system are calculated. No work is done on the system due to shafts or movement of fluid, or to deform the system boundaries. Potential and kinetic energy terms are neglected.

Wet paper, that is pulp, before sticking on the Yankee cylinder surface is 60% composed of water. The temperature of the pulp at the entrance of the cylinder is assumed to be 30°C. The temperature of the product stream, T21, is assumed to be constant and around 92°C. Fresh air entering the system in streams 3, 4 and 6 is heated up to T3°C (about 150°C) at the first heat exchanger before it is fed to the system. Energy generation occurs as a result of the combustion of natural gas with the feed air. Natural gas is assumed to be composed of methane only depending on the analysis of the gas made by Botas as presented in Appendix C. Combustion reaction is assumed to be taking place with 100% conversion and at the reaction temperature, Trxn.

The amount of heat energy lost by the overall system per hour can be observed for a specific product, Product-1, in Table 5.13. Table 5-13 involves the intensive system parameters for the specific product and the heat flow of the streams entering and leaving the overall system, System 1. Appendix A can be referred for the details of calculations presented in Table 5.13. As a result of the total mass balance applied for Product-1, it is found out that on the order of 10^6 kJ/h heat is lost by the system.

Table 5.13: Total Energy Balance and Data on the Overall System

For a Specific Product

Energy Balance for Product-1 on System 1				
	Stream #	Temperature (°C)	Pressure (bar)	Heat Flow Rate (kJ / h)
In	3, 4, 6	273		$1.721*10^6$
	8, 9	29.1	1.4	$3.095*10^3$
	20	30		$6.451*10^5$
	50		9.5	$1.941*10^7$
		Total in		$2.178*10^7$
Generation	Burners	458		$1.645*10^7$
Out	13	286		$1.848*10^7$
	21	92		$5.006*10^5$
	51	177		$1.444*10^7$
		Total out		$3.342*10^7$
Rate of net heat loss through system boundaries, Q				$4.807*10^6$
Energy required for removal of water (Wr) at T21, Hv				$1.074*10^7$
Efficiency				28.1%

The rate of the net heat loss through the system boundaries is in the range of 2.95 to 4.80 kJ/h observing the total mass balance results for different products presented in Appendix B.

The rate of heat energy required to evaporate the water in the wet paper at paper temperature (T21) is found as $1.074 \cdot 10^7$ kJ/h for Product-1. However, the amount of heat supplied by the system to meet the drying requirements is about 3.5 times as much. System efficiency defined as the ratio of energy required to evaporate the water in the paper to energy input through the system boundaries, is calculated to be 28.1%.

Considering the energy consumption and the cost, 28.1% is an inefficient value. Nevertheless, the system considered is very large, where there are a lot of occasions for leakage and intake of mass and heat. Efficiency of a more specific system in the Yankee-Hood dryer would be greater.

5.2.2 Shell-Hood Interface, System 4

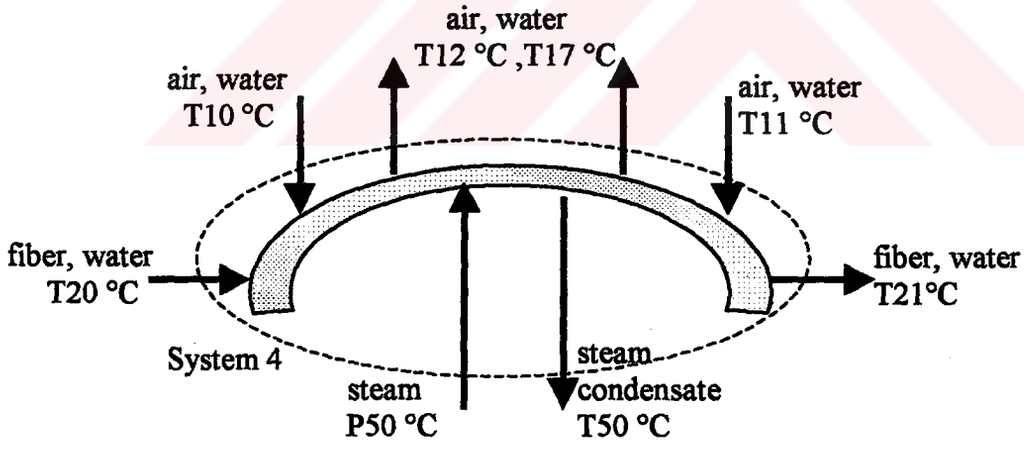

Figure 5.5: Flow Streams at Shell-Hood Interface, System 4

Only the hood and the paper are involved in System 4. It is a smaller and more specific system than the overall system. Some parts of the hood such as the burners are left out of the boundaries. System 4 is simply sketched in Figure 5.4 with the symbols of the corresponding intensive parameters.

Several assumptions are made in order to be able to apply the energy balance at the shell-hood interface. The high temperature air streams entering and especially leaving the system contain important amount of water vapor. Thus, moisture contents of the air streams entering (streams 10 and 11) and leaving (streams 12 and 17) the system are required. The Mill with a Zirconium Humidity Analyzer continuously measures moisture content of the exhaust stream, stream 13. Moisture content of streams 12 and 13 are the same. Knowing the moisture content of stream 12 (h12) and having been found the amount of water removed by the wet side (Wrwh) in mass balance calculations, the amount of water in wet side streams are calculated. Since there is no specific information or measurement about the moisture content of the dry side streams and only the amount of water removed (Wrdh) is known, moisture content of stream 11 (h11) is accepted to be equal to the design value. Results of these calculations for the wet and dry sides are given in Table 5.14.

Table 5.14: Water Content of Wet- and Dry-Side Streams Required for the Energy Balance at the Shell-Hood Interface

	Known or Already Calculated Values		Water Content Results	
Wet Side	H12	0.448 g water/kg dry air	W12	11390 kg/h
	M12	36800 kg/h	W10	8791 kg/h
	Wrwh	2594 kg/h	h10	0.339 g water/kg dry air
Dry Side	H11	0.219 g water/kg dry air	W11	7732 kg/h
	M11	43040 kg/h	W17	9855 kg/h
	Wrdh	2123 kg/h	h17	0.283 g water/kg dry air

Using the water and air mass flow rate data, enthalpies of streams 10, 11, 12 and 17 are calculated. The enthalpies of the streams involved in System 4 together with the temperature data and the results of the energy balance are presented in Table 5.15.

Table 5.15: Data and Energy Balance at the Shell-Hood Interface (System 4)

Heat transferred	**Stream**	**Temperature (°C)**		**Symbol**	**Heat Transfer Rate (kJ/h)**
By entering streams	20	T20	30	H20	6.451E+5
	50	T50	177	H50	1.941E+7
	10	T10	452	H10	3.822E+7
	11	T11	456	H11	3.940E+7
By leaving streams	21	T21	92	H21	5.006E+5
	51	T50	177	H51	1.444E+7
	12	T12	337	H12	3.831E+7
	17	T17	365	H17	3.621E+7
By net mass transferred	Miwh	T10	452	HMiwh	-2.187E+5
	Midh	T11	456	HMidh	-2.208E+5
Rate of net heat trans. through system boundaries				Q	-7.774E+6

According to Table 5.15, about 7.8 million kilo-joules of heat per hour is lost through System 4 boundaries, which is more than that lost through System 1, i.e., the overall system, boundaries.

A comparison of the results of the total mass and energy balances applied on the overall system (system 1) and the shell-hood interface (system 4) is presented briefly in Table 5.16. It is indicated in the table that, rate of net mass transfer in both systems is almost the same meaning that net mass transfer is mainly controlled at the paper surface-hood interface. The negative sign indicates that there is air leakage to

the surroundings at the gap between the hood and the cylinder. Rate of net heat transfer is to the same order of magnitude in both systems. It is greater for System 4 due to lower temperature reading of the recycle streams 12 and 17 and higher reading of the blowing streams 10 and 11. Since the pipelines transferring the hot air between the large drying machinery are long, temperature variation along the air transfer lines is inevitable.

Table 5.16: Comparison of Energy and Mass Balance Results for Systems 1 and 4

Comparison of Systems 1 and 4		
Rate of Net Transfer Through System Boundary (Product-1)		
System	Heat (kJ/h)	Mass (kg/h)
System 1: Cylinder + Hood + Burners	-4.807E+6	-979.422
System 4: Cylinder-Hood Interface	-7.774E+6	-976.989

5.2.3 Heat Transfer From Steam and Air to the Paper Web Through the Resistances

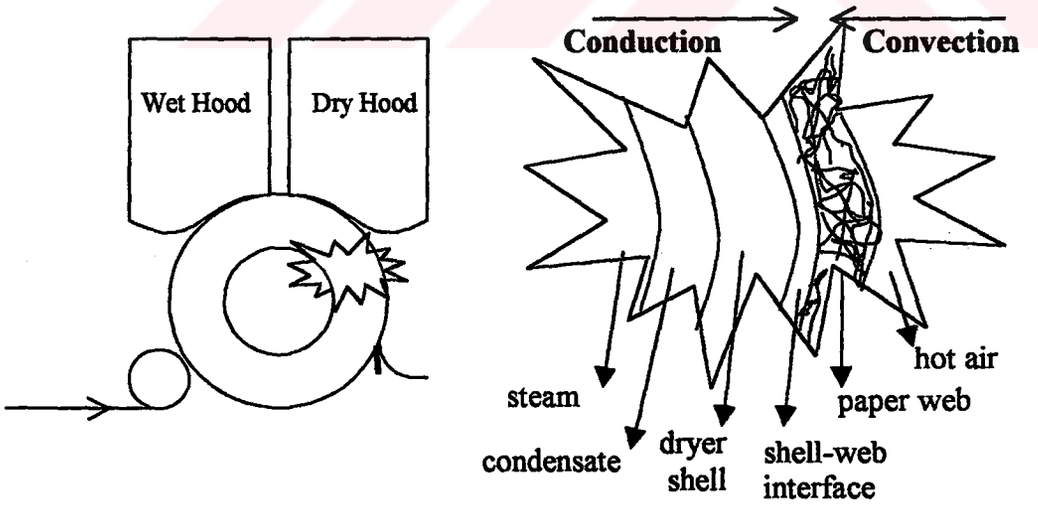

Figure 5.6: Thermal Resistances and the Two Way Heat Transfer

The effect of each thermal resistance on the overall heat transfer rate between the steam and the paper web with the hood air above it is to be determined. This is important due to the fact that overall drying rate is significantly affected by the heat transfer process taking place between these layers. Transfer of heat to paper by two mechanisms, conduction from steam and convection from air, is represented in Figure 5.5. The resistances in series are the steam condensate, cast-iron shell, shell-paper interface, and paper [10].

Paper sheet does not cover the entire cylinder surface. It sticks on the Yankee cylinder at θ=0° at the press roll and cylinder contact point. It wraps 314° as shown in Figure 5.7. Hood region starts at θ=22° with the wet hood and the dry hood starts at θ=164°. Totally the hood wraps 257°, that is, the paper surface is not totally covered by the hood. Actually, 22° at the entrance on the Yankee cylinder and 36° at the exit are not covered by the hood, and the paper sheet in these regions is in contact with the ambient.

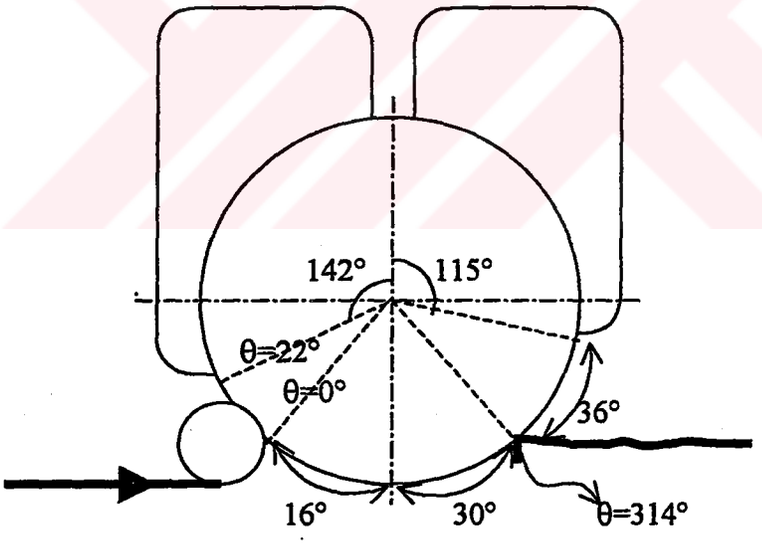

Figure 5.7: Angular View of the Yankee Cylinder

5.2.3.1 Moisture Profile Along the Paper Sheet on the Yankee Surface

In the calculations, paper sheet is assumed thin enough that temperature and moisture content variation in thickness direction is unimportant. This assumption has been proved to be true for tissue paper by Karlsson and Heikkila [32]. In spite of the fact that circumferential sheet temperature increases in machine direction, it is assumed to be uniform since Ahrens [28] has shown the uniform sheet temperature model to be appropriate for low grades of paper such as tissue paper.

Moisture profile is assumed to decrease linearly with the wrap angle, θ, in the hood region as paper gets dry based on the measurements by Lindeborg [35] and Ahrens [28]. Since the initial (60%) and the final (6%) paper moisture contents for İpek Kağıt are known, the equation of the moisture profile obtained by Ahrens is replotted assuming it is linear in the hood region between θ=22 and θ=278, the angle where the sheet leaves the Yankee. Finally, moisture profile as a function of wrap angle, that is, MC(θ) versus θ, is presented in Figure 5.8.

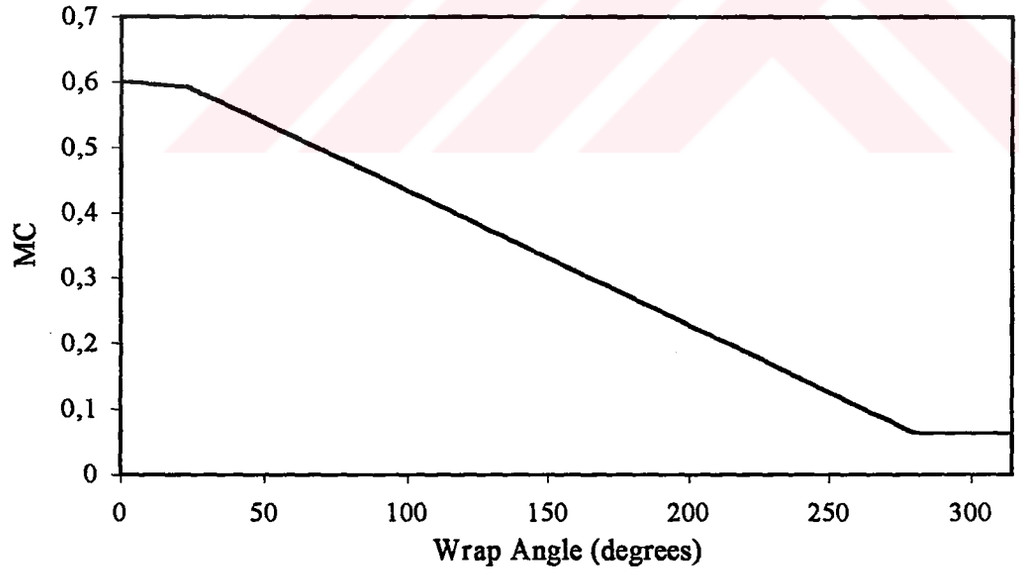

Figure 5.8: Moisture Content versus Wrap Angle

5.2.3.2 Heat Transfer Coefficients

Paper conductivity as a function of wrap angle is presented in Figure 5.9. Han's calculations for tissue paper referred by Seyed-Yagoobi et al. [24] in Table 3.2 state that thermal conductivity of wet tissue paper is 0.216 W/m·K and that of dry tissue paper is 0.144 W/m·K. Since there could be found no relation for the dependence of paper conductivity on wrap angle or moisture content for tissue paper, it is assumed to change linearly with respect to wrap angle within the hood area and is represented as kp(θ).

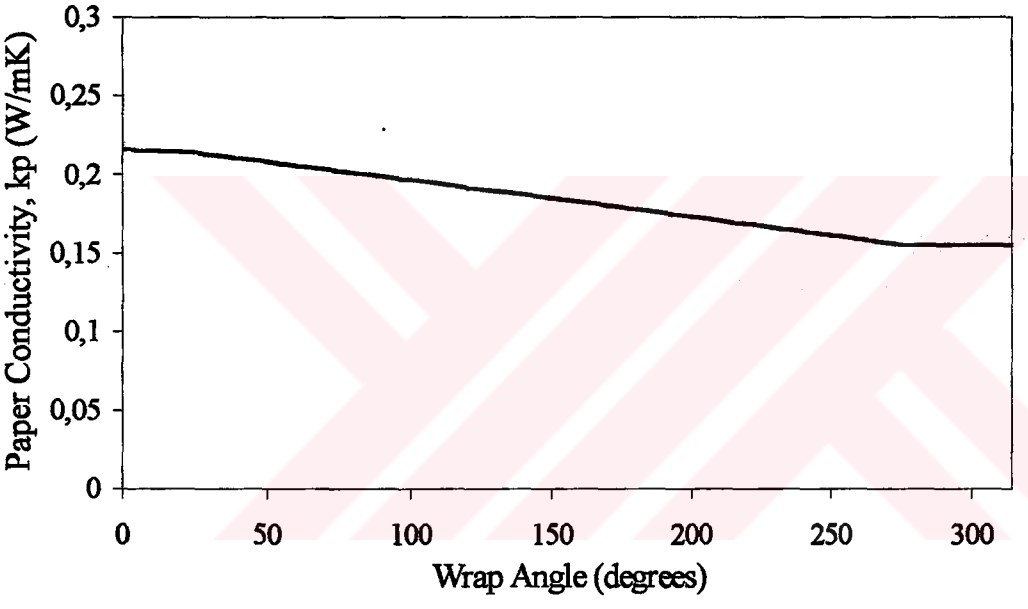

Figure 5.9: Paper Conductivity Changing Locally on the Cylinder Surface

Heat transfer coefficient for the shell-web interface, that is, the contact coefficient, for tissue paper is a function of the moisture content as shown in Equation (5.3), where α and β are heat transfer coefficients in units of $W/m^2 \cdot K$:

$$hint(\theta) := \alpha + \beta \cdot \frac{MC(\theta)}{1 - MC(\theta)} \tag{5.3}$$

The equation was found by Ahrens [28] and used in the analysis of a system resembling the one in İpek Kağıt with similar operating conditions. Since water conductivity is greater than air conductivity and dry-fiber conductivity, contact coefficient is expected to decrease with decreasing moisture content as shown in Figure 5.10.

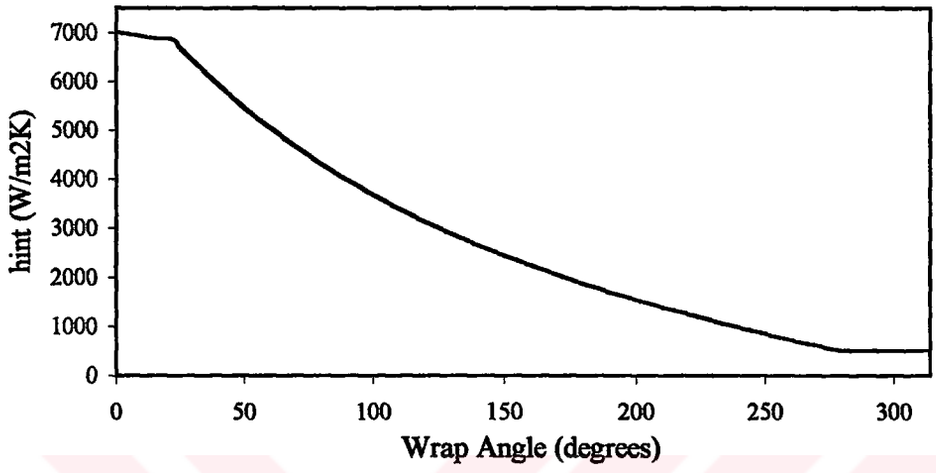

Figure 5.10: Yankee Shell-Paper Web Interface Heat Transfer Coefficient (Contact Coefficient) versus Wrap Angle

Steam condensing heat transfer coefficient, hcond, is determined approximately considering the rimming condition due to high speeds of the Yankee cylinder, 1200-1700 m/min. The respective values presented in Table 3.3 and found in other literature as high as 3500 $W/m^2 \cdot K$ are considered [33], [27], [28], [13]. Ahrens [28] used 1703 $W/m^2 \cdot K$ for a system very similar to the one studied in this study. Consequently, assuming constant condensate temperature and thickness all inside the shell and improved heat transfer due to the existence of ribs, the condensate coefficient is given an average value of 2000 $W/m^2 \cdot K$.

Convective heat transfer coefficient of the high-speed hot air from the hoods, ha, is assumed to be constant and 227.1 $W/m^2 \cdot K$ as used by Ahrens [28]. This value is evaluated to be valid due to the fact that convective heat transfer coefficient is 25-250 $W/m^2 \cdot K$ for gases in forced convection [36].

Thermal conductivity of the Yankee shell made of cast iron is assumed to be constant and equal to 310 Btu/(sq.ft)(h) [37] since the steam temperature inside the cylinder is generally constant around 170-180°C. It is assumed that Yankee shell surface temperature is constant during rotation. Actually, there is only a short period of temperature fall as the wet and cool web is pressed on to the shell at the contact point at the entrance. However, especially the area wrapped by the hood is of consideration and variations in surface temperature are ignored.

A comparison of all of the heat transfer resistances and the overall resistance is possible in Figure 5.11.

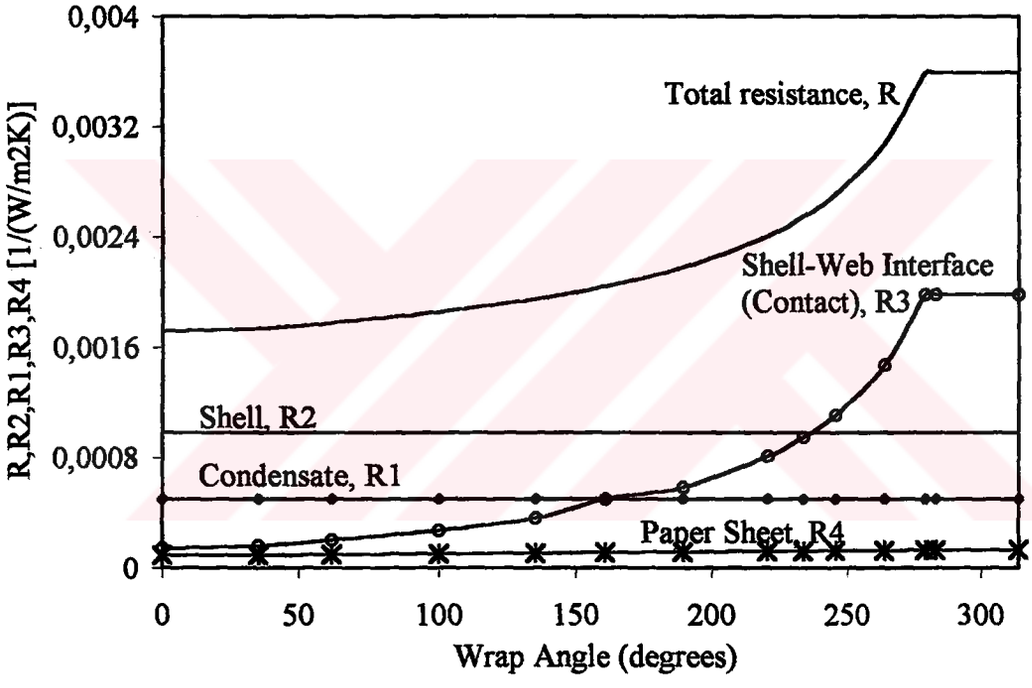

Figure 5.11: Thermal Resistances With Respect To Wrap Angle

It can be seen in Figure 5.11 that the resistance to heat transfer at the shell-paper interface increases the most as the sheet gets dry towards the end of the dry hood. It has strong dependency on moisture content and so even shapes the overall

resistance curve. Thermal conductivity of the paper sheet is also dependent on moisture content in a linear manner as shown in Figure 5.9. However, examining Figure 5.11 for the reciprocals of the heat transfer coefficients, i.e., for the resistances, this dependency is not as conspicuous as the moisture content dependency of the thermal resistance at the shell-paper interface. Heat transfer coefficient at the shell-paper interface, i.e., the contact coefficient, decreases crucially hindering the amount of heat transferred to the paper sheet, thereby increasing the overall resistance to heat transfer. Overall resistance for thermal conduction, R, is calculated as a function of the wrap angle using the equation for resistances in series:

$$R(\theta) = R1 + R2 + R3(\theta) + R4(\theta) \tag{5.4}$$

and the overall heat transfer coefficient is equal to the reciprocal of the overall thermal resistance:

$$U(\theta) = [R(\theta)]^{-1} \tag{5.5}$$

Overall heat transfer coefficient, U, decreases with decreasing water amount at the shell-paper interface on the cylinder and in the paper sheet.

Thermal conduction and convection resistances with their thickness and temperature are presented in Table 5.17 for different moisture contents of the paper sheet. The three certain locations on the Yankee Cylinder are the start of the wet hood (θ=22°), connection of the two hoods (θ=176°), and the end of the dry hood (θ=279°). Both Figure 5.11 and Table 5.17 indicate that dryer shell is the largest and paper web is the smallest resistance to heat transfer.

The validity of the assumptions made in evaluating the heat transfer coefficients is checked by comparing the values with those determined by Han [38] in Table 5.18.

Table 5.17: Conduction and Convection Resistances at Certain Angles ($\theta = 22°, 164°, 279°$) on the Yankee Cylinder

Thermal Resistances Affecting the Overall Heat Transfer Rate							
	Temperature (°C)	Thickness (mm)	Heat Transfer Coefficient	Thermal Resistivity (W/m^2K)·10^4			
				Wrap-Angle, θ degrees			
				θ	22	164	279
Steam-condensate	177	4-8	Hcond	R1	5.0	5.0	5.0
Dryer shell	150	48.6	Kshell	R2	9.8	9.8	9.8
Shell-web interface			Hint(θ)	R3(θ)	1.5	4.6	19.4
Paper web	92	0.02	Kp(θ)	R4(θ)	0.9	1.1	1.3
Blowing Air	450		ha	1/ha	44.0	44.0	44.0

Table 5.18: Heat Transfer Coefficients Determined by Han [h, Btu/(h)(ft^2)(°F)]

	Present Study			**Han's Study** [38]							
Grade	Tissue			Tissue				Paper		Board	
Caliper	0.02 mm			0.5 points				2 points		10 points	
Speed	1500 m/min			3000 ft/min ~1000 m/min				2000 ft/min		1000 ft/min	
Heat Trans. Coef.	$W/m^2 \cdot °C$					Btu/(h)(ft^2)(°F)					
	θ:22	θ:164	θ:279	Wet	Dry	Wet	Dry	Wet	Dry	Wet	Dry
Condns.	2000	2000	2000	852	852	150	150	300	400	500	600
Shell	1019	1019	1019	852	852	150	150	300	300	300	300
Contact	6667	2174	515	2272	1988	400	350	250	200	200	100
Web	11111	9091	7692	17040	11360	3000	2000	1000	400	400	50
Overall	581	487	281	341	341	62	60	90	70	80	30

For easy comparison of the heat transfer coefficients used in this study with those of Han's, condensate, shell, shell-paper interface, and paper values used in the calculations and the values found by Han [38] for tissue, paper and board are summarized in Table 5.18. The heat transfer coefficients recorded by Han [38] in units of Btu/(h)(ft^2)(°F) are converted into SI units in W/m^2·°C for ease of comparison. The present calculation values are given for the wet tissue at 22° and 164° and for dry tissue at 279°. It is seen that the values used in the present calculation are very close to those determined by Han [38].

Condensate coefficient is constant in both studies but the value used in this study is greater than Han's. This is due to the fact that cylinder speed is greater in the present study and the cylinder is ribbed, which enhances the heat transfer rate. Shell coefficients are constant and almost the same, only the shell coefficient used in this study is greater. This may be due to thinner shell thickness and improved conductivity of the shell material. The contact coefficient at the beginning of the wet hood at 22°, 6667 W/m^2·°C, is much greater than the one Han [38] determined for wet conditions, 2272 W/m^2·°C, but it is almost the same with the value at 164°, 2174 W/m^2·°C. Both the wet and dry web heat transfer coefficients used by Han are greater than those used in the present study. Since the values used in the present study are also calculated based on Han's study presented in another study [24] also shown in Table 3.2, the difference between the heat transfer coefficients might be due to the paper thickness (caliper).

In conclusion, heat transfer coefficients calculated in this study based on several assumptions are close to the values published by Han [38] with small variations. Therefore, heat transfer rate calculations carried with these heat transfer coefficients are reliable.

5.2.3.3 Heat Transferred To Paper Sheet By Conduction And Convection

It is required to be able to evaluate and compare the amount of heat transferred to the paper sheet at any point on the Yankee cylinder. Therefore, heat

conduction from steam to paper (Qstp), heat convection from air to paper (Qap), and their total (Qp) are calculated as point values at each angle on the paper sheet:

$$Qstp(\theta) = U(\theta) \cdot (C \cdot w \cdot (Tst - Tp)) \cdot 3600 \div 1000 \quad (5.6)$$

$$Qap(\theta) = ha \cdot A \cdot (Ta - Tp) \cdot 3600 \div 1000 \quad (5.7)$$

$$Qp(\theta) = Qap(\theta) + Qstp(\theta) \quad (5.8)$$

The total amount of heat supplied by both mechanisms is calculated by taking the sum of the point values at each angle over the wrap angle ranges specified in Table 15.19.

Table 5.19: Effects of Conduction and Convection on Drying (Product-1)

Heat Transfer Direction	**Wrap Angle (θ degrees)**	**Symbol**	**Rate of Heat Transfer (kJ/h)**
From air to paper	22→279	Qap	$8.129 \cdot 10^6$
From steam to paper	0→314	Qstp	$4.816 \cdot 10^6$
From steam to cylinder	314→360	Qstc	$0.325 \cdot 10^6$
Total heat given by steam (Qstp+Qstc)		Qst	$5.141 \cdot 10^6$
Heat transferred to paper (Qap+Qstp)		Qp	$1.295 \cdot 10^7$
Total heat given by air and steam (Qap+Qst)		Qast	$1.327 \cdot 10^7$
Heat given by condensation of steam		Hls50	$4.97 \cdot 10^6$
Heat required to vaporize water (Wr)		Hv	$1.074 \cdot 10^6$

The results presented in Table 5.19 indicate that about 6% of the heat supplied by steam is lost through the uncovered bottom part of the cylinder, which has an angle of 46°. The amount of heat lost at this bare part of the cylinder is equal to 2.5% of the total heat given by air and steam. 62.8% of the heat given to paper is

from air while 37.2% is from steam. Steam and air contribution in the total heat supplied is 36.3% and 61.2% respectively.

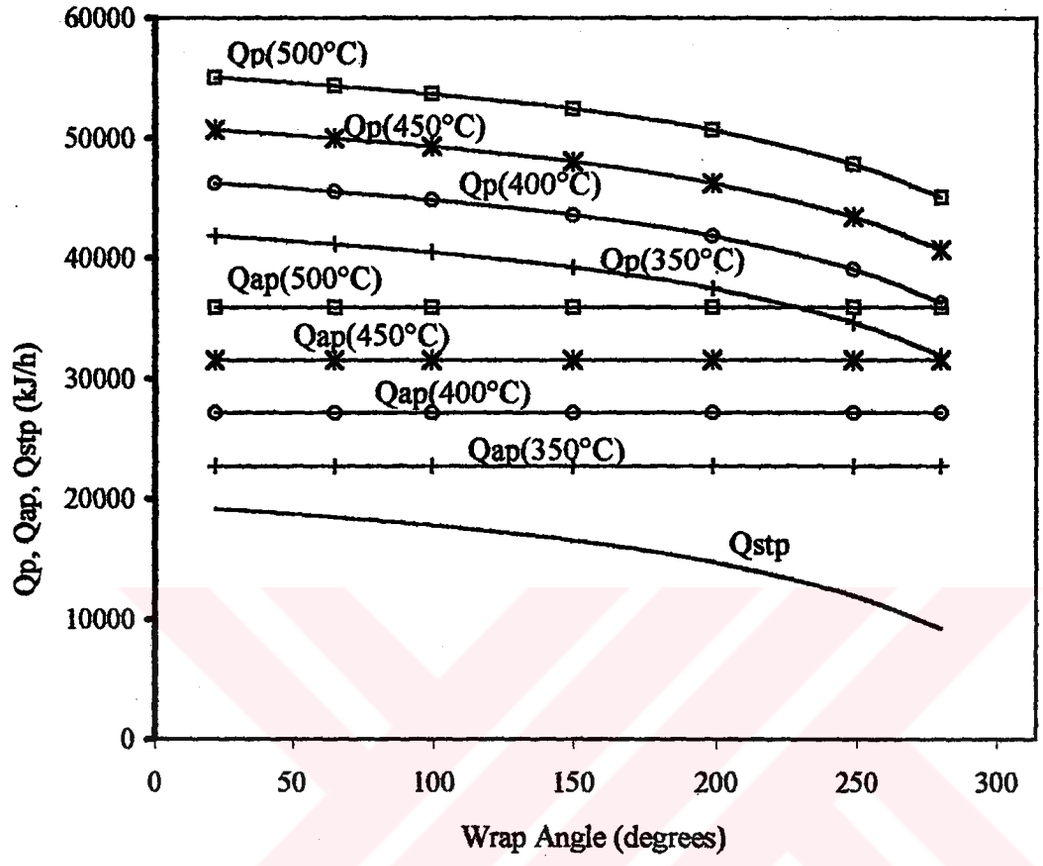

Figure 5.12: Point Values for Rate of Heat Transfer to Paper at Different Air Blowing Temperatures Versus Wrap Angle (θ=22° to 279°)

Point values of rate of heat transferred from air (Qap), steam (Qstp) and both (Qp) to the paper sheet are calculated at each angle under the hood between 22° and 279° since blowing air is only active in this region. As the sheet is dried during its transfer from the wet end to the dry end on the Yankee shell, web moisture content decreases causing the contact and paper heat transfer coefficients to decrease. Therefore, at each point towards the end of the hoods, the rate of heat that can be

steam to the paper surface (Qstp) decreases as can be seen in Figure 5.12. Rate of heat transfer from air is calculated for 350, 400, 450 and 500°C, which are in the actual air temperature range of the real system. Rate of heat transfer from air increases as air temperature increases and it is the same at all points under the hood since air heat transfer coefficient and the paper temperature are assumed to be constant. The contribution of air to total amount of heat transferred is found to be greater than that of steam and it is found to increase as air temperature increases. At 350°C, 59% of the total heat given to paper is supplied by air, while at 500°C, air contribution increases to 69%.

CHAPTER 6

ANALYSIS OF THE DRYING PARAMETERS AND THE OPTIMUM CONDITIONS

The same final product can be produced by changing different drying parameters and keeping the rate of paper production constant. With reference from literature, the most effective drying parameters are the air supply velocity in each end of air cap (blowing air velocity), hood temperatures, steam pressure in cylinder and exhaust air humidity [15], [12]. In the present study, only the air velocity, air temperature and the steam pressure are considered. However, in literature, exhaust air humidity is greatly stressed [39]. Total energy, ET, can be written as a function of the drying parameters:

ET=f1(blow velocity)+f2(steam pressure)+f3(air temperature, blow velocity) (7.1)

Energy consumption is from three different sources used in the system: Natural gas, steam and electricity. Gas consumption is a function of the blowing air temperature and velocity. Steam consumption is a function of the steam pressure in the cylinder. Electricity consumption is a function of the blowing air velocity.

For a certain product, thermal energy required to dry the product to the desired moisture content is constant. Thermal energy is the sum of the energy from gas and from steam. Since it is constant, the variation of energy from steam and from air with respect to air temperature is presented in Figure 6.1, which is a result of the solutions with heat transfer coefficients. When the air temperature increases, energy from air increases and energy from steam decreases for a constant thermal drying rate.

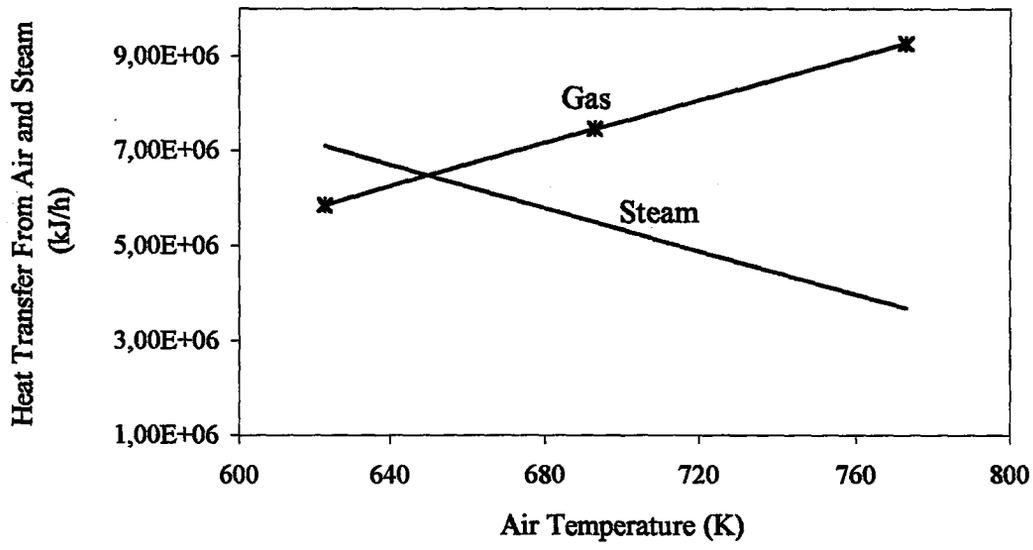

Figure 6.1: Heat Transfer Rates of Air and Steam at Varying Air Temperatures Calculated Using the Thermal Resistances

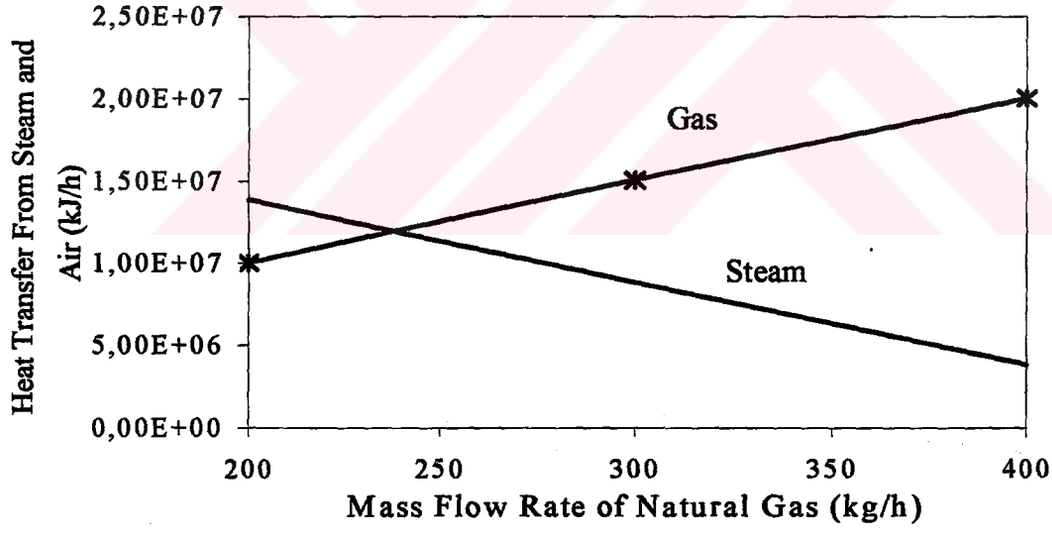

Figure 6.2: Heat Transfer Rate of Steam and Air versus Mass Flow Rate of Natural Gas Calculated for the Overall System

Considering only variation in steam pressure and air temperaure for constant drying rate, energy from steam decreases while that from air increases. As can be seen in Figures 6.1 and 6.2, heat flow rate of air increases as air temperature and mass flow rate of natural gas increases for constant air mass flow rate. Drying rate is kept constant for an increase in the temperature of the air causes a decrease in the pressure of the steam. As the amount of natural gas fed to the system increases, temperature of the blowing air increases as presented in Figure 6.3 for constant mass flow of air.

For a certain mass flow rate of air determined at a certain temperature, 700 K, keeping the mass flow rate constant, the variation in the energy consumed by gas is presented in Figure 6.4 and the variation in the enthalpy of the blowing air is presented in Figure 6.5. Both the energy consumption by gas and thus the enthalpy of the blowing air increase with increasing blowing air temperature at constant mass flow rate of air.

For constant drying energy, as air temperature increases, air mass flow rate decreases as shown in Figure 6.6, or if more air is blown on to the paper surface then the air temperature must be decreased. However, the opposite is true when the drying energy is not constant. Then, as shown in figure 6.7, air with higher velocities is blown onto the paper for higher air temperatures. The physical reason for this is that tissue paper is much thinner and more delicate than higher grades of paper. The very high temperatures applied on the surface may damage or burn the web. Therefore, it must be blown faster onto the web surface so that removing the moisture out of the web, it will quickly sweep away.

Figures 6.8 indicates that for increasing drying rates, electricity consumption increases due to increasing air temperature because of the decreasing volumetric efficiency and the requirement of higher air impingement velocities above the paper to prevent web burning. As the electricity consumption increases, Figure 6.9 presents the consequent increase in total cost of electricity.

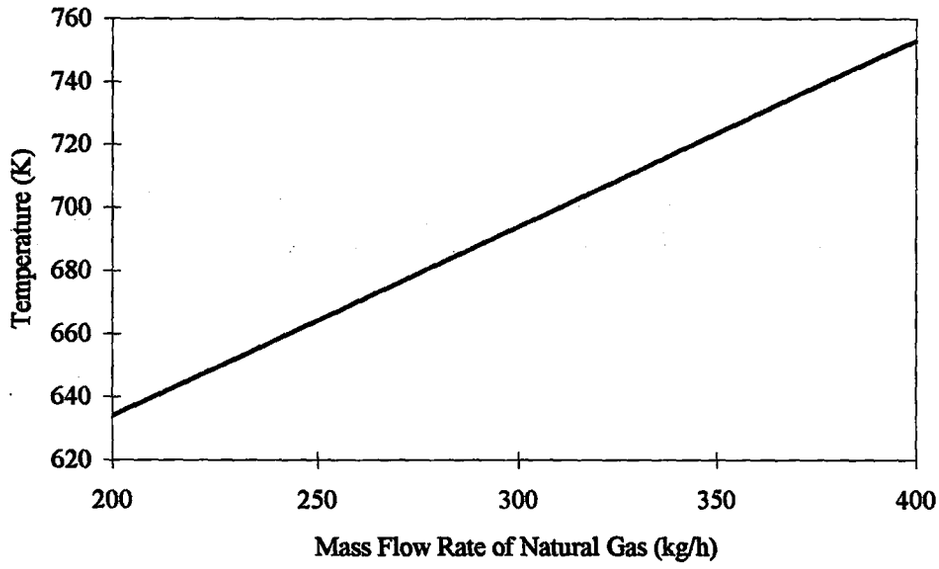

Figure 6.3: Variation of Air Temperature by Consumption of Natural Gas

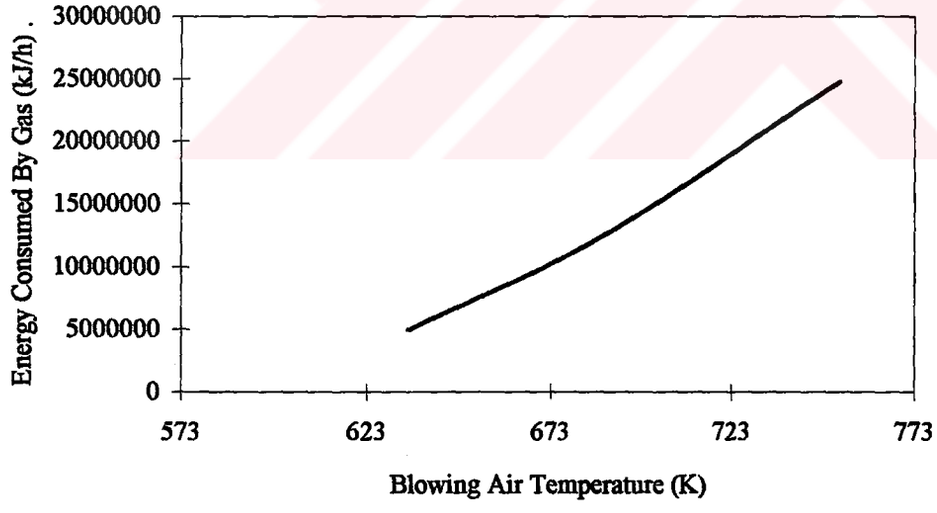

Figure 6.4: Energy Consumed by Gas as the Air Blowing Temperature Increases

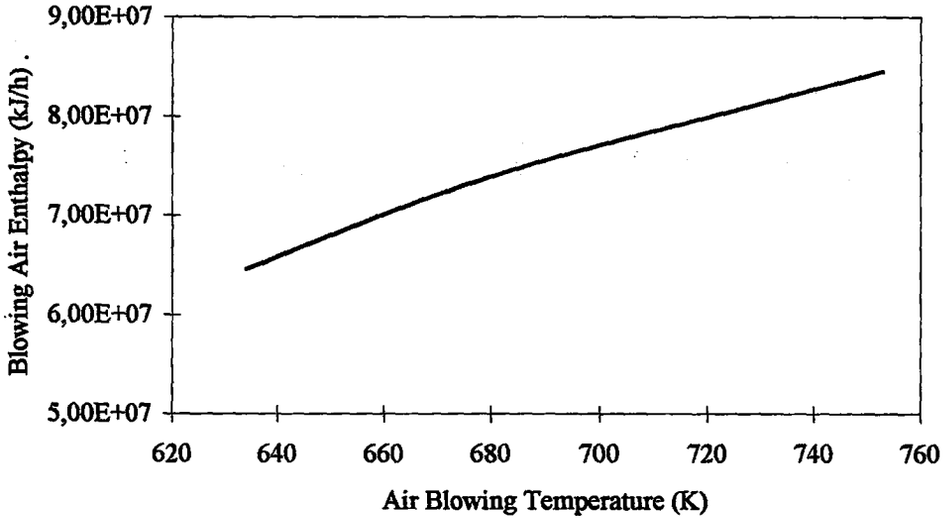

Figure 6.5: Enthalpy of Blowing Air Changing With Air Temperature

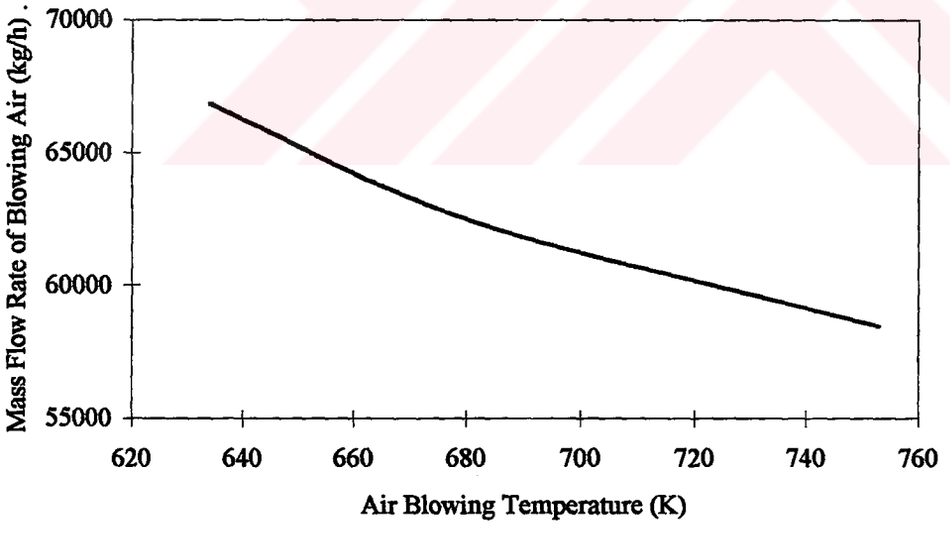

Figure 6.6:Mass Flow Rate of Blowing Air Changing With Air Temperature For Constant Drying Energy

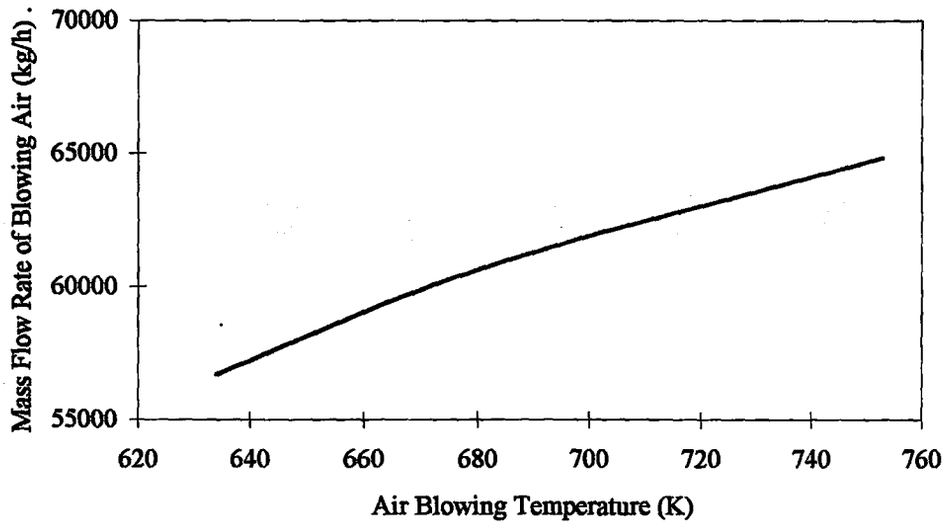

Figure 6.7: Mass Flow Rate of Blowing Air for Increasing Drying Energy

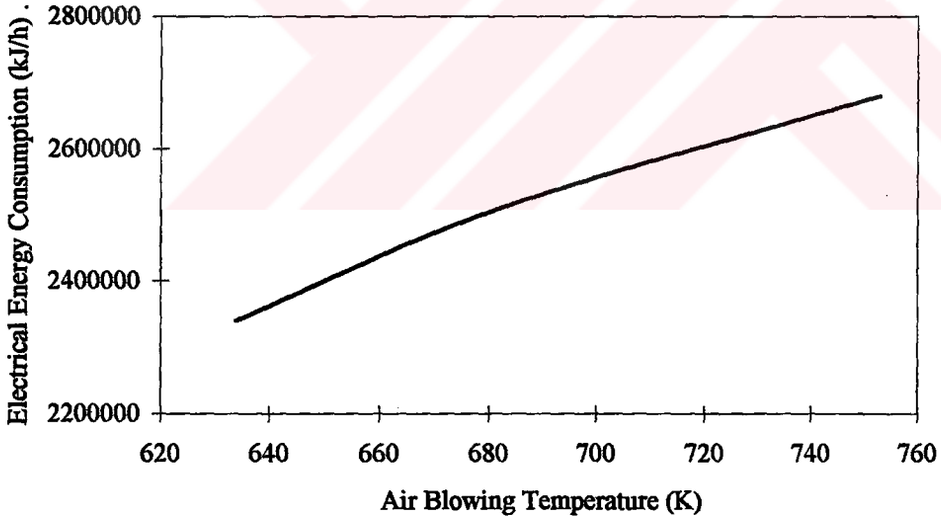

Figure 6.8: Electricity Consumption Changing With Air Temperature For Increasing Drying Energy

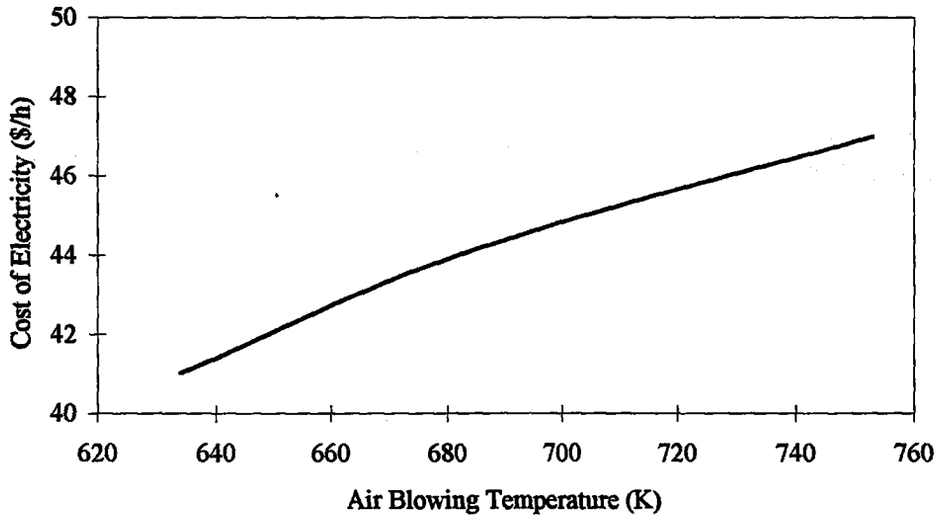

Figure 6.9: Cost of Electricity Changing With Air Temperature For Increasing Drying Energy

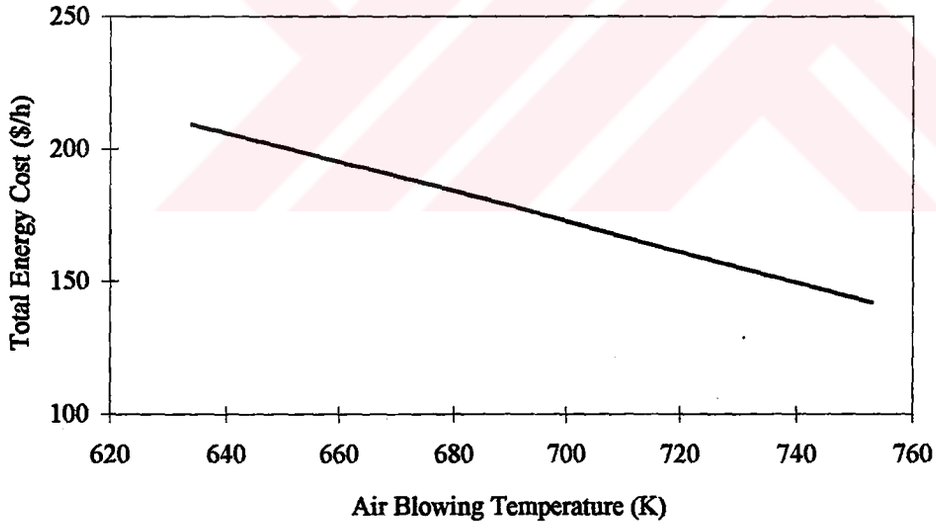

Figure 6.10: Total Cost Changing With Air Temperature For Constant Drying Energy

Finally, it is shown in Figure 6.10 that, in contrast with the previous case, if the drying rate is constant, then the total cost decreases with increasing air temperature since the amount of air blown onto the paper and therefore the electricity consumption will decrease. Besides natural gas is much cheaper than electricity, and decrease in electricity consumption causes great decreases in total costs.

Generally, contribution of gas in the total energy use is more. In general, energy from gas is about 45-55%, energy from steam is 35-45%, and energy from electricity is 10-15% of the total consumption.

Electricity is the most expensive among the other energy types used in the industry, namely gas and steam. According to the values obtained from the İpek Kağıt mill, the cost of electricity is 62.7 $/1000 kWh while the costs of steam and gas are 28 $/1000 kWh and 14.9 $/1000 kWh, respectively. Electricity consumption is the smallest among gas and steam due to its high cost, but it should be minimized since even a small increase or decrease in the consumption of electricity would affect the total cost with great savings.

CHAPTER 7

CONCLUSIONS

The Yankee-Hood dryer section of the paper machine at the İpek Kağıt tissue-paper mill in Yalova was analyzed in terms of mass and energy. The analysis was carried on three main systems: The overall system, shell-hood interface, and the system involving the layers of resistance to heat transfer between steam, paper web and air. Mass flow rate and moisture content of each stream was determined.

Mass analysis showed that there is always mass spill out of the hood. The spill is mainly of air since the water balance was found to be consistent. As a result of the mass balances made for the overall system in System 1 and for the cylinder surface and hood system, it was seen that the rate of net mass transfer in both systems is almost the same. Consequently, it was suggested that the mass lost through system boundaries is mainly controlled at the paper surface and hood interface.

Energy analysis showed that the spill is through the 20 mm to 50 mm clearance at the shell-hood intersection area, between the shell surface and the below side of the hood. The hood is under depression since it takes up about 4-5 tons/h of water vapor out of the paper sheet on the Yankee cylinder surface. The leakage of air through the pipelines before the hood is also possible but according to the present analysis indicating high thermal losses, the spill is by the hot impingement air. This high-velocity air is blown onto the sheet surface and vacuumed back after sweeping the sheet surface. It is probable that some of this air blown with great force cannot be vacuumed at the open sides and is let to escape to the ambient. The leakage is suggested to be especially cross-machine at the entrance and exit of the hood since

the clearance between the cylinder and the hood increases at these points as a result of the bending of the hood due to high temperature and gravity.

As a result of the analysis of the Yankee-hood dryer in terms of thermal energy for eight products and operating conditions in practice, the overall system was found to be 28.1-29.4% efficient. Efficiency was defined as the ratio of the energy required to evaporate the water to energy input through the system boundaries. Thus, the resulting efficiencies indicate that almost 3.5 times the actual amount of energy required is being expended by the overall system, which is very inefficient and costly. Seyed-Yagoobi et al. [40] has mentioned that an assessment of industrial drying made by an Energy Department indicated that dryer efficiencies (defined as the ratio of theoretical energy for evaporation to actual energy consumed) ranged as low as 10% for some dryer configurations and was typically on the order of 40-45%. Consequently, the resulting efficiency is not uncommon in the industry since drying is extremely energy inefficient and represents a major production bottleneck in many industrial processes, but needs to be increased.

The improvement of the overall efficiency is strongly dependent on the reduction of thermal losses. Thermal losses are caused by spill out of the hood, hot air leakages within the system and heat losses through the walls of the long pipelines that transfer the heated air from the hoods to the paper surface and back to the hoods. The higher rate of net heat transfer found as a result of the energy balance at the shell-hood interface is due to great thermal losses taking place at the hot air streams 10, 11, 12 and 17 between the burners and the hood. Air temperature is read in the Mill when it has its maximum temperature just at the exit of the burner. Air temperature decreases due to heat loss through the pipe walls as it is transferred to the hood. The temperature of the recycle stream is read just before the entrance to the burner when it has its minimum temperature due to heat losses through the pipeline. If the temperature readings of the blowing air at the nozzles and the recycle air in the hoods were possible, heat loss at the interface would come out to be less than that at System 1, which means higher efficiency. Consequently, it confirmed that pipeline insulation in İpek Kağıt is not very effective in preventing heat losses.

The efficiency calculated for the conduction and convection mechanisms through the resistance layers from steam and air to the paper sheet was calculated to be 84%. Efficiency of the two-way mechanism is strongly dependent on the heat transfer coefficients of the media from and through which heat is transferred. Heat transfer coefficients for the condensate and shell were assumed to be constant at any angle of the cylinder. The contact and the paper coefficients were calculated as functions of paper moisture content that was assumed to change linearly with the hood wrap angle. Several assumptions for paper were made for the ease of calculations due to the microscopic thickness of the tissue paper. Finally, it was found out that about 55-65% of the heat supplied to paper is from air while 35-45% is from steam depending on the temperature of the air. Rate of heat transferred from steam does not show much variation since the cylinder is generally operated at the maximum pressure.

As the market has changed, demand of low cost and low basis weight tissues is increasing. The performance of a high-speed tissue machine depends greatly on how it is managed from its design, the project phase, the start up and finally, the optimization.

The interaction of steam consumption with gas consumption and electricity is analyzed in this study. The effect of increasing air temperature on air mass flow rate at constant and increasing drying energy cases are examined. It is found out that electricity consumption is very effective on the total energy cost. Electricity is not used in direct drying of the paper sheet in İpek Kağıt, it is used to turn the fans to blow the hot air on to the paper in the Yankee-Hood system. It is also used to transfer the air from the recovery unit to the dry side and from the dry side to the wet side. However, only the electricity consumed by the blowing fans are considered in this study. Results of the calculations on electricity consumption changing due to air temperature with the resulting changes in the total cost are presented as graphs concluding that electricity use should be minimized.

REFERENCES

1. S. Y. Salama, B. S. Minsker and Olsen K.G., 'Competitive Position of Natural Gas: Industrial Solids Drying', Energy and Environmental Analysis 1987, Inc., Arlington, VA.

2. M. H. Chiogioji, 'Industrial Energy Conservation', Marcel Dekker, New York, NY, 1979.

3. J. A. Hinds, A. N. Neogi, 'The Dynamic Computer Simulation of a Paper Machine Dryer', Proceedings of the Technical Association of the Pulp and Paper Industry, Engineering Conference 1982, Book I, TAPPI Press, Atlanta, GA, pp. 117-123.

4. 'Encyclopedia Britannica', W. Benton, Pub., Encyclopedia Britannica, Inc., 1971, Vol. 17.

5. 'Kirk-Othmer Encyclopedia of Chemical Technology', 4th Ed., John Wiley and Sons, Inc, New York, USA, 1996, Vol. 18.

6. O. Polat, R. H. Crotogino and W.J.M. Douglas, 'Through-Drying of Paper: A Review', Advances in Drying, Ed.by A.S. Mujumdar, Hemisphere Publishing Cor., Washington, 1984 Vol. 3, pp. 263-299.

7. L. A. Kirk, 'A Literature Review of Computer Simulation of Paper Drying', Advances in Drying, Ed.by A.S. Mujumdar, Hemisphere Publishing Cor., Washington, 1984, Vol.. 3, pp. 1-37.

8. J. E. Kline, 'Paper and Paperboard Manufacturing and Converting Fundamentals', 1982, TAPPI Press, Atlanta.

9. 'Pulp and Paper Manufacture - Paper Making and Paperboard Making', Ed. R.G. Macdonald and J.N. Franklin, 2nd Ed, McGraw Hill, New York, 1969, Vol. III, pp.437-533.

10. J. L. Chance, 'Overview of the Dryer Section', TAPPI Seminar Notes:1989, Practical Aspects of Pressing and Drying, Atlanta, USA, 1989, Vol. 62, pp. 121-137.

11. C. Morini, 'The Approach to the Next General of Air Tissue Drying', Tissue Making '98- High Performance Tissue Production, May 7-8, Karlstad, Sweden.

12. K. Toivonen, 'Yankee Drying of Soft Tissue Paper', Svensk Papperstidning 1982, Vol. 85, Iss. 12, pp. R107-R114.

13. D. W. Appel and S. H. Hong, 'Condensate Distribution and Its Efforts on Heat Transfer in Steam-Heated Dryers', Pulp Paper Magazine Of Canada 1969, Vol. 70, Iss. 4, p. 66.

14. F.O. Oliver, 'Dry-Creping of Tissue Paper - A Review of Basic Factors', Tappi Journal 1980, Vol 63, Iss 12, pp. 91-95.

15. V. Schukov, 'High-Speed paper Tissue Yankee Hood drying System', Engineering Digest 1989, Toronto, Vol. 35, Iss. 4, pp. 14-15.

16. V. Schukov and A. Heberl, 'Humidity and its Effect on Thermal Efficiency of Yankee Hoods', TAPPI Journal 1988, Vol. 71, Iss. 7, pp. 68-70.

17. J.Seyed-Yagoobi, D. O. Bell and M.C. Asensio, 'Heat and Mass Transfer in a Paper Sheet During Drying', Journal of Heat Transfer, Transactions of the ASME 1992, Vol. 114, pp.538-541.

18. M. C. Asensio and J. Seyed-Yagoobi, 'Simulation of Paper-Drying Systems With Incorporation of an Experimental Drum/Paper Thermal Contact Conductance Relationship', Transactions of the ASME, Journal of Energy Resources Technology 1993, Vol. 115, Iss. 4, pp. 291-300.

19. D. Wahren, 'Pulp and Paper Drying Helsinki Symposium 1991', Paperi ja Puu-Paper and Timber 1991, Vol. 73, Iss. 8, pp. 737-740.

20. S. Ramaswamy and R. A. Holm, 'Analysis of Heat and Mass Transfer During Drying of Paper/Board', Drying Technology 1999, Vol. 17, Iss. 1-2, pp.49-72.

21. J. Lehtinen, 'The Heat Pipe Process in Intraweb Heat Transfer in Hot Surface Paper Drying, Paperi ja Puu-Paper and Timber 1992, Vol. 74, Iss. 7, pp. 560-571.

22. J. F. Bond, A. S. Mujumdar, A. R. P. Van-Heiningen and W. J. M. Douglas, 'Drying Paper by Impinging Jets of Superheated Steam. Part 2: Comparison of Steam and Air as Drying Fluids', Canadian Journal of Chemical Engineering 1994, Vol. 72, Iss. 3, pp. 452-456.

23. B. Wilhemson, L. Fagerhol and L. Nilsson, 'An Experimental Study of Contact Coefficients in Paper Drying', TAPPI 1994, Vol. 77, Iss. 5, pp. 159-168.

24. J. Seyed-Yagoobi, K. H. Ng and L.S. Fletcher, 'Thermal Contact Conductance of a Bone-Dry Paper Handsheet/Metal Interface', Journal of Heat Transfer, Transactions of ASME 1992, Vol. 114, pp. 326-330.

25. M. C. Asensio, J. Seyed-Yagoobi and L. S. Fletcher, 'Thermal Contact Conductance of a Moist Paper Handsheet Metal Interface for Paper Drying Applications', Journal of Heat Transfer, Transactions of the ASME 1993, Vol. 115, Iss. 4, pp.1051-1053.

26. A. Meinecke, T. Chau Huu, and H. Loser, Das Papier 1988, 42(10A): V159.

27. B. Wilhemsson, S. Stenstrom, L. Nilsson, R. Krook, H. Persson and R. Wimmerstedt , 'Modeling Multicylinder Paper Drying – Validation of a New Simulation Program', TAPPI Journal 1996, Vol. 79, Iss. 4, pp. 157-167.

28. F. W. Ahrens, 'Effect of shell Thermal Dynamics on Predictions of a Yankee Dryer Model', ASME Heat Transfer Division 1995, Vol. HTD 317-2, pp. 427-435.

29. O. Brauns and A. L. Jansson, 'Heat Transmission in the Drying of Paper on a Yankee Cylinder', Svensk Paperstidning 1957, Vol.60, No. 17, pp. 621-631.

30. T. Sundberg, N. Andersson, K. Lofgren and L. Osterberg, 'Heat Transfer in MG Drying', Svensk Paperstidning 1968, Vol.71, No. 8, pp. 317-324.

31. L. W. Zabel, 'The Application of an Analaog Computer to a Paper Manufacturing Problem', TAPPI Journal 1959, Vol. 42, No. 8, pp. 687-690.

32. M. Karlsson and P. Heikkila, 'Computer Simulation of Yankee Drying', Drying '87, A.S. Mujumdar , Ed., 1987, Hemisphere, Washington, USA, pp. 194-202.

33. A. R. Pearson, 'Modeling Paper Machine Drying on a Microcomputer', TAPPI 1986, Vol. 69, Iss. 9, pp.194-195.

34. R. A. Reese, 'Revised TAPPI Drying-Rate Curves', TAPPI Journal 1988, Vol. 71, Iss. 12, pp. 231-233.

35. C. Lindeborg, 'A Method for Analysis of Cross-Direction Drying Performance in a Paper Machine, TAPPI 1982, Vol. 65, Iss. 10, pp. 119-122.

36. F. P. Incropera and D. P. De Witt, 'Fundamentals of Heat and Mass Transfer', 3rd Ed., John Wiley and Sons, Inc., New York, USA, 1990.

37. 'Chemical Engineers' Handbook', J.H. Perry: Editor-in-Chief, 4th Ed., McGraw-Hill, Inc., New York, USA, 1963.

38. S .T. Han, 'Drying of Paper', TAPPI Journal 1970, Vol. 53, Iss. 6, pp. 1034-1046.

39. T. K. Wahlberg, A. Hallgren and B. Axelsson, 'Minimizing the Total Drying Energy on a Tissue Paper Machine', TAPPI Journal 1985, Vol. 68, Iss. 3, pp.86-91.

40. D. O. Bell, J. Seyed-Yagoobi and L. S. Fletcher, 'Recent Develeopments in Paper Drying', Advances in Drying, Ed.by A.S. Mujumdar, Hemisphere Publishing Cor., Washington, D.C., 1984, Vol.. 3, pp. 203-261.

APPENDIX A

A.1 MASS BALANCE

A.1.1 Mass Flow Rates and Overall Mass Balance

Mass flow rate of Natural Gas

$$M8 = NG8 \cdot dng \cdot (P8 \div 1.013) \cdot ((273 + 15) \div T8) \cdot \quad (A.1)$$

$$M9 = NG9 \cdot dng \cdot (P8 \div 1.013) \cdot ((273 + 15) \div T8) \cdot \quad (A.2)$$

Mass flow rate of exhaust air (kg/h)

$$M13 = E13 \cdot (h13 + 1000) \quad (A.3)$$

Mass flow rate of paper produced (kg/h)

$$M21 = VY \cdot (1 - CF) \cdot (60 \cdot (m21 \div 1000) \cdot w) \quad (A.4)$$

$$Mp21 = M21 \cdot (1 - x21) \quad (A.5)$$

Mass flow rate of pulp (kg/h)

$$Mp20 = Mp21 \quad (A.6)$$

$$M20 = Mp20 \div (1 - x20) \quad (A.7)$$

Mass flow rate of steam (kg/h)

$$M50 = Mbt + Mms \quad (A.8)$$

$$M51 = M50 \quad (A.9)$$

$$Mcy = Mbt \div 1.5 \quad (A.10)$$

$$Msy = M50 - Mcy \quad (A.11)$$

Rate of total mass lost by the system (kg/h)

$$Min + Mout + Mgen - Mcon + Mi = Macc \quad (A.12)$$

$$Mgen - Mcon = 0 \quad (A.13)$$

$$Macc = 0 \quad (A.14)$$

$$Min - Mout + Mi = 0 \quad (A.15)$$

$$Ma = M3 + M4 + M6 \quad (A.16)$$

$$Mng = M8 + M9 \quad (A.17)$$

$$Min = Ma + Mng + M20 \quad (A.18)$$

$$Mout = M21 + M13 \quad (A.19)$$

$$Mi = Mout + Min \quad (A.20)$$

A.1.2 Water Balance

Rate of water removal (kg/h)

$$Wr = M20 - M21 \quad (A.21)$$

$$Win - Wout + Wgen - Wcon - Wl = Wacc \quad (A.22)$$

Water in, from air (kg/h)

$$W3 = M3 \cdot h3 \cdot 10^{-3} \quad (A.23)$$

$$W4 = M4 \cdot h3 \cdot 10^{-3} \quad (A.24)$$

$$W6 = M6 \cdot h3 \cdot 10^{-3} \quad (A.25)$$

Water in, from natural gas (kg/h)

$$W8 = M8 \cdot h8 \quad (A.26)$$

$$W9 = M9 \cdot h8 \quad (A.27)$$

Water in, from pulp at the entrance of Yankee (kg/h)

$$W20 = M20 - Mp20 \quad (A.28)$$

Water out, from exhaust air (kg/h)

$$W13 = E13 \cdot h8 \quad (A.29)$$

Water out, from paper at the exit of Yankee (kg/h)

$$W21 = M21 \cdot x21 \quad (A.30)$$

Water generated from NG combustion (kg/h)

$$W8c = 2 \cdot M8 \cdot (18 \div MWng) \quad (A.31)$$

$$W9c = 2 \cdot M9 \cdot (18 \div MWng) \quad (A.32)$$

Total water in to, out of and generated in the system (kg/h)

$$Win = W20 + Wa \quad (A.33)$$

$$Wout = W13 + W21 \quad (A.34)$$

$$Wgen = W8c + W9c \quad (A.35)$$

$$Wcon = 0 \quad (A.36)$$

$$Wacc = 0 \quad (A.37)$$

Water lost from system (kg/h)

$$W1 = Win - Wout + Wgen - Wcon - Wacc \quad (A.38)$$

A.1.3 Mass Balance On Wet And Dry Sides

A.1.3.1 Wet Side

$$\alpha = 0.63 \quad (A.39)$$

$$\beta = 0.55 \quad (A.40)$$

$$Wiwh = Mi \cdot \alpha \quad (A.41)$$

$$Wrwh = Wr \cdot \beta \quad (A.42)$$

$$M10 - M12 + Miwh + Wrwh = 0 \quad (A.43)$$

$$\lambda w \cdot M12 - M13 = 0 \quad (A.44)$$

$$M14 - M12 + M13 = 0 \quad (A.45)$$

$$M14 + M15 - M16 = 0 \quad (A.46)$$

$$M16 - M10 + M8 = 0 \quad (A.47)$$

A.1.3.2 Dry Side

$$Midh = Mi \cdot (1 - \alpha) \quad (A.48)$$

$$Wrdh = Wr \cdot (1 - \beta) \quad (A.49)$$

$$(M4 + M6 + M9 + Wrdh + Midh) - M15 = 0 \quad (A.50)$$

$$M11 - M17 + Midh + Wrdh = 0 \quad (A.51)$$

$$M6 + M17 - M18 = 0 \quad \text{(A.52)}$$

$$\lambda w \cdot M18 - M19 = 0 \quad \text{(A.53)}$$

$$M4 + M9 - M11 + M19 = 0 \quad \text{(A.54)}$$

A.2 ENERGY BALANCE ON SYSTEM 1

Energy input through system boundary (kJ/h)

Energy in from pulp

$$Hp20 = Mp20 \cdot CPf \cdot (T20 - Tref) \quad (A.55)$$

$$Hw20 = W20 \cdot HIT20 \quad (A.56)$$

$$H20 = Hp20 + Hw20 \quad (A.57)$$

Energy in from entering air

$$Ha = Ma \cdot CPa \cdot (T3 - Tref) \quad (A.58)$$

Energy in from Natural Gas

$$Hg = Mng \cdot CPng \cdot (T8 - Tref) \quad (A.59)$$

$$HinI = H20 + Ha + Hg \quad (A.60)$$

Energy in from entering steam

$$H50 = M50 \cdot HgP50 \quad (A.61)$$

$$HinII = H50 \quad (A.62)$$

$$Hin = HinI + HinII \quad (A.63)$$

Energy output through system boundary (kJ/h)

Energy output from pulp

$$Hp21 = Mp21 \cdot CPf \cdot (T21 - Tref) \quad (A.64)$$

$$Hw21 = W21 \cdot HIT21 \quad (A.65)$$

$$H21 = Hp21 + Hw21 \quad (A.66)$$

Energy out from exhaust dry air

$$Ha13 = E13 \cdot 1000 \cdot CPa \cdot (T13 - Tref) \quad (A.67)$$

Energy out from exhaust water vapor

$$Hw13 = W13 \cdot HgT13 \quad (A.68)$$

$$H13 = Ha13 \cdot Hw13 \quad (A.69)$$

$$HoutI = H21 + H13 \quad (A.70)$$

Energy out from leaving steam and condensate

$$H51s = Msy \cdot HgT51 \quad (A.71)$$

$$H51c = Mcy \cdot HIT51 \quad (A.72)$$

$$HoutII = H51s + H51c \quad (A.73)$$

$$Hout = HoutI + HoutII \quad (A.74)$$

Energy Generation within the system (kJ / h)

$$Hrxn = Mng \cdot Hng \quad (A.75)$$

$$Hsen = na \cdot \int_{Tref}^{Trxn} 6.173+0.04697 \cdot 10^{-2} \cdot T + 0.1147 \cdot 10^{-5} \cdot T^2 + 0.4696 \cdot 10^{-9} \cdot T^3 \cdot dT \quad (A.76)$$

$$Hgen = Hrxn + Hsen \quad (A.77)$$

Net Energy tranfer by heat (kJ / h)

$$Q = Hin + Hgen - Hout \quad (A.78)$$

Energy required to evaporate Wr (kJ / h)

$$Hv = Wr \cdot HT21 \quad (A.79)$$

$$e = Hv \div (Hin + Hgen) \quad (A.80)$$

A.3 MASS AND ENERGY BALANCE ON SYSTEM 4

A.3.1 Moisture Content of Streams

Stream 12

$$M12 = Ma12 + W12 = Ma12 \cdot (1 + h12) \quad (A.81)$$

$$W12 = M12 - Ma12 \quad (A.82)$$

Stream 10 (A.83)

$$W10 = W12 - Wrwh \quad (A.84)$$

$$Ma10 = M10 - W10 \quad (A.85)$$

$$h10 = W10 \div Ma10 \quad (A.86)$$

Stream11

$$Ma11 = M11 \div (1 + h11) \quad (A.87)$$

$$W11 = M11 - Ma11 \quad (A.88)$$

Stream17

$$W17 = M17 - W17 \quad (A.89)$$

$$h17 = W17 \div Ma17 \quad (A.90)$$

A.3.2 Total Mass Balance Around System 4

$$M20 + M10 + M11 + Mih = M21 + M12 + M17 \quad (A.91)$$

$$Mih = (M21 + M12 + M17) - (M20 + M10 + M11) \quad (A.92)$$

A.3.3 Total energy balance over the system 4

$$Q + Ein = Eout \tag{A.93}$$

$$Hp20 = Mp20 \cdot Cpf \cdot (T20 - Tref) \tag{A.94}$$

$$Hp21 = Mp21 \cdot Cpf \cdot (T21 - Tref) \tag{A.95}$$

$$Hw20 = W20 \cdot HlT20 \tag{A.96}$$

$$H20 = Hp20 + Hw20 \tag{A.97}$$

$$Hw21 = W21 \cdot HlT21 \tag{A.98}$$

$$Hw20 = W20 \cdot HgP50 \tag{A.99}$$

$$H51s = Msy \cdot HgT51 \tag{A.100}$$

$$H51c = Mcy \cdot HlT51 \tag{A.101}$$

$$H51 = Mcy \cdot HlT51 + Msy \cdot HgT51 \tag{A.102}$$

$$Ha10 = Ma10 \cdot CPa \cdot (T10 - Tref) \tag{A.103}$$

$$Ha12 = Ma12 \cdot CPa \cdot (T12 - Tref) \tag{A.104}$$

$$Hw10 = W10 \cdot HgT10 \tag{A.105}$$

$$H10 = Ha10 + Hw10 \tag{A.106}$$

$$Hw12 = W12 \cdot HgT12 \tag{A.107}$$

$$H12 = Ha12 + Hw12 \tag{A.108}$$

$$Ha11 = Ma11 \cdot CPa \cdot (T11 - Tref) \tag{A.109}$$

$$Ha17 = Ma17 \cdot CPa \cdot (T17 - Tref) \quad \text{(A.110)}$$

$$Hw11 = W11 \cdot HgT11 \quad \text{(A.111)}$$

$$H11 = Ha11 + Hw11 \quad \text{(A.112)}$$

$$Hw17 = W17 \cdot HgT17 \quad \text{(A.113)}$$

$$H17 = Ha17 + Hw17 \quad \text{(A.114)}$$

$$Hmiwh = Miwh \cdot CPa \cdot (T10 - Tref) \quad \text{(A.115)}$$

$$Hmidh = Midh \cdot CPa \cdot (T10 - Tref) \quad \text{(A.116)}$$

A.4 HEAT TRANSFER BETWEEN STEAM AND WEB

A.4.1 Heat Transfer Coefficients

$$Slope1 = -3 \cdot 10^{-4} \quad \text{(A.117)}$$

$$Slope2 = -2.06 \cdot 10^{-3} \quad \text{(A.118)}$$

$$c1 = 0.6 \quad \text{(A.119)}$$

$$c2 = 0.64 \quad \text{(A.120)}$$

$$x21 = 0.063 \quad \text{(A.121)}$$

$$\text{If } 0 \le \theta \le 22, \quad MC(\theta) = slope1 \cdot \theta + c1 \quad \text{(A.122)}$$

$$\text{If } 22 < \theta \le 279, \quad MC(\theta) = slope2 \cdot \theta + c2 \quad \text{(A.123)}$$

$$\text{If } 279 < \theta \le 314, \quad MC(\theta) = x21 \quad \text{(A.124)}$$

$$Slope3 = -8 \cdot 10^{-5} \quad \text{(A.125)}$$

$$Slope4 = -2.35 \cdot 10^{-4} \quad \text{(A.126)}$$

$$c3 = 0.216 \quad \text{(A.127)}$$

$$c4 = 0.22 \quad \text{(A.128)}$$

$$\text{If } 0 \le \theta \le 22, \quad kp(\theta) = slope3 \cdot \theta + c3 \quad \text{(A.129)}$$

$$\text{If } 22 < \theta \le 279, \quad kp(\theta) = slope4 \cdot \theta + c4 \quad \text{(A.130)}$$

$$\text{If } 279 < \theta \le 314, \quad kp(\theta) = 0.155 \quad \text{(A.131)}$$

$$\alpha = 198.7\ W / m^2K \quad (A.132)$$

$$\beta = 4542\ W / m^2K \quad (A.133)$$

$$hint(\theta) = \alpha + \beta \cdot [\, MC(\theta) \div (1 - MC(\theta)) \,] \quad (A.134)$$

$$R1 = 1 \div hcond \quad (A.135)$$

$$R2 = tshell \div kshell \quad (A.136)$$

$$R3(\theta) = 1 \div hint(\theta) \quad (A.137)$$

$$R4(\theta) = tp \div kp(\theta) \quad (A.138)$$

A.4.2 Point Values of Heat Transfer From Air And Steam

$$C = (1 \div 360) \cdot \pi \cdot D \quad (A.139)$$

$$A = C \cdot w \quad (A.140)$$

$$Qstp(\theta) = U(\theta) \cdot (C \cdot w \cdot (Tst - Tp)) \cdot (3600/1000) \quad (A.141)$$

$$Qap(\theta) = h(a) \cdot A \cdot (Ta - Tp) \cdot (3600/1000) \quad (A.142)$$

$$Qp(\theta) = Qstp(\theta) + Qap(\theta) \quad (A143)$$

$$Qstpflux = Qstp(\theta) \div (A \cdot 3600) \quad (A144)$$

A.4.3 Point Values of Heat Transferred At Different Air Temperatures

$$Qap0(\theta) = ha \cdot A \cdot (Ta0 - Tp) \cdot (3600/1000) \quad (A.144)$$

$$Qp0(\theta) = Qstp(\theta) + Qap0(\theta) \quad \text{(A.145)}$$

$$Qap1(\theta) = h(a) \cdot A \cdot (Ta1 - Tp) \cdot (3600/1000) \quad \text{(A.146)}$$

$$Qp1(\theta) = Qstp(\theta) + Qap1(\theta) \quad \text{(A.147)}$$

$$Qap2(\theta) = h(a) \cdot A \cdot (Ta2 - Tp) \cdot (3600/1000) \quad \text{(A.148)}$$

$$Qp2(\theta) = Qstp(\theta) + Qap2(\theta) \quad \text{(A.149)}$$

A.4.4 Total Heat Transferred By Air and Steam

$$Qstcloss = (1 \div (R1 + R2)) \cdot (C \cdot w \cdot (360 - 314)) \cdot (Tst\ (150 + 273)) \quad \text{(A.150)}$$
$$(3600 \div 1000)$$

$$Qap = \sum_{22}^{279} Qap(\theta) \quad \text{(A.151)}$$

$$Qstp = \sum_{0}^{314} Qsp(\theta) \quad \text{(A.152)}$$

A.4.5 Drying Parameters

$$GRi = \sum_{22}^{279} ha \cdot A \cdot (Ta - Tp) \cdot \frac{3600}{1000} \quad \text{(A.153)}$$

$$SR = \sum U(\theta) \cdot [C \cdot w \cdot (Tst - Tp)] \cdot \frac{3600}{1000} \quad \text{(A.154)}$$

$$ER = \sum_{\theta=0}^{279} ha \cdot A \cdot (Ta - Tp) \cdot \frac{3600}{1000} + \left[\sum_{\theta=0}^{314} U(\theta) \cdot (C \cdot w \cdot (Tst - Tp)) \cdot \frac{3600}{1000} \right] \qquad (A.155)$$

Table B.1: Data Sheet For Product-1

Product 1 Servis Peçete VY = 1500 m/min m = 16.8 g/m^2									
Yankee and paper properties (Streams 20 & 21)		Properties of feed Natural Gas (Streams 8 & 9)		Properties of exhaust air (Stream 13)		Properties of feed air (Streams 3, 4, 6)		Properties of steam (Streams 50, 51)	
VY	1500	NG8	148	E13	12.2	M3	2200	Mbt	2450
VR	1291	NG9	194	h13	448	M4	3200	Mms	4542
w	2.7	P8	1.4	T13	559	M6	8200	P50	9.5
m21	16.8	h8	0	HgT13	2771	h3	1.25	T51	450
x20	0.6	T8	302.1			T3	419	HgP50	2775
x21	0.063	Trxn	731			CPa	1.046	HgT51	2775
CF	0.139	dng	0.728					HIT51	749
CPf	1.8828	MWng	16.325					HT21	2773
T20	303	RDng	0.564						
T21	365	CPng	2.3012						
HIT20	124	Hng	50078						
HIT21	385								
Tref = 298 K									

Table B.2: Data Sheet For Product-2

Product 2 Servis peçete 2 VY = 1479 m/min. m = 17 g/m^2									
Yankee and paper properties (Streams 20 & 21)		Properties of feed Natural Gas (Streams 8 & 9)		Properties of exhaust air (Stream 13)		Properties of feed air (Streams 3, 4, 6)		Properties of steam (Streams 50, 51)	
VY	1479	NG8	129	E13	11.7	M3	2000	Mbt	2751
VR	1305	NG9	188	h13	445	M4	3000	Mms	4592
w	2.7	P8	1.4	T13	563	M6	8300	P50	8.8
m21	17	H8	0	HgT13	2765.53	h3	1.25	T51	447
x20	0.596	T8	305.3			T3	425	HgP50	2772.5
x21	0.0616	Trxn	726			CPa	1.046	HgT51	2772
CF	0.141	Dng	0.728					HIT51	735.7
CPf	1.8828	MWng	16.325					HT21	2773
T20	303	RDng	0.564						
T21	365	CPng	2.9288						
HIT20	124.4	Hng	50078.2						
HIT21	385.3								
Tref = 298 K									

Table B.3: Data Sheet For Product-3

Product 3 UltraSolo 1 VY = 1630 m/min m = 16.7 g/m^2									
Yankee and paper properties (Streams 20 & 21)		Properties of feed Natural Gas (Streams 8 & 9)		Properties of exhaust air (Stream 13)		Properties of feed air (Streams 3, 4, 6)		Properties of steam (Streams 50, 51)	
VY	1630	NG8	131	E13	12.4	M3	2000	Mbt	2569
VR	1304	NG9	175	h13	448	M4	2800	Mms	4601
w	2.7	P8	1.4	T13	560	M6	8500	P50	9.5
m21	16.7	h8	0	HgT13	2770.3	h3	1.25	T51	450
x20	0.6	T8	302.1			T3	547	HgP50	2775.4
x21	0.0587	Trxn	699			CPa	1.046	HgT51	2774.9
CF	0.20	dng	0.728					HIT51	749
CPf	1.8828	MWng	16.325					HT21	2773
T20	303	RDng	0.564						
T21	365	CPng	2.9288						
HIT20	124.4	Hng	50078.2						
HIT21	385.3								
Tref = 298 K									

Table B.4: Data Sheet For Product-4

Product 4 UltraSolo 2 VY = 1640 m/min. m = 16.7 g/m^2									
Yankee and paper properties (Streams 20 & 21)		Properties of feed Natural Gas (Streams 8 & 9)		Properties of exhaust air (Stream 13)		Properties of feed air (Streams 3, 4, 6)		Properties of steam (Streams 50, 51)	
VY	1640	NG8	135	E13	12.5	M3	2000	Mbt	2603
VR	1314	NG9	185	h13	441	M4	2900	Mms	4592
w	2.7	P8	1.4	T13	550	M6	8400	P50	9.5
m21	16.7	h8	0	HgT13	2782.6	h3	1.25	T51	450
x20	0.6	T8	301.4			T3	417	HgP50	2775.4
x21	0.06	Trxn	711			CPa	1.046	HgT51	2774.9
CF	0.199	dng	0.728					HIT51	749
CPf	1.8828	MWng	16.325					HT21	2773
T20	303	RDng	0.564						
T21	365	CPng	2.9288						
HIT20	124.4	Hng	50078.2						
HIT21	385.3								
Tref = 298 K									

Table B.5: Data Sheet For Product-5

Product 5 UltraSolo 3 VY = 1650 m/min. m = 16.7 g/m^2									
Yankee and paper properties (Streams 20 & 21)		Properties of feed Natural Gas (Streams 8 & 9)		Properties of exhaust air (Stream 13)		Properties of feed air (Streams 3, 4, 6)		Properties of steam (Streams 50, 51)	
VY	1650	NG8	136	E13	12.4	M3	2000	Mbt	2673
VR	1320	NG9	186	h13	451	M4	2900	Mms	4525
w	2.7	P8	1.4	T13	552	M6	8500	P50	9.5
m21	16.7	h8	0	HgT13	2762.35	h3	1.25	T51	450
x20	0.6	T8	302.1			T3	418	HgP50	2775.4
x21	0.06	Trxn	711			CPa	1.046	HgT51	2774.9
CF	0.2	dng	0.728					HIT51	749
CPf	1.8828	MWng	16.325					HT21	2773
T20	303	RDng	0.564						
T21	365	CPng	2.9288						
HIT20	124	Hng	50078.158						
HIT21	385								
Tref = 298 K									

Table B.6: Data Sheet For Product-6

Product 6 Israel Hai Paper 2 VY = 1575 m/min m = 17.4 g/m^2									
Yankee and paper properties (Streams 20 & 21)		Properties of feed Natural Gas (Streams 8 & 9)		Properties of exhaust air (Stream 13)		Properties of feed air (Streams 3, 4, 6)		Properties of steam (Streams 50, 51)	
VY	1575	NG8	138	E13	12.5	M3	2000	Mbt	2685
VR	1263	NG9	185	h13	445	M4	2900	Mms	4524
w	2.7	P8	1.4	T13	565	M6	8100	P50	9.7
m21	17.4	h8	0	HgT13	2762.35	h3	1.25	T51	451
x20	0.6	T8	300.1			T3	427	HgP50	2776.4
x21	0.055	Trxn	732			CPa	1.046	HgT51	2775.8
CF	0.198	dng	0.728					HIT51	753.4
CPf	1.8828	MWng	16.325					HT21	2273
T20	303	RDng	0.564						
T21	365	CPng	2.9288						
HIT20	124.4	Hng	50078.2						
HIT21	385.3								
Tref = 298 K									

Table B.7: Data Sheet For Product-7

Product 7 Syria Ghabra 1 VY = 1600 m/min. m = 17 g/m^2									
Yankee and paper properties (Streams 20 & 21)		Properties of feed Natural Gas (Streams 8 & 9)		Properties of exhaust air (Stream 13)		Properties of feed air (Streams 3, 4, 6)		Properties of steam (Streams 50, 51)	
VY	1600	NG8	134	E13	12.1	M3	2000	Mbt	2865
VR	1278	NG9	174	h13	453	M4	2800	Mms	4587
w	2.7	P8	1.4	T13	551	M6	8400	P50	9.5
m21	17.03	h8	0	HgT13	2781.37	h3	1.25	T51	450
x20	0.6	T8	300.6			T3	416	HgP50	2775.4
x21	0.06	Trxn	709			CPa	1.046	HgT51	2774.9
CF	0.201	dng	0.728					HIT51	749
CPf	1.8828	MWng	16.325					HT21	2773
T20	303	RDng	0.564						
T21	365	CPng	2.9288						
HIT20	124.4	Hng	50078.2						
HIT21	385.3								
Tref = 298 K									

Table B.8: Data Sheet For Product-8

Product 8 Syria Ghabra 2 VY = 1620 m/min m = 16.2 g/m^2									
Yankee and paper properties (Streams 20 & 21)		Properties of feed Natural Gas (Streams 8 & 9)		Properties of exhaust air (Stream 13)		Properties of feed air (Streams 3, 4, 6)		Properties of steam (Streams 50, 51)	
VY	1620	NG8	138	E13	11.7	M3	2100	Mbt	2884
VR	1305	NG9	184	h13	454	M4	3000	Mms	4410
w	2.7	P8	1.4	T13	555	M6	8300	P50	8.8
m21	16.20	h8	0	HgT13	2776.45	h3	1.25	T51	447
x20	0.6	T8	300.6			T3	414	HgP50	2772.5
x21	0.06	Trxn	715			CPa	1.046	HgT51	2772
CF	0.194	dng	0.728					HIT51	735.7
CPf	1.8828	MWng	16.325					HT21	2773
T20	303	RDng	0.564						
T21	365	CPng	2.9288						
HIT20	124.4	Hng	50078.2						
HIT21	385.3								
Tref = 298 K									

Table B.9: Overall Mass Balance for Different Paper Grades
(Pressure 8.8-9.7 bar, Reaction Temperature 426-459°C,
Exhaust Air Humidity 441-454 g water/kg dry air)

Product	Basis weight g/m^2	Exit moisture (%)	Water removed kg/h
Product-1	16.8	6.3	4717
Product-2	17.0	6.1	4709
Product-3	16.7	5.9	4774
Product-4	16.7	6.0	4799
Product-5	16.7	6.0	4821
Product-6	17.4	5.5	4851
Product-7	17.0	6.0	4760
Product-8	16.2	6.0	4624

Table B.10: Overall Energy Balance for Different Paper Grades
(Pressure 8.8-9.7 bar, Reaction Temperature 426-459°C,
Exhaust Air Humidity 441-454 g water/kg dry air)

Product	Yankee Velocity m/min	Rate of net mass transfer kg/h	$Q*10^{-6}$ kJ/h	Efficiency %
Product-1	1500	-979	4.81	28.1
Product-2	1479	-496	4.12	28.4
Product-3	1630	-412	3.04	29.4
Product-4	1640	-394	3.70	29.1
Product-5	1650	-537	3.91	28.9
Product-6	1575	-100	4.13	29.0
Product-7	1600	-675	4.27	28.6
Product-8	1620	-1322	4.45	28.3

APPENDIX C

Table C.1 : Natural Gas at Karamürsel, winter conditions

		% Volume	Weight (g)
Methane	CH_4	97,81844282	15,651
Ethane	C_2H_6	1,358266472	0,407
Propane	C_3H_8	0,263198837	0,116
Butane	C_4H_{10}	0,078293665	0,045
Pentane	C_5H_{12}	0,002575616	0,002
Nitrogen	N_2	0,454936603	0,127
Carbon Dioxide.	CO_2	0,021600319	0,010
	C_6	0,002685667	0,002

Table C.2 : Natural Gas at Karamürsel, summer conditions

		% Volume	Weight (g)
Methane	CH_4	95,7456343	15,319
Ethane	C_2H_6	2,212260994	0,664
Propane	C_3H_8	0,403962523	0,178
Butane	C_4H_{10}	0,049692201	0,029
Pentane	C_5H_{12}	0,003059095	0,002
Nitrogen	N_2	0,427948329	0,120
Carbon Dioxide.	CO_2	0,025371107	0,011
	C_6	0,003043787	0,002